The Structure–Property Relationship of Aryl-Substituted Tetrathiafulvalene Vinylogues

By

© Stephen Bouzan

A dissertation submitted to the School of Graduate Studies

in partial fulfillment of the requirements for

the degree of Master of Science

Department of Chemistry

Faculty of Science

Memorial University

St. John’s, Newfoundland and Labrador, Canada

May 2015

Table of Contents

Chapter 4 Conclusion and Future Work

Appendices: NMR Spectra for New Compounds

Abstract

Tetrathiafulvalene (TTF) is well known in the discipline of materials chemistry for its excellent electron donating properties. For decades, considerable efforts have been made to design and synthesize novel π-extended analogues of TTF (ex-TTFs) in order to exploit the application in electronic and optoelectronic devices. Of the vast array of ex-TTFs known so far, the class of vinylogous derivatives of TTF (TTFVs) has attracted the interest of many research groups. TTFVs are ideal candidates for organic-based electronics as they have a low band gap and rich electroactivity. This has posed the need to further investigate the interesting and inherently peculiar nature of TTFV; in particular, the structure-property relationship that exists with aryl based TTFVs has been a focus of this thesis work. Through the use of aryl substituents conformational control of TTFV has been demonstrated. The use of a 1-naphthyl substituent allowed a neutral TTFV to take an unprecedented *trans* conformation as a result of significant allylic strain. Additionally, an unprecedented tricyclic S-containing heterocycle was produced via *ortho* brominated aryl substituents. Finally, a group of alkynylated phenyl-TTFVs were synthesized and characterized. The molecular properties of all the new TTFV and related compounds have been studied by single crystal X-ray diffraction, UV-Vis absorption spectroscopy, and cyclic voltammetry

List of Figures

List of Schemes

List of Abbreviations and Symbols

APCI	atmospheric pressure chemical ionization
aq	aqueous
C_{60}	buckminsterfullerene
calcd	calculated
CTC	charge transfer complex
CV	cyclic voltammetry
d	doublet
DFT	density functional theory
DMF	N,N-dimethylformamide
Et	ethyl
FTIR	Fourier transform infrared (spectroscopy)
g	gram(s)
h	hour(s)
HOMO	highest occupied molecular orbital
IR	infrared (spectroscopy)
K	kelvin
LUMO	lowest unoccupied molecular orbital
m	multiplet
m/z	mass to charge ratio
Me	methyl
MHz	megahertz
min	minute(s)
mL	milliliter(s)

mol	mole(s)
mp	melting point
MS	mass spectrometry
nm	nanometer(s)
NMR	nuclear magnetic resonance (spectroscopy)
Ph	phenyl
ppm	parts per million
rt	room temperature
s	second(s) or singlet
SAM	self-assembled monolayer
t	triplet
THF	tetrahydrofuran
TMS	trimethylsilyl
TMSA	trimethylsilylacetylene
TTF	tetrathiafulvalene
TTFV	tetrathiafulvalene vinylogue
TTFAQ	tetrathiafulvalene anthraquinone
UV-Vis	ultraviolet-visible
V	volt(s)
XRD	X-Ray diffraction
δ	chemical shift
BLA	bond length alternation
EC	electrochemical-chemical

Acknowledgments

There are many people I would like to thank for the wonderful experiences I have had at Memorial University. First of all, I would like to thank my supervisor Dr. Yuming Zhao for giving me the opportunity to work with him and for showing me the joys of organic chemistry. His kind, caring, and positive attitude made for an excellent learning atmosphere during my research. I could not have asked for a better supervisor.

I would also like to thank all of the members of my research group as well as those from the Pansare research group as they have made my time during my masters here at M.U.N. a pleasure. Most of all I would like to especially thank Karimulla Mulla, Kaivalya Kulkarni, and RakeshThorat for all their patience, dedication, and guidance. It would have been exceptionally difficult were it not for their help throughout my program. I wish them the best of luck in their endeavors, especially Kaivalya.

I would also like to extend my thanks to the staff and faculty of the Chemistry Department as they have offered me a great education and many memorable experiences. I also wish to thank C-Cart for their help and assistance with the instruments. Lastly, I would like to thank my parents for their tremendous support throughout my program. Without them none of this would have been possible.

Chapter 1 Introduction

1.1 A Brief Overview of the Emergence and History of Tetrathiafulvalene

Tetrathiafulvalene (TTF) is a sulfur-containing heterocyclic compound (see structure **1** in Figure 1.1) which has attracted enormous research interest in the disciplines of chemistry and materials engineering for well over eighty years.[1, 2] Initially its appearance was the result of some non-targeted byproducts that were reported sporadically throughout the literature prior to 1970 and dating as far back as 1926.[3-5] The landmark work inaugurating the beginning of TTF chemistry was the synthesis of TTF reported in the early 1970s by three groups independently and nearly simultaneously (Wudl in 1970,[6] Hünig[7] and Coffen[8] in 1971). Prior to these works, the significance of TTF in the field of chemistry and materials science remained unrecognized due to the lack of characterization of its properties. It was because of the seminal studies by Wudl[9] and others[10-13] on the conductivity and superconductivity of TTF-containing complexes that the unique electronic properties of TTF began to draw broad attention from the scientific community. Ever since then, tremendous interest in this relatively simple organosulfur compound has been generated, which opened the door to a new discipline, organic molecule-based electronics.[14-17]

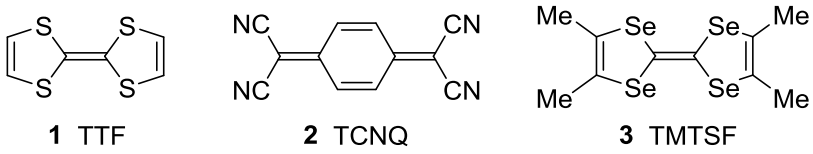

Figure 1.1 Molecular structures of TTF, TCNQ, and TMTSF.

The early milestones in TTF chemistry began with the creation of the first organic conductor $[TTF]^{+}Cl^{-}$ in 1972.[9] Further examination of this salt revealed that the π-electron donating nature of TTF enabled a unique packing arrangement in the solid state, such that the TTF moieties were stacked in alignment with their central double bond. The result was an increase in molecular orbital interactions which yielded an abnormally high electrical conductivity along the direction of the stacking. The metal-like behavior of such a TTF charge-transfer salt prompted a surge of research on TTF based compounds. Shortly after $[TTF]^{+}Cl^{-}$ was reported, another charge-transfer complex (CTC) was discovered in 1973.[10] Through the combination of the π-donating TTF and the strong electron acceptor 7,7,8,8-tetracyano-*p*-quinodimethane (TCNQ, **2** in Figure 1.1) a truly astonishing and remarkable CTC was generated. This TTF-TCNQ complex displayed substantial improvement in its electrical conductivity over the $[TTF]^{+}Cl^{-}$ salt predecessor. Differences between the electrical conductivities of both complexes arise from the segregated molecular stacking motifs in the TTF-TCNQ complex. Effectively the packing motif enables intermolecular charge transfer from the TTF to the TCNQ generating an array of delocalized electrons which are responsible for the extraordinary electrical conductance. In fact, the electrical conductivity of the TTF-TCNQ CTC

(~10^5(Ωcm)$^{-}$1) was determined to be several orders of magnitude higher than that of respective organic materials. Furthermore, with a Peierls transition (a form of lattice distortion) from metal to insulator at 54 K, the TTF-TCNQ charge-transfer complex was widely deemed as "the first organic metal".[10] Although this TTF-TCNQ result was quite bedazzling, it was not the last outstanding contribution to be made from the TTF family. A few years later, in 1980, the hexafluorophosphate salt of tetramethyltetraselenafulvalene (TMTSF, **3** in Figure 1.1) $[TMTSF]_2PF_6$, was found to show superconductivity,[13] and this exciting discovery inaugurated the era of organic superconductors. $[TMTSF]_2PF_6$ has been commonly referred to as Bechgaard's salt,[18] which demonstrates the importance and significance of TTFs within the realm of solid-state physics. Today, its incredible properties continue to stimulate the invention and development of newer, more complex and useful molecular electronic and optoelectronic materials.[16, 19-22]

1.2 Properties of TTF

As shown in Figure 1.1, the structure of TTF consists of two 1,3-dithiole rings connected via a single carbon-carbon double bond. Although its structure may appear to be simple and relatively small in size, its most important feature at first glance still can be easily overlooked, which is its π-electron delocalization properties. The peculiar and intriguing electronic properties of TTF are truly remarkable and offer a wide range of avenues to explore in the disciplines of chemistry, engineering, and materials sciences.

According to the classical resonance model, TTF in the neutral state appears as though it is a non-aromatic 14 π-electron bicyclic system. The structure of TTF deviates from being planar as a result of the C-S-C bond angle in the five-membered dithiole ring which favors an angle of 90°.[23] TTF can be easily oxidized to form the respective radical cation and dication in a stepwise manner.[1] After releasing one electron, the yellow-colored neutral TTF is converted to a purple-colored radical cation species, TTF^{+}, which can be further oxidized to form a dark green-colored dicationic species TTF^{2+} after the second electron is taken away (Figure 1.2). The case where sequential single-electron transfers occur twice is known as the normal potential scenario, which is typically observed in multi-step redox reactions when the intermediates are thermodynamically stable.

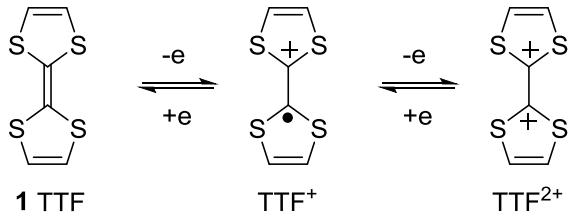

Figure 1.2 Sequential oxidation of TTF.

According to the Hückel's rule, the two dithiole rings in neutral TTF are non-aromatic. In the oxidized state, however, the 1,3-dithiolium ring shows aromaticity and hence deliveries stability under normal conditions.[1] Particularly, dicationic TTF is stabilized by the gaining of double aromaticity, while the destabilizing intramolecular coulombic repulsion between the two closely positioned cationic centers can be minimized by adopting a perpendicular orientation between the two dithiolium units.[8]

One of the more important aspects of these fascinating cationic aromatic species is that they oxidize sequentially and reversibly within a convenient potential window. Oxidation of neutral TTF to its radical cation and dication occur at relatively low oxidation potentials at $E_{½}^{1}$ = +0.34 V and $E_{½}^{2}$ = 0.78 V respectively versus Ag/AgCl in MeCN.[1, 14] Moreover, the oxidation potentials can be modified or tuned through attachment of electron-donating or withdrawing substituents to the backbone of TTF.[14, 24, 25] Specifically, the addition of electron-withdrawing substituents increases the oxidation potentials for the entire molecule. In contrast, the opposite trend is observed with the attachment of electron-donating groups. This selective modulation of TTF's oxidation potentials effectively controls the energy gap between the highest occupied molecular orbital (HOMO) and lowest unoccupied molecular orbital (LUMO). Owing to its high-lying HOMO, TTF is often conjugated with electron acceptors with low-lying LUMOs to generate "ensembles" for the preparation of low-bandgap organic semiconductors.[26-28] Although in theory any moiety can act as both electron donor and electron acceptor, electrochemically amphoteric molecules are kind of rare in practice. The difficulty stems from the fact that molecules that typically display this characteristic behavior do not have easily accessible potential windows or do not form stable redox states.[14, 25] Molecules that do exhibit this type of behavior also tend to have a high degree of π-conjugation or exist as donor-acceptor pairs.

TTF also demonstrates distinctive UV-Vis absorption properties in its neutral state as well as its two oxidized states. Furthermore it readily forms dimers, highly ordered stacking motifs, two-dimensional sheets stabilized by π–π interactions, and non-covalent

sulfur–sulfur contact.[29-31] Lastly, TTF is fairly robust as a result of its thermodynamic stability, which renders it an attractive material for many synthetic transformations. One of the only notable downsides to TTF is its sensitivity towards strongly acidic conditions and strongly oxidizing environments.[17, 32-34]

1.3 Synthetic Routes to TTF

The synthetic chemistry of TTF has been highly developed since its debut in the early 1970s. For nearly 40 years, a vast array of synthetic methods for TTF and TTF derivatives has been investigated and established.[1, 14] Several of these methods have been thoroughly reviewed in the literature by experts in the fields of organic synthesis, heterocyclic chemistry, materials chemistry, and sulfur chemistry. Today one can easily find a paper in an important chemistry journal related to TTF-based science, even though the topic of TTF synthesis continues to receive updates as well as improvements to the current methodologies; in particular, the synthetic routes to the parent TTF structure as well as its two most significant precursors, the thione and dithiolium salt. The commonly used synthetic routes to these specific targets are briefly outlined in Figures 1.3 and 1.4 respectively.

With copious options available to chemists, the synthesis of TTF is commonly approached by one of three different methods. These methods include but are not limited to phosphite-promoted couplings, base-catalyzed couplings, and Wittig-type olefination reactions.[1, 14, 35, 36] The generally "preferred" methods are outlined in Figure 1.5, which

give facile synthetic access to both symmetric and asymmetric TTF products. In particular, the use of phosphite-based couplings allows TTF to be prepared in relatively high yields with few synthetic steps.

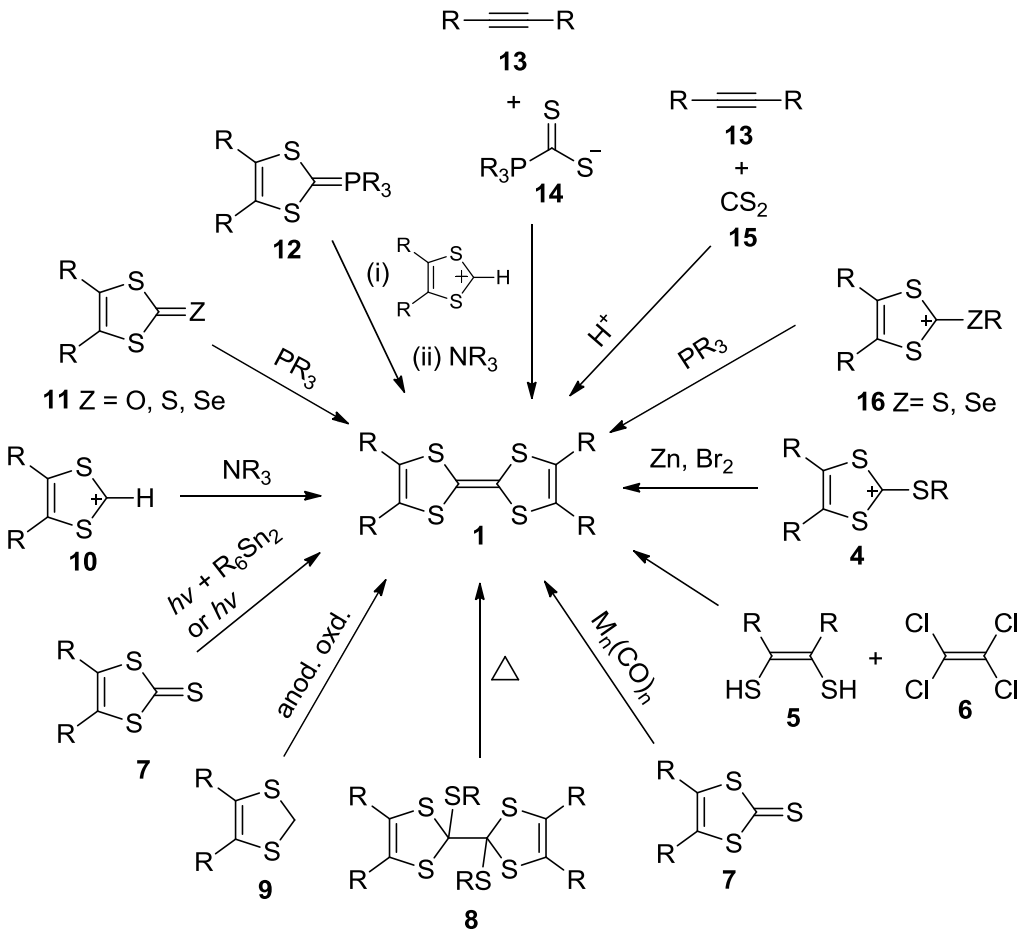

Figure 1.3 Summary of general synthetic methods for preparation of the parent TTF.[14, 37]

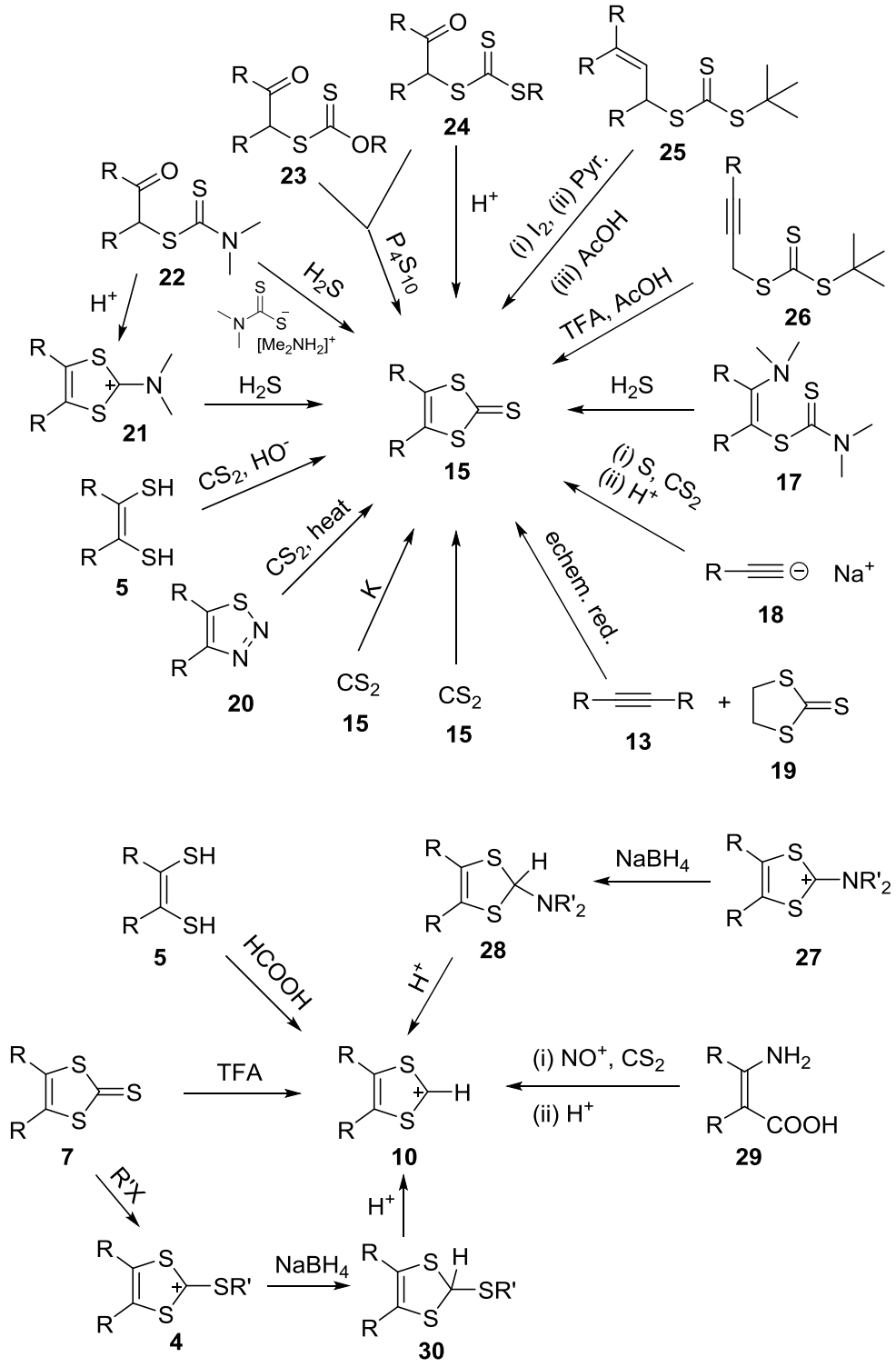

Figure 1.4 Synthetic methods for thione and dithiolium salt precursors.[14, 37]

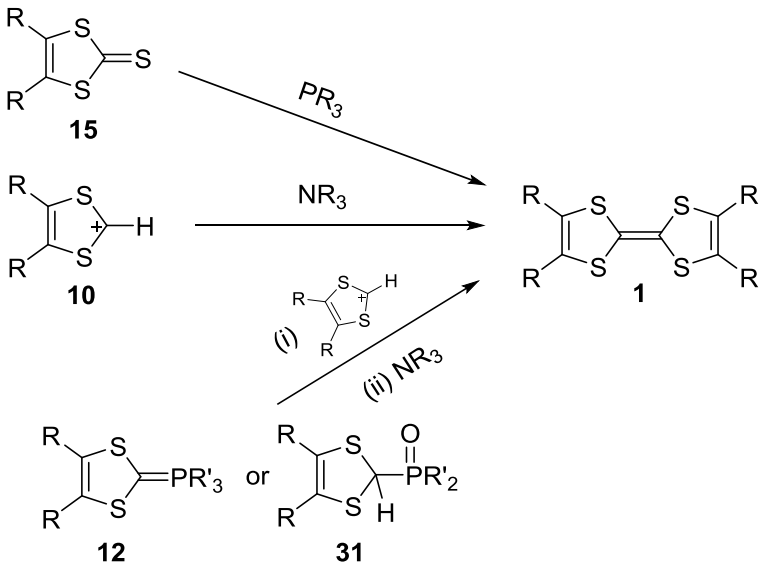

Figure 1.5 Preferred synthetic routes to TTF.

A notable and facile methodology for large-scale production of TTF was developed by Hoyer in 1979.[38] The method capitalizes on cheap and readily available starting materials, i.e. carbon disulfide and alkali metals such as sodium metal. The synthetic sequences involve two key steps: (i) the production of a zinc-coordinated dithiolate salt, and (ii) the addition of an alkyl halide as an electrophile to form the thione product. The details of these synthetic steps are outlined in Figure 1.6 and the mechanism is described in Figure 1.7.[39]

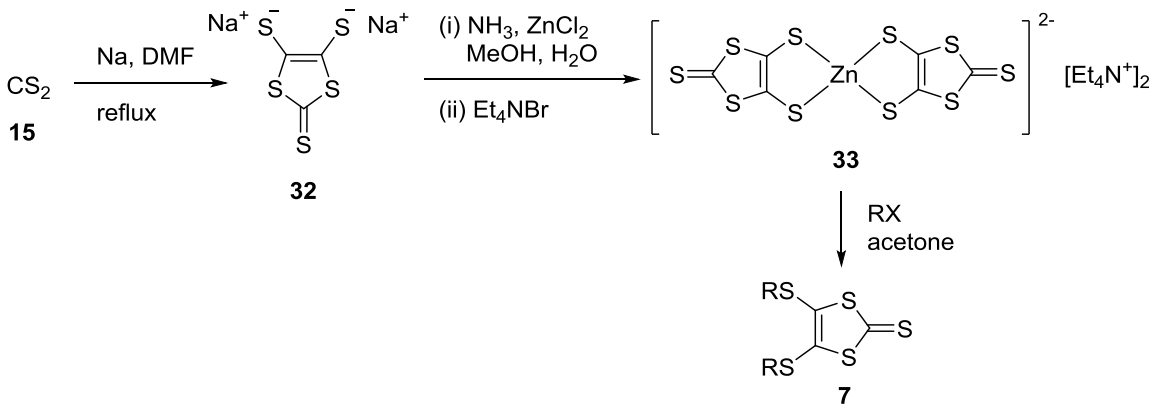

Figure 1.6 An efficient large-scale synthetic method for thione **7**.

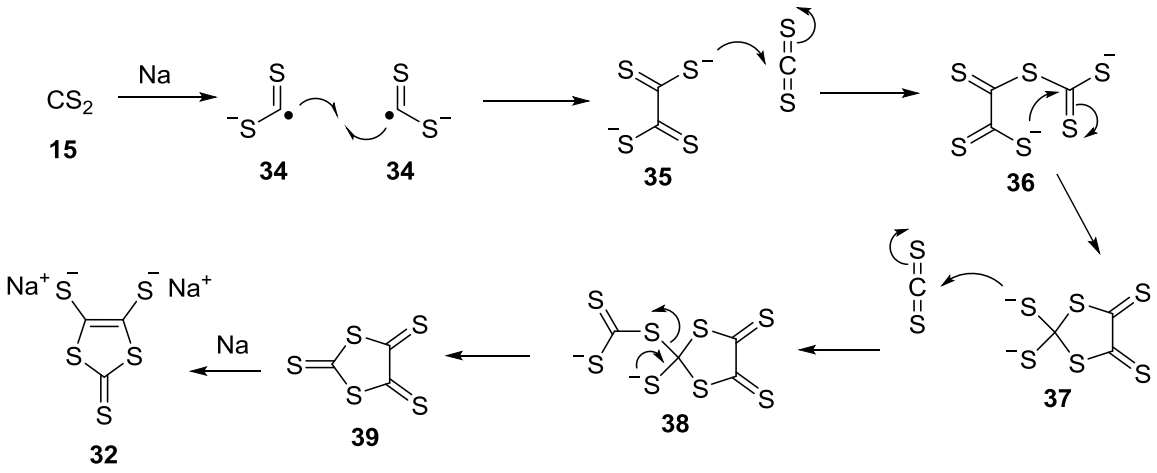

Figure 1.7 Mechanism for the formation of bis(thiolate) precursor **32**.

Collectively these synthetic routes to TTF have allowed a wide range of TTF and related analogues or derivatives to be prepared, which in turn greatly benefited the material design and synthesis in which various TTF components can be conveniently

incorporated into other molecular or macromolecular systems to form meaningful structural and functional materials. Improvement of these methods will fuel up the continuous growth of TTF chemistry and further aid prospective technological development and transfer.

1.4 Applications of TTF

Owing to their unique and appealing electronic and electrochemical properties, TTF and its derivatives have been extensively used as active components in various electronic and optoelectronic applications.[1, 16, 20, 21, 24, 28] Since the number of TTF-based functional materials and devices is enormous and still growing rapidly in the literature, the following section only focuses on a few important examples to illustrate TTF-enabled material design and device fabrication ranging from chemosensors, to molecular machines, to molecular switches.

The first example is a class of crown ether-annulated TTFs **40** and **41** designed by Echegoyen and co-workers (see Figure 1.8).[40] The 18-crown-6 units in these hybrid compounds were designed to serve as cation receptors, and the event of cation binding could be detected by monitoring the changes in the oxidation potentials of adjacent TTF moieties which act as reporters. These sensors were anchored to the surface of gold electrodes through Au-S bonds, forming robust self-assembled monolayers (SAMs). Such features deliver electrochemical sensing function toward various metal cations, and

the sensor systems give extraordinary stability and require rather simple procedures to prepare and operate.

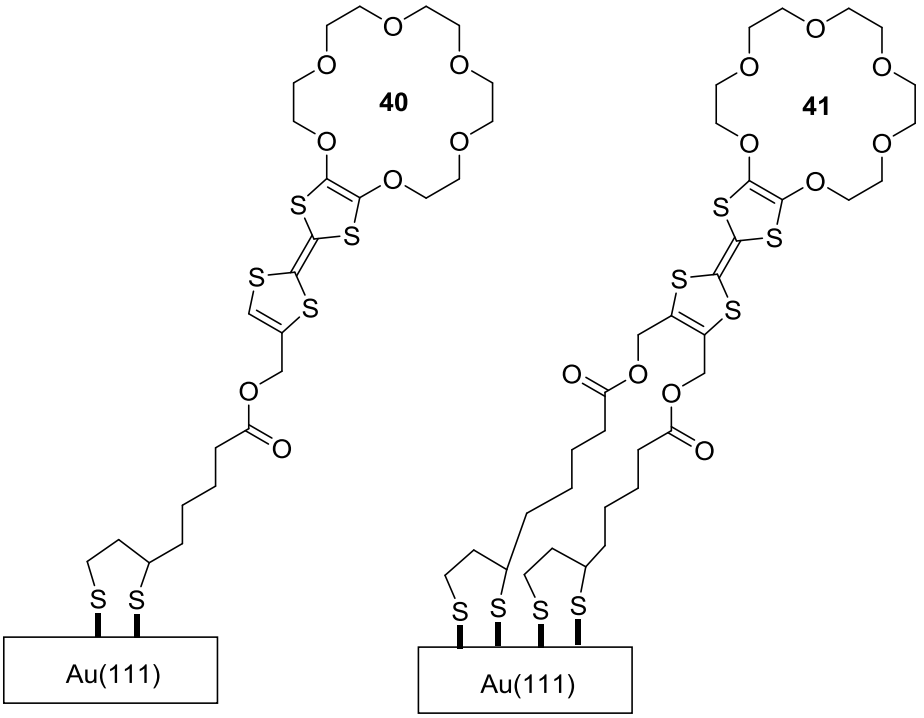

Figure 1.8 SAMs of TTF-crown ether derivatives **40** and **41** as cation sensors.

TTF can be integrated into rotaxane-based structures to achieve the function of "molecular shuttles". For example, Becher and Stoddart reported a TTF-based amphiphilic bistable rotaxane system,[41] which was synthesized as a mixture of two translational isomers, the green-colored form **42** to the red-colored form **43** (Figure 1.9) at room temperature in an approximate ratio of 1:1. The activation energy for the shuttling of the macrocycle unit ($CBPQT^{2+}$) was found to be significant (24kcal/mol). As a result,

the two isomers could be isolated by chromatography and characterized by ^{1}H NMR and UV-Vis spectroscopy to investigate the kinetic properties.

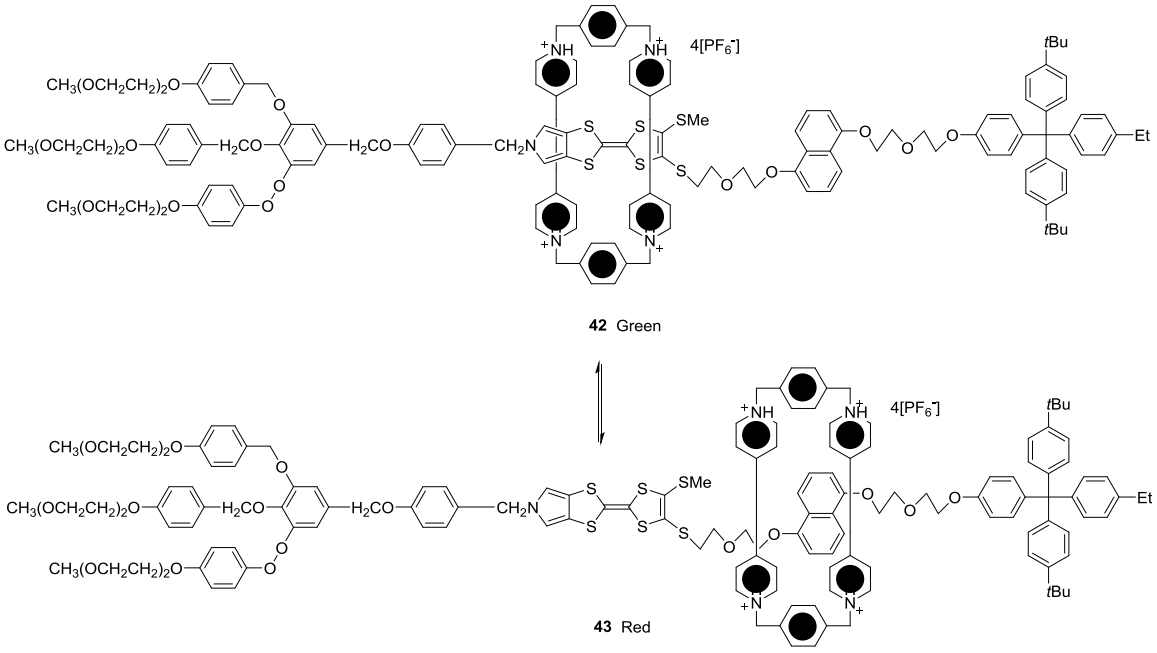

Figure 1.9 A molecular shuttle built on a TTF-based rotaxane.

Prato and Martín in 1996 reported the first class of TTF-C_{60} fullerene dyads (**44**, Figure 1.10),[42] in which the electron-donating TTF moiety is covalently linked to the electron-acceptor C_{60} unit via a C-C bond or vinyl bridges. Absorption of light in these molecules first promoted the C_{60} unit into an excited state, which was followed by a facile intramolecular electron transfer from TTF to C_{60}. Evidence for the electron transfer was established based on steady-state and time-dependent photolysis experiments, and the lifetimes for the charge-separation (CS) states in these systems are in the range of 1-2 ns.

The photophysical properties render these compounds potentially useful candidates for organic photovoltaic materials.

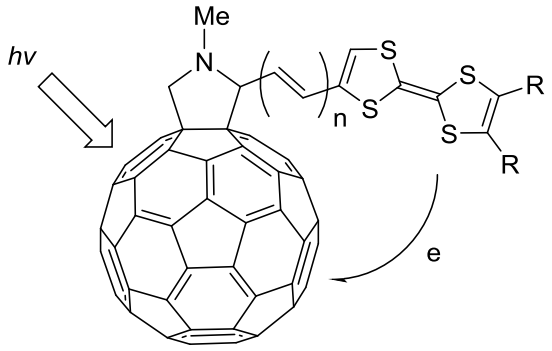

44 R = H, SMe, $(SCH_2)_2$
n = 0, 1, 2

Figure 1.10 TTF-C_{60} based donor/acceptor dyads **44**.

Becher and co-workers prepared a TTF derivative **45** which was directly annulated to a porphyrin chromophore (Figure 11).[43] Compound **45** is almost non-fluorescent as a result of the strong quenching effect provide by the electron-donating TTF unit. The compound, however, can be transformed into a fluorescent species by oxidation of the TTF unit with $FeCl_3$. As such, porphyrin-TTF **45** acts as a fluorescent molecular switch under the control of redox stimuli.

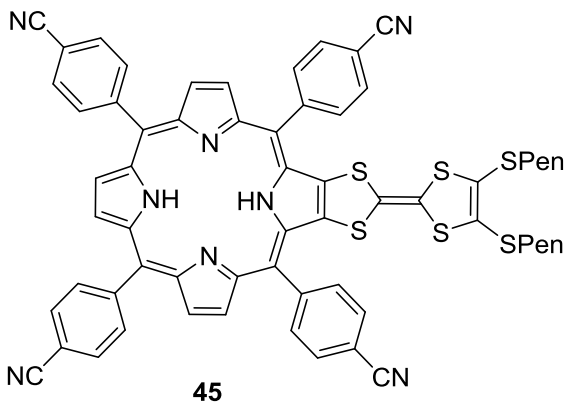

45

Figure 1.11 A porphyrin-annulated TTF **45** functioning as a fluorescent molecular switch.

The selected examples mentioned above only cast a very brief highlight on some of the many applications of TTF. It is worth mentioning that, aside from materials chemistry, the application of TTF has also extended itself into many other disciplines of science and technology. Presently, TTF-oriented research has also led to a considerable development of the so-called π-extended TTF analogues,[14, 15, 44, 45] which in turn offer tremendous promise with respect to the fabrication of novel organic electronic and optoelectronic materials and devices. The following sections thus deal with the fundamental properties and applicability of some important π-extended TTF analogues.

1.5 π-Extended TTFs

With the parent tetrathiafulvalene (TTF) well characterized and understood, a vast array of TTF-derived molecular systems has been reported in the literature. Besides TTF,

the research focus on the expanded TTF frameworks has been gradually taking a central stage in current TTF chemistry; in particular, the past two decades witnessed a surge in the investigations on the family of so-called π-extended TTFs which contain various π-conjugated units (e.g., alkenyl, alkynyl, and aryl) to increase the degree of π-delocalization between the two dithiole rings. Structurally, the π-extension can be achieved by having π-units either inserted between the two dithiole rings of TTF or annulated with the dithiole rings. Primarily there are two common types of exTTFs, those with vinylene and those with acene-type spacers. One notable example of exTTFs contains an anthraquinoid (AQ) central bridge between the two dithiole rings， and hence they are often referred to as TTFAQs.[14, 46-48] A representative structure, TTFAQ **46**, is shown in Figure 1.12. This molecule in the neutral state adopts a saddle shape or butterfly-like conformation. Instead of the normal potential scenario (*i.e.*, $E_{ox}^{1} < E_{ox}^{2}$) observed in the parent TTF, the oxidation of TTFAQ directly leads to the formation of dicationic TTFAQ.[48] This type of oxidation is known as an inverted potential (*i.e.*, $E_{ox}^{1} > E_{ox}^{2}$) scenario, which is associated with a dramatic structural change within the molecule as shown in Figure 1.12.[14] In the neutral state, the TTFAQ takes a saddle-like geometry, while in the dicationic state the central anthracene becomes planar and the two dithiolium rings rotate to a perpendicular orientation with respect to the central anthracene unit.[14, 49]

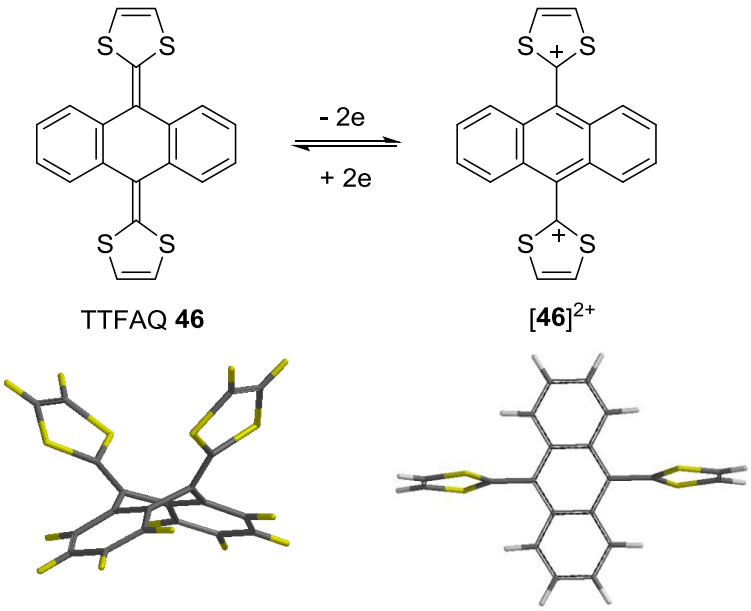

Figure 1.12 Redox reaction of TTFAQ **46** and conformational changes associated with it.

It is important to note that, upon oxidation, both the dithiole rings and the central anthracene become aromatic. The resulting $[TTFAQ]^{2+}$ adopts a conformation to minimize *peri*-hydrogen interactions as well as to maximize π-conjugation.[14] The unusually strong gain in aromaticity displayed during the two-electron oxidation of TTFAQ makes the TTFAQ dication possess a lower oxidation potential than that of the TTFAQ radical cation (~200 mV lower). This is a significant factor behind the fascinating electrochemical phenomenon known as inverted potential.[14, 50] This type of electrochemical behavior makes TTFAQ an excellent electron donor and, moreover, the saddle-like conformation of TTFAQ in the neutral state creates a unique π-concavity that

is suitable to act as the receptor for certain large spherical π-conjugated molecules, such as buckminsterfullerenes.

Through the insertion of a vinyl spacer between the two dithiole rings another type of ex-TTFs is formed. This new type of ex-TTFs is commonly referred to as tetrathiafulvalene vinylogues (TTFVs) or vinylogous tetrathiafulvalenes in the literature.[51-53] The early work on TTFVs was focused on their improved electron-donating properties compared to TTF, because the extended vinyl bridge reduces the Columbic repulsion between the two dithiolium rings in the oxidized states.[53] Typically, unsubstituted TTFV **47** takes a planar transoid conformation in the neutral state (Figure 1.13). TTFV **47** favors to lose two electrons sequentially under chemical or electrochemical conditions to form radical cation $\mathbf{47}^{+}$ and dication $\mathbf{47}^{2+}$, respectively, while its *trans* conformation remains unchanged during the oxidation steps. In contrast, the conformation of aryl (particularly phenyl) substituted TTFVs (e.g. **48** in Figure 1.13) prefers a *pseudo-cis* conformation in the neutral state. The dihedral bond angle between the two vinyl units varies significantly depending on the steric demands and other intramolecular interactions between the aryl rings. Aryl-substituted TTFV **48** undergoes a simultaneous two-electron transfer, an electrochemical behavior similar to that of TTFAQ (i.e. inverted potential), and the resulting aryl-TTFV dication dramatically changes the conformation to a *trans* geometry due to the strong electrostatic repulsion between the two positively charged dithiolium rings (see Figure 1.13).

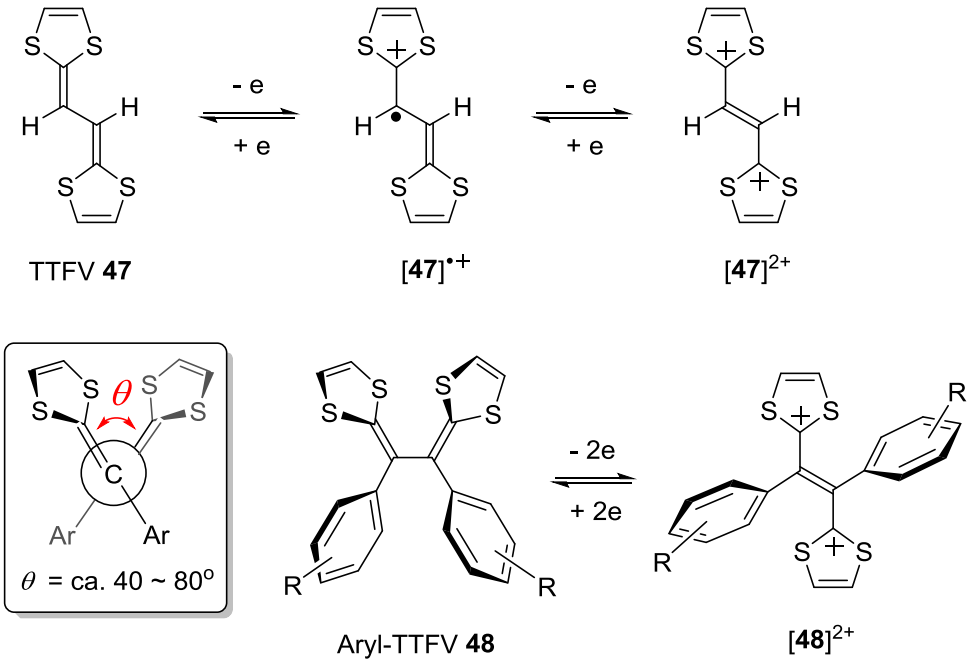

Figure 1.13 TTFV substituent effects on oxidation.

The skeletons of aryl-substituted TTFVs can be constructed by various synthetic methods.[54-57] The most commonly used one is the oxidative dimerization of corresponding aryl-dithiafulvene (DTF) precursors. Figure 1.14 illustrates the general mechanism for such type of reactions. In general, the dimerization reaction begins with the DTF precursor being oxidized into a radical cation by an oxidant (step I, Figure 1.14).[58, 59] As the concentration of the DTF radical cation builds up, a bimolecular reaction follows (step II, Figure 1.14), in which two molecules of DTF radical are combined via a new C-C bond formation process. The resulting dication intermediate then undergoes a double deprotonation (step III, Figure 1.14) to yield the TTFV product, which would then be quickly oxidized into TTFV dication under the oxidative reaction

environment. Once the dimerization is accomplished, a reductive workup is performed to regenerate the desired neutral TTFV product (step V, Figure 1.14).

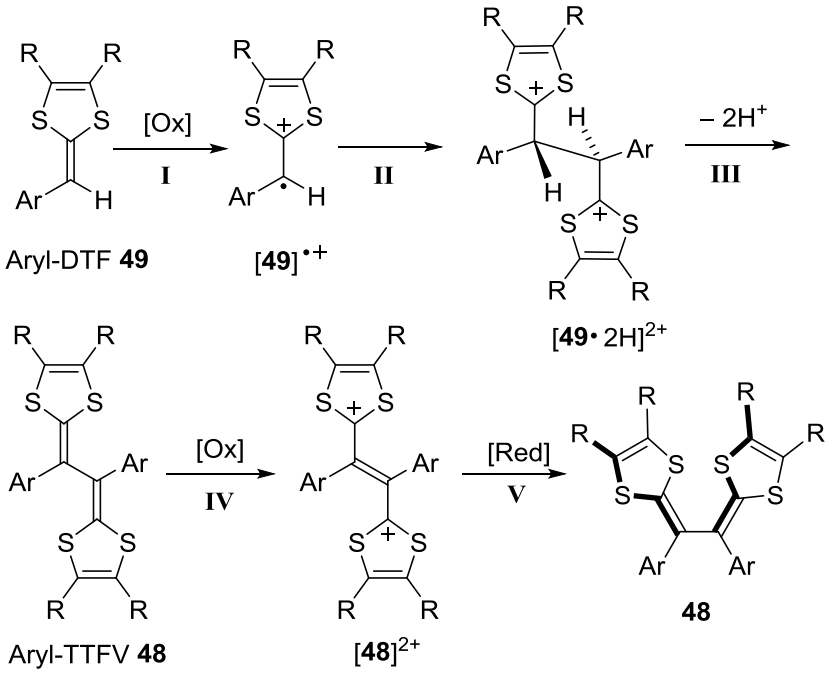

Figure 1.14 General mechanism for oxidative dimerization of an aryl-substituted DTF.

1.6 Applications of ex-TTFs in Molecular Devices

With their extended π-surface and excellent electron donating properties, it is no surprise that various ex-TTFs have been extensively used in the development of molecular and supramolecular systems with novel electronic and optoelectronic functions.[15, 17, 25, 53] Specifically the application of ex-TTFs into guest-host type molecular recognition has attracted significant attention in recent years. Guest-host chemistry in general deals with the complexation of a guest molecule with a suitable host molecule

through noncovalent attraction, such as π-π stacking, van der Waals forces, and hydrogen bonding. The guest and host molecules have to be complementary in either shapes (e.g. concave/convex interaction) or electronic nature (e.g. donor-acceptor interaction). This renders certain ex-TTFs perfect candidates for forming guest-host complexes with spherical shaped nanocarbons, such as fullerenes. Martín and co-workers in 2006 reported a type of bis(TTFAQ)-based molecular tweezers **50** (Figure 1.15),[44] which can form a 1:1 complex with C_{60} fullerene in chlorobenzene. The binding constant was measured to be 2.98×10^3 M^{-1}. When the solvent system was switched to $CHCl_3/CS_2$, however, the complexation behavior was dramatically changed to a stepwise 2:1 and 2:2 binding mode.

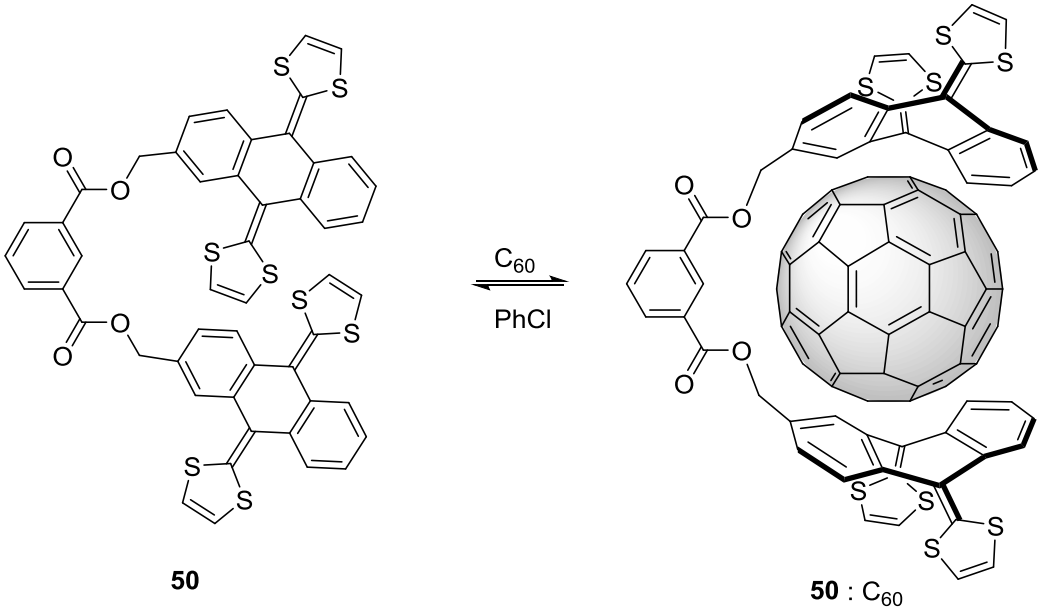

Figure 1.15 Complexation of C_{60} with bis(TTFAQ) **50**.

Mulla and Zhao recently synthesized a class of TTFV-based molecular tweezers **51** and macrocycle **52** (see Figure 1.16) using Cu-catalyzed alkyne azide coupling as the key synthetic step.[60] Compound **51** was found to selectively bind to C_{70} fullerene in the presence of an excess amount of C_{60}, while macrocycle **52** can effectively complex with either C_{60} or C_{70} fullerene at 1:1 and 1:2 ratios. For both compounds, the binding with fullerenes results in notable enhancement of fluorescence emission. Hence these compounds can be used as efficient fluorescent sensors for fullerenes.

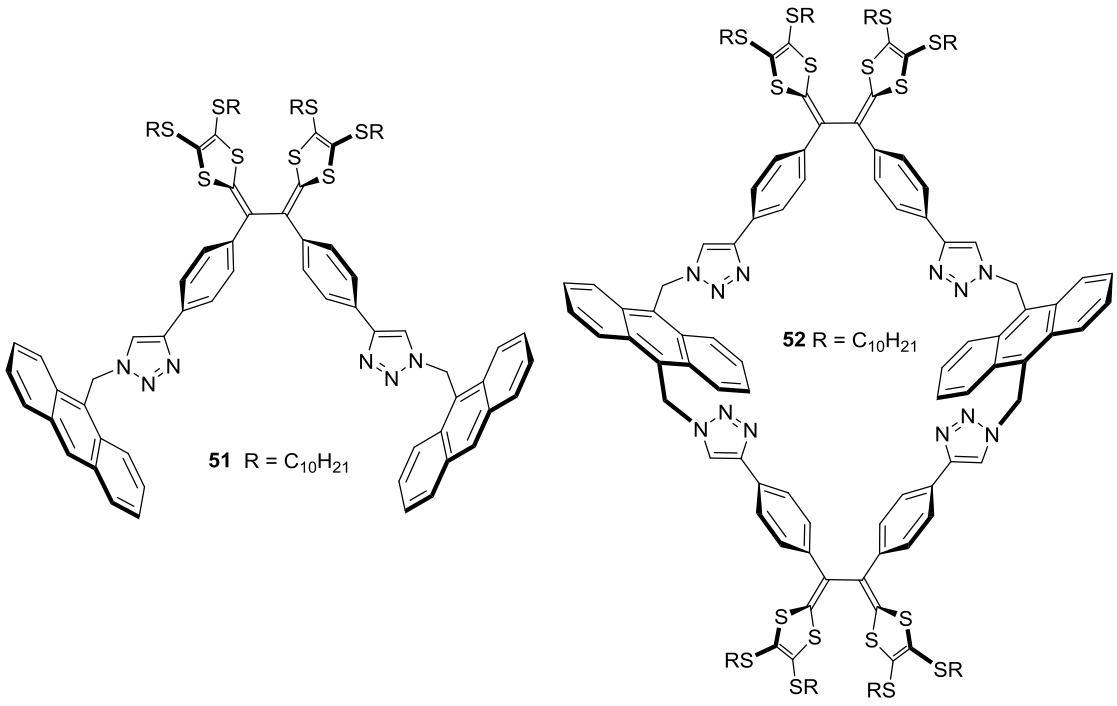

Figure 1.16 TTFV-based molecular tweezers **51** and macrocycle **52**.

In 2014, the Zhao and Adronov groups collaboratively investigated a class of TTFV-fluorene co-polymer **53**, which show controlled reversible interactions with single-walled

carbon nanotubes (SWNTs).[61] In the neutral state, the polymer adopts a folded conformation to wrap around the carbon nanotube through π-stacking (Figure 1.17). The polymer-SWNT supramolecular complexes form stable suspension in typical organic solvents. Upon addition of a strong organic acid, trifluoroacetic acid (TFA), the TTFV moieties in the polymer can be protonated to change into a *trans* conformation. As such the entire polymer backbone is unfolded and detached from the carbon nanotube, giving released pristine SWNTs free of the polymer. This method may be useful for device applications where pure SWNTs are desired after solution-phase processing with polymer dispersants.

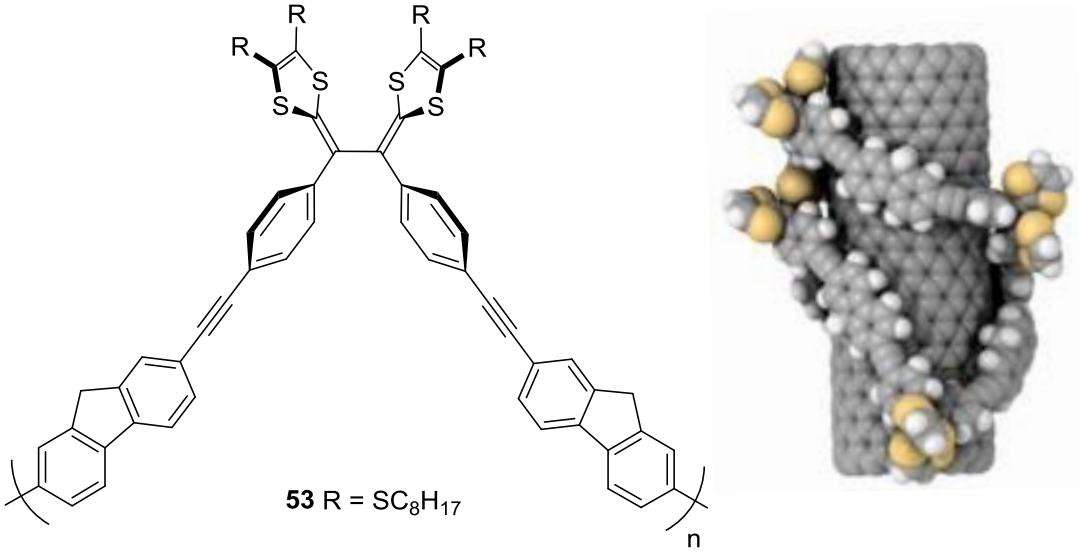

Figure 1.17 The structure of TTFV-fluorene polymer **53** (left) and calculated model of **53** wrapping around a SWNT (right).

Aside from the examples mentioned above, ex-TTFs and related analogues have also been widely applied in many other areas of science and technology, ranging from the development of artificial photosynthetic systems, to supramolecular assemblies, to molecular logic gates and clips to fabrication of electrochromic and non-linear optical devices, just to name a few. More details can be found in a number of important review articles.[14, 16, 17, 19, 53, 62, 63]

1.7 Outline of This Thesis

With a vast array of TTF-based systems reported in the literature, it is important to develop an in-depth understanding of how the fundamental properties and reactivity of TTF derivatives are affected by molecular structures, degree of π-conjugation, and substituent effect. Acquisition of this knowledge will be greatly helpful in the design and preparation of new π-extended TTF derivatives with enhanced or unprecedented properties for various applications.

This thesis work is particularly focused on investigating the synthesis and properties of tetrarthiafulvalene vinylogues (TTFVs). In Chapter 2, the synthesis of a group of aryl-substituted dithiafulvenes (DTFs) is described. These compounds serve as the precursors to corresponding TTFV systems, while iodine-induced oxidative dimerization is used as the key synthetic method. In addition, a class of alkynyl-substituted exTTFs is prepared via the Pd/Cu-catalyzed cross coupling and homocoupling methodologies. In Chapter 3, the structure, electronic, and redox properties of the synthesized TTFVs and related

compounds are investigated by single-crystal X-ray diffraction (XRD) analysis, UV-Vis spectroscopy, and cyclic voltammetry. Some of the experimental results can be reasonably correlated with the structural and electronic effects imposed by substituent groups attached to the TTFV group, providing some understanding of the structure-property relationship. Finally, in Chapter 4 a summary of the entire thesis work is provided and new directions that may lead to more intriguing TTFV-based nanomaterials and devices are discussed.

1.8 References

1. Yamada, J.-i.; Sugimoto, T., *TTF Chemistry: Fundamentals and Applications of Tetrathiafulvalene*. Springer-Verlag: Berlin, 2004.

2. Jorgensen, T.; Hansen, T. K.; Becher, J., Tetrathiafulvalenes as Building-Blocks in Supramolecular Chemistry. *Chem. Soc. Rev.* **1994**, *23*, 41-51.

3. Hurtley, W. R. H.; Smiles, S., CCXLI.-ortho-Dithiolbenzene. *J. Chem. Soc.* **1926**, *129*, 1821-1828.

4. Hurtley, W. R. H.; Smiles, S., CCXCIX.-2 : 2'-Bis-1 : 3-benzdithiolene. *J. Chem. Soc.* **1926**, *129*, 2263-2270.

5. Prinzbach, H.; Berger, H.; Lüttringhaus, A., Proton Activity of the 1,3-Dithiolium System. *Angew. Chem., Int. Ed. Engl.* **1965**, *4*, 435-435.

6. Wudl, F.; Smith, G. M.; Hufnagel, E. J., Bis-1,3-dithiolium Chloride: An Unusually Stable Organic Radical Cation. *J. Chem. Soc. D: Chem. Commun.* **1970**, 1453-1454.

7. Zahradník, R.; Čársky, P.; Hünig, S.; Kiesslich, G.; Scheutzow, D., Conjugated Radicals. VII. Tetrathiofulvalene and a Note on Sulfur-Containing Conjugated Radicals. *Int. J. Sulfur Chem. Part C* **1971**, *6*, 109-122.

8. Coffen, D. L.; Chambers, J. Q.; Williams, D. R.; Garrett, P. E.; Canfield, N. D., Tetrathioethylenes. *J. Am. Chem. Soc.* **1971**, *93*, 2258-2268.

9. Wudl, F.; Wobschall, D.; Hufnagel, E. J., Electrical Conductivity by the Bis(1,3-dithiole)-bis(1,3-dithiolium) System. *J. Am. Chem. Soc.* **1972**, *94*, 670-672.

10. Ferraris, J.; Cowan, D. O.; Walatka, V.; Perlstein, J. H., Electron Transfer in a New Highly Conducting Donor-Acceptor Complex. *J. Am. Chem. Soc.* **1973**, *95*, 948-949.

11. Coleman, L. B.; Cohen, M. J.; Sandman, D. J.; Yamagishi, F. G.; Garito, A. F.; Heeger, A. J., Superconducting Fluctuations and the Peierls Instability in an Organic Solid. *Solid State Commun.* **1973**, *12*, 1125-1132.

12. Andrieux, A.; Duroure, C.; Jérome, D.; Bechgaard, K., The Metallic State of the Organic Conductor TMTSF-DMTCNQ at Low Temperature under Pressure. *J. Phys. Lett.* **1979**, *40*, 381-383.

13. Jérome, D.; Mazaud, A.; Ribault, M.; Bechgaard, K., Superconductivity in a Synthetic Organic Conductor $(TMTSF)_2PF_6$. *J. Phys. Lett.* **1980**, *41*, 95-98.

14. Bendikov, M.; Wudl, F.; Perepichka, D. F., Tetrathiafulvalenes, Oligoacenenes, and Their Buckminsterfullerene Derivatives: The Brick and Mortar of Organic Electronics. *Chem. Rev.* **2004**, *104*, 4891-4946.

15. Brunetti, F. G.; Lopez, J. L.; Atienza, C.; Martin, N., π-Extended TTF: a Versatile Molecule for Organic Electronics. *J. Mater. Chem.* **2012**, *22*, 4188-4205.

16. Segura, J. L.; Martín, N., New Concepts in Tetrathiafulvalene Chemistry. *Angew. Chem. Int. Ed.* **2001**, *40*, 1372-1409.

17. Canevet, D.; Salle, M.; Zhang, G.; Zhang, D.; Zhu, D., Tetrathiafulvalene (TTF) Derivatives: Key Building-Blocks for Switchable Processes. *Chem. Commun.* **2009**, 2245-2269.

18. Pouget, J., P.; Ravy, S., Structural Aspects of the Bechgaard Salts and Related Compounds. *J. Phys. I France* **1996**, *6*, 1501-1525.

19. Yamada, J.-i.; Akutsu, H.; Nishikawa, H.; Kikuchi, K., New Trends in the Synthesis of π-Electron Donors for Molecular Conductors and Superconductors. *Chem. Rev.* **2004**, *104*, 5057-5084.

20. Mori, T., Organic Conductors with Unusual Band Fillings. *Chem. Rev.* **2004**, *104*, 4947-4970.

21. Enoki, T.; Miyazaki, A., Magnetic TTF-Based Charge-Transfer Complexes. *Chem. Rev.* **2004**, *104*, 5449-5478.

22. Shibaeva, R. P.; Yagubskii, E. B., Molecular Conductors and Superconductors Based on Trihalides of BEDT-TTF and Some of Its Analogues. *Chem. Rev.* **2004**, *104*, 5347-5378.

23. Pou-Amérigo, R.; Ortí, E.; Merchán, M.; Rubio, M.; Viruela, P. M., Electronic Transitions in Tetrathiafulvalene and Its Radical Cation: A Theoretical Contribution. *J. Phys. Chem. A* **2001**, *106*, 631-640.

24. Bryce, M. R., Tetrathiafulvalenes as π-Electron Donors for Intramolecular Charge-Transfer Materials. *Adv. Mater.* **1999**, *11*, 11-23.

25. Roncali, J., Linearly Extended π-Donors: When Tetrathiafulvalene Meets Conjugated Oligomers and Polymers. *J. Mater. Chem.* **1997**, *7*, 2307-2321.

26. Brisset, H.; Thobie-Gautier, C.; Jubault, M.; Gorgues, A.; Roncali, J., Small Bandgap Molecular Semiconductors Based on Rigidified Tetrathiafulvalene-Bithiophene Hybrid Conjugated Systems. *J. Chem. Soc., Chem. Commun.* **1994**, 1765-1766.

27. Martín, N.; Sánchez, L.; Herranz, M. Á.; Illescas, B.; Guldi, D. M., Electronic Communication in Tetrathiafulvalene (TTF)/C_{60} Systems: Toward Molecular Solar Energy Conversion Materials? *Acc. Chem. Res.* **2007**, *40*, 1015-1024.

28. Dong, H.; Wang, C.; Hu, W., High Performance Organic Semiconductors for Field-Effect Transistors. *Chem. Commun.* **2010**, *46*, 5211-5222.

29. Yoshizawa, M.; Kumazawa, K.; Fujita, M., Room-Temperature and Solution-State Observation of the Mixed-Valence Cation Radical Dimer of Tetrathiafulvalene, $[(TTF)_2]^{+\bullet}$, within a Self-Assembled Cage. *J. Am. Chem. Soc.* **2005**, *127*, 13456-13457.

30. Tachikawa, T.; Izuoka, A.; Kumai, R.; Sugawara, T.; Sugawara, Y., Preparation and Properties of Double-Bridged BEDT-TTF Dimer and Its Perchlorate Salt. *Solid State Commun.* **1992**, *82*, 19-22.

31. Bozio, R.; Zanon, I.; Girlando, A.; Pecile, C., Vibrational Spectroscopy of Molecular Constituents of One-dimensional Organic Conductors. Tetrathiofulvalene (TTF), TTF^+, and $(TTF^+)_2$ Dimer. *J. Chem. Phys.* **1979**, *71*, 2282-2293.

32. Farnia, G.; Sandonà, G.; Marcuzzi, F., Formation of Non-stoichiometric Salts of Tetrathiafulvalene in An Acidic Medium. *Adv. Mater.* **1996**, *8*, 742-745.

33. Kobayashi, Y.; Yoshioka, M.; Saigo, K.; Hashizume, D.; Ogura, T., Hydrogen-Bonding-Assisted Self-Doping in Tetrathiafulvalene (TTF) Conductor. *J. Am. Chem. Soc.* **2009**, *131*, 9995-10002.

34. Nielsen, M. B.; Sauer, S. P. A., On the Aromaticity of Tetrathiafulvalene Cations. *Chem. Phys. Lett.* **2008**, *453*, 136-139.

35. Gorgues, A.; Hudhomme, P.; Sallé, M., Highly Functionalized Tetrathiafulvalenes: Riding along the Synthetic Trail from Electrophilic Alkynes. *Chem. Rev.* **2004**, *104*, 5151-5184.

36. Fabre, J. M., Synthesis Strategies and Chemistry of Nonsymmetrically Substituted Tetrachalcogenafulvalenes. *Chem. Rev.* **2004**, *104*, 5133-5150.

37. Schukat, G.; Richter, A. M.; Fanghänel, E., Synthesis, Reactions, and Selected Physico-Chemical Properties of 1,3-and 1,2-Tetrachalcogenafulvalenes. *Sulfur Reports* **1987**, *7*, 155-231.

38. Steimecke, G.; Sieler, H.-J.; Kirmse, R.; Hoyer, E., 1.3-Dithio-2-Thion-4.5-Dithiolat Aus Schwefelkphlenstoff Und Alkalimetall. *Phosphorus and Sulfur and the Related Elements* **1979**, *7*, 49-55.

39. Svenstrup, N.; Becher, J., The Organic Chemistry of 1,3-Dithiole-2-thione-4,5-dithiolate (DMIT). *Synthesis* **1995**, *1995*, 215-235.

40. Liu, H.; Liu, S.; Echegoyen, L., Remarkably Stable Self-assembled Monolayers of New Crown-Ether Annelated Tetrathiafulvalene Derivatives and Their Cation Recognition Properties. *Chem. Commun.* **1999**, 1493-1494.

41. Jeppesen, J. O.; Perkins, J.; Becher, J.; Stoddart, J. F., Slow Shuttling in an Amphiphilic Bistable [2]Rotaxane Incorporating a Tetrathiafulvalene Unit. *Angew. Chem. Int. Ed.* **2001**, *40*, 1216-1221.

42. Martín, N.; Sánchez, L.; Seoane, C.; Andreu, R.; Garín, J.; Orduna, J., Semiconducting Charge Transfer Complexes from [60]Fullerene-Tetrathiafulvalene (C_{60}-TTF) Systems. *Tetrahedron Lett.* **1996**, *37*, 5979-5982.

43. Li, H.; Jeppesen, J. O.; Levillain, E.; Becher, J., A mono-TTF-annulated Porphyrin as a Fluorescence Switch. *Chem. Commun.* **2003**, 846-847.

44. Pérez, E. M.; Sánchez, L.; Fernández, G.; Martín, N., exTTF as a Building Block for Fullerene Receptors. Unexpected Solvent-Dependent Positive Homotropic Cooperativity. *J. Am. Chem. Soc.* **2006**, *128*, 7172-7173.

45. Frere, P.; Skabara, P. J., Salts of Extended Tetrathiafulvalene Analogues: Relationships Between Molecular Structure, Electrochemical Properties and Solid State Organisation. *Chem. Soc. Rev.* **2005**, *34*, 69-98.

46. Moore, A. J.; Bryce, M. R., Generation and Trapping of Phosphorus Stabilized 4,5-Ethylenedithio-1,3-dithiol-2-ide Carbanions: Synthesis of Ethylenedithio-1,3-dithiafulvalenes. *Synthesis* **1991**, *1991*, 26-28.

47. Akiba, K.-y.; Ishikawa, K.; Inamoto, N., Synthesis of 1,4-Dithiafulvenes and 1,4-Dithiafulvalenes by Carbonyl Olefination Using 2-Dimethoxyphosphinyl-1,3-benzodithiole. *Bull. Chem. Soc. Jpn.* **1978**, *51*, 2674-2683.

48. Bryce, M. R.; Moore, A. J., A New Highly-conjugated TTF Analogue: Synthesis, Electrochemistry and a Conducting TCNQ Complex of 9,10-Anthracenediylidene-2,2′-bis(4,5-dimethyl-1,3-dithiole). *Synth. Met.* **1988**, *25*, 203-205.

49. Bryce, M. R.; Coffin, M. A.; Hursthouse, M. B.; Karaulov, A. I.; Müllen, K.; Scheich, H., Synthesis, X-ray Crystal Structure and Multistage Redox Properties of a Severely-distorted Tetrathiafulvalene Donor. *Tetrahedron Lett.* **1991**, *32*, 6029-6032.

50. Perepichka, D. F.; Bryce, M. R.; Perepichka, I. F.; Lyubchik, S. B.; Christensen, C. A.; Godbert, N.; Batsanov, A. S.; Levillain, E.; McInnes, E. J. L.; Zhao, J. P., A (π-

Extended Tetrathiafulvalene)−Fluorene Conjugate. Unusual Electrochemistry and Charge Transfer Properties: The First Observation of a Covalent D^{2+}−σ−$A^{\bullet-}$ Redox State. *J. Am. Chem. Soc.* **2002**, *124*, 14227-14238.

51. Yamashita, Y.; Tomura, M.; Badruz Zaman, M., Synthesis and Properties of Novel Tetrathiafulvalene Vinylogues. *Chem. Commun.* **1998**, 1657-1658.

52. Guerro, M.; Lorcy, D., A Simple Route to Novel Functionalized Tetrathiafulvalene Vinylogues. *Tetrahedron Lett.* **2005**, *46*, 5499-5502.

53. Zhao, Y.; Chen, G.; Mulla, K.; Mahmud, I.; Liang, S.; Dongare, P.; Thompson, D. W.; Dawe, L. N.; Bouzan, S., Tetrathiafulvalene Vinylogues as Versatile Building Blocks for New Organic Materials. *Pure & Appl. Chem.* **2012**, *84*, 1005-1025.

54. Sugimoto, T.; Awaji, H.; Sugimoto, I.; Misaki, Y.; Kawase, T.; Yoneda, S.; Yoshida, Z.; Kobayashi, T.; Anzai, H., Ethylene Analogs of Tetrathiafulvalene and Tetraselenafulvalene: New Donors for Organic Metals. *Chem. Mater.* **1989**, *1*, 535-547.

55. Hansen, T. K.; Lakshmikantham, M. V.; Cava, M. P.; Metzger, R. M.; Becher, J., Synthesis and Properties of New p-Donor Sulfur Heterocycles. *J. Org. Chem.* **1991**, *56*, 2720-2722.

56. Moore, A. J.; Bryce, M. R.; Batsanov, A. S.; Green, A.; Howard, J. A. K.; McKervey, A.; McGuigan, P.; Ledoux, I.; Orti, E.; Viruela, R.; Viruela, P. M.; Tarbit, B., New 1,3-Dithiol-2-ylidene Donor-p-Acceptor Chromophores with Intramolecular Charge-Transfer Properties, and Related Donor-p-Donor Molecules: Synthesis, Electrochemistry, X-ray Crystal Structures, Non-linear Optical Properties and Theoretical Calculations. *J. Mater. Chem.* **1998**, *8*, 1173-1184.

57. Bryce, M. R.; Coffin, M. A.; Clegg, W., New Vinylogous Tetrathiafulvalene p-Electron Donors with Peripheral Alkylseleno Substitution. *J. Org. Chem.* **1992**, *57*, 1696-1699.

58. Hapiot, P.; Lorcy, D.; Tallec, A.; Carlier, R.; Robert, A., Mechanism of Dimerization of 1,4-Dithiafulvenes into TTF Vinylogues. *J. Phys. Chem.* **1996**, *100*, 14823-14827.

59. Carlier, R.; Hapiot, P.; Lorcy, D.; Robert, A.; Tallec, A., Electrosynthesis and Redox Behavior of Vinylogous TTF Displaying Strong Conformational Changes Associated with Electron Transfers. *Electrochim. Acta* **2001**, *46*, 3269-3277.

60. Mulla, K.; Shaik, H.; Thompson, D. W.; Zhao, Y., TTFV-Based Molecular Tweezers and Macrocycles as Receptors for Fullerenes. *Org. Lett.* **2013**, *15*, 4532-4535.

61. Liang, S.; Zhao, Y.; Adronov, A., Selective and Reversible Noncovalent Functionalization of Single-Walled Carbon Nanotubes by a pH-Responsive Vinylogous Tetrathiafulvalene–Fluorene Copolymer. *J. Am. Chem. Soc.* **2013**, *136*, 970-977.

62. Bryce, M. R., Functionalised Tetrathiafulvalenes: New Applications as Versatile π-Electron Systems in Materials Chemistry. *J. Mater. Chem.* **2000**, *10*, 589-598.

63. Nielsen, M. B.; Lomholt, C.; Becher, J., Tetrathiafulvalenes as Building Blocks in Supramolecular Chemistry II. *Chem. Soc. Rev.* **2000**, *29*, 153-164.

Chapter 2 Synthesis of Aryl-Substituted TTFV Derivatives

2.1 Introduction

As briefly introduced in Chapter 1, the unique redox activity and switching properties of an intriguing class of π-extended TTF analogues, namely tetrathiafulvene vinylogues (TTFVs), has prompted a surging interest over the past few years in using them as molecular building blocks for nanoscale electronic and optoelectronic materials/devices.[1] The initial interest in TTFVs began in the mid 1980s, when Yoshida and co-workers[2] first reported the synthesis and characterization of 2,2'-ethanediylidenebis(1,3-dithiole) **54** (Figure 2.1). The study soon sparked an active pursuit for analogous π-extended TTFV systems; for example, compounds **54**-**57** (Figure 1) were reported by the groups of Yoshita,[3] Bryce,[4, 5] Misaki,[6] and Becher[7] from the late 1980s to the late 1990s. In their studies, much characterization efforts have been dedicated to determining the single-crystal structures and measuring the conductivity of the charge-transfer (C-T) complexes between the TTFVs and other organic electron-acceptors (e.g. TCNQ). These TTFVs were found to act as better electron donors than TTF, owing to their extended π-framework and reduced on-site coulombic repulsion. Structurally, the TTFVs without any substituents attached to the vinylic positions favor a planar, *s*-trans

conformation in both the neutral and oxidized (cation and dication) states. Electrochemically, the TTFVs undergo stepwise monoelectronic transfers to form radical cations and dications, which is evidenced by the observation of two distinctive oxidation peaks in their cyclic voltammograms.

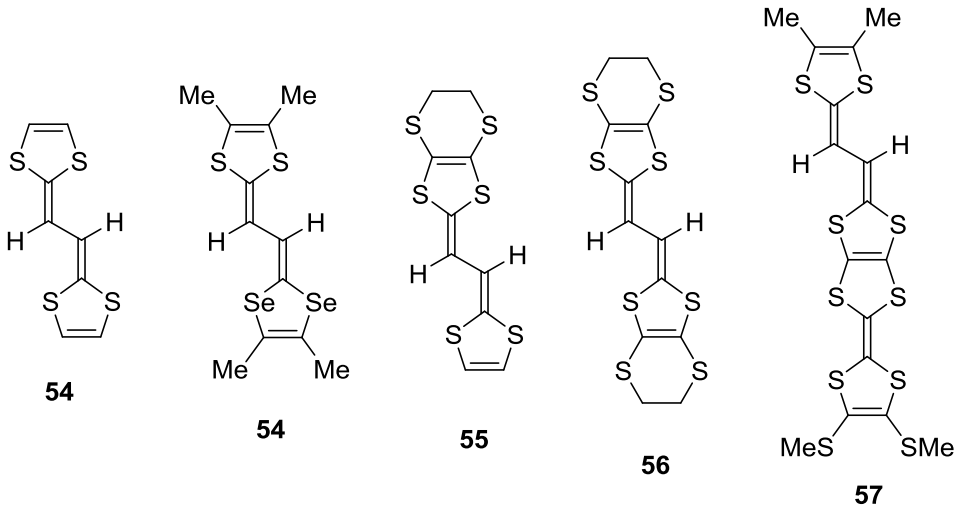

Figure 2.1 Examples of TTFVs with vinylidene positions unsubstituted.

Functionalization of various aryl groups at the vinylic positions provides another type of TTFVs. The aryl substitution added considerable steric crowdedness, making the aryl-substituted (henceforth referred to as aryl-TTFVs) adopt a twisted conformation in the neutral state. For instance, in 2000 Hapiot and co-workers[8] calculated the structures of a phenyl-TTFV **58** (Figure 2.2) and its radical cation and dication by the density functional theory (DTF) method (B3LYP/6-31G* level of theory). The neutral molecule of **58** takes a twisted, *pseudo-cis* conformation, while the radical cation and dication both

shows a planar, *trans* conformation along the dithiolium and vinyl skeleton. The two phenyl rings in the oxidized states rotate to be perpendicular to the central TTFV planar.

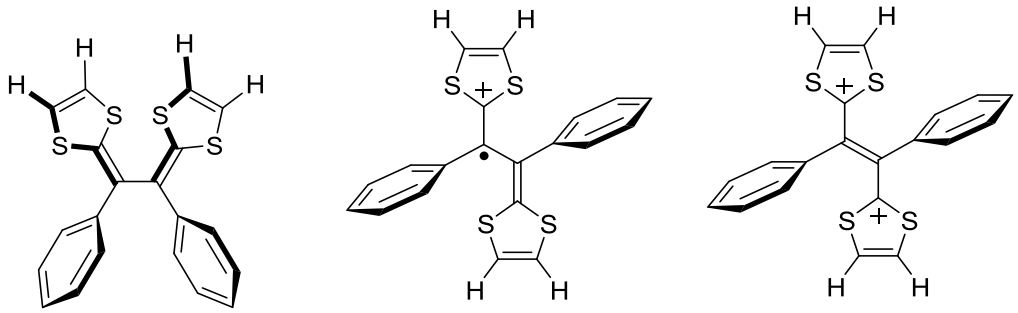

Figure 2.2 Preferred Conformations of phenyl-TTFV **58** and its radical cation and dication.

The dramatic *pseudo-cis* to *trans* conformational changes associated with the oxidation of phenyl-TTFV have also been confirmed by the X-ray single crystallographic data for a number analogous phenyl-TTFVs.[8-13] Based on the existing crystallographic data, two well-known TTFV researchers, Hapiot and Lorcy, in their paper published in *J. Org. Chem*. in 2007 made a general statement, "*Indeed, all the neutral TTFVs (R) substituted on the central conjugation exhibit non-planar structures, due to steric hindrance*."[14] This generalization appears to be reasonable at the first glance; however, a careful survey of the previous literature of TTFV chemistry reveals a contradiction to the hypothesis proposed by Yamashita in 1998. In Yamashita' work, a group of TTFV derivatives bearing various substituted phenyl groups were synthesized and characterized. The cyclic voltammogram of 2,6-difluorophenyl substituted TTFV **59** (Figure 2.3) was

noticed to show two reversible one-electron oxidation waves similar to the non-substituted TTFV. Yamashita rationalized that this was because "*the TTFV skeletons are planar when there are o-substituents, which increase the steric interactions and make the phenyl parts twist from the π-conjugated framework.*" Although Yamashita's proposed *ortho*-steric effect is logically sound and can reasonably explain the cyclic voltammetric properties of **59**, the actual X-ray structure of **59** (CCDC 223592) shows a twist, *cis*-like TTFV framework instead of the predicted *s-trans* conformation.[12]

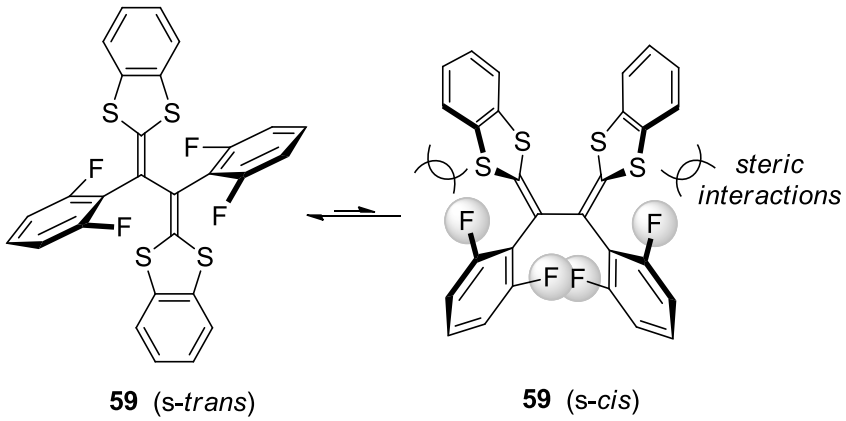

Figure 2.3 Two possible conformations of 2,6-difluorophenyl-TTFV **59**.

If Yamashita's steric argument still remains valid, much bulkier groups than fluorine should be placed at the *ortho*-position(s) of the phenyl groups to force the formation of a fully planar, *trans* TTFV framework. In theory, modification of the TTFV conformation can effectively alter the electronic and solid-state packing properties, which in turn offers a useful design approach for new TTFV-based electronic and optoelectronic materials. Prior to this thesis work, there have been no literature reports showing

substituted TTFVs with a planar, *s-trans* structure at the central conjugated unit. To address such fundamental properties of TTFVs, a series of new aryl-TTFVs (**60**-**67**, Figure 2.4) was designed and synthesized.

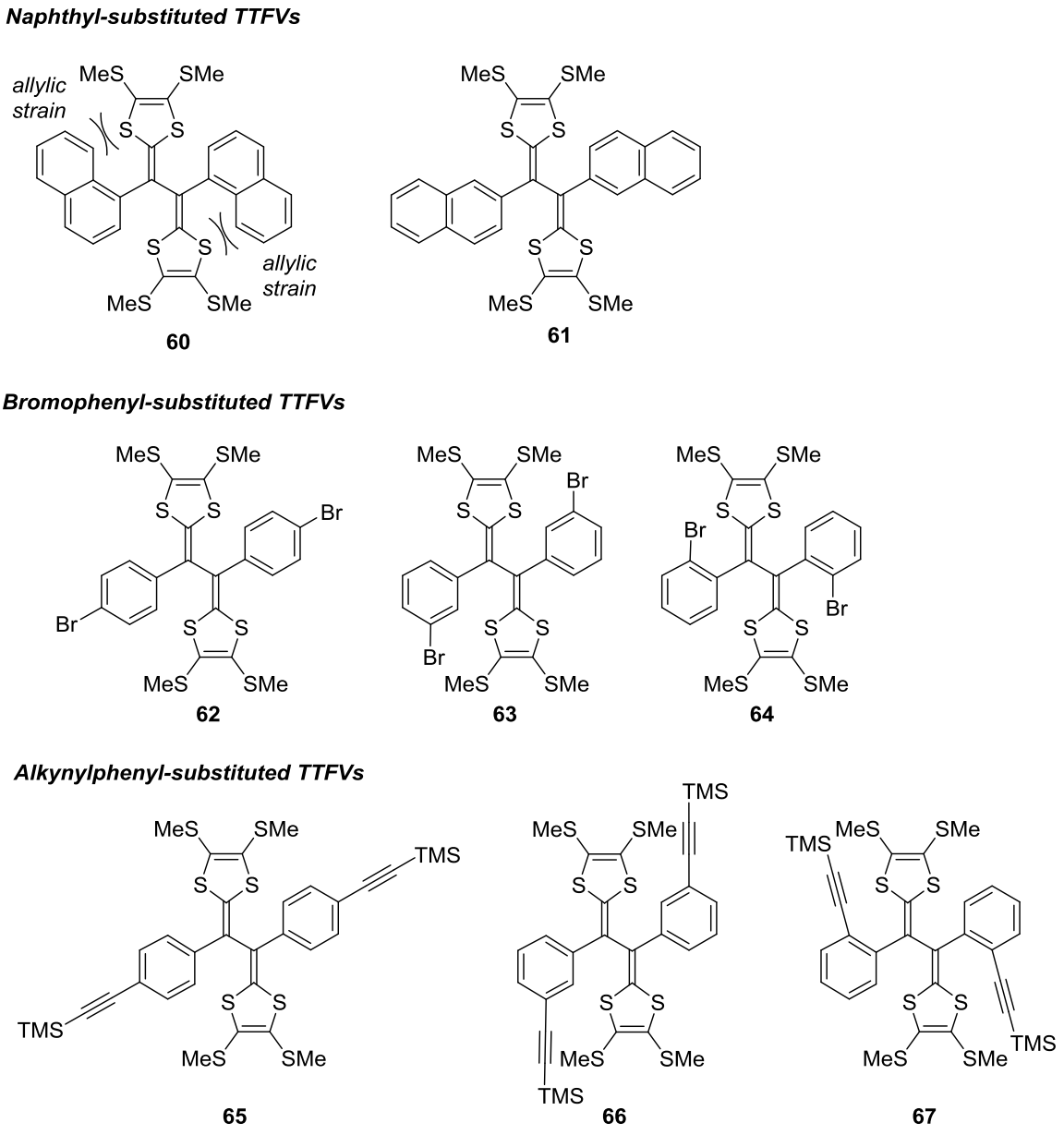

Figure 2.4 New aryl-TTFVs **60**-**67** investigated in this thesis work.

As shown in Figure 2.3, aryl-TTFVs **60**-**67** can be categorized into three groups. Compounds **60** and **61** constitute the naphthyl-substituted derivatives, wherein the steric effect as well as the extended π-conjugation of naphthalene is expected to give rise to interesting conformational and solid-state packing properties. In particular, in the case of 1-naphthyl-TTFV **60**, a significant effect of allylic strain can be envisaged if the molecule takes a twisted, non-planar conformation. To avoid this interaction, a favorable conformation would be that the two naphthyl groups become perpendicular to the central TTFV unit, which in turn naturally assumes a planar, *s-trans* conformation. Compounds **62**-**64** are bromophenyl-substituted TTFVs, which allow a comparative study of the steric and inductive effects of bromo groups on the structural and electronic properties of TTFV derivatives. Finally, three alkynylphenyl-TTFV isomers **65**-**67** are targeted in this work. These compounds can not only help to better understand the structure-property relationships for substituted TTFVs, but also may serve as building blocks for the preparation of novel π-extended macromolecular systems using various alkynye-based coupling reactions.

Synthetically, all the target compounds can be readily prepared via the oxidative dimerization of corresponding aryl-dithiafulvene (aryl-DTF) precursors, the mechanism of which is mentioned in the previous chapter (see Figure 1.14 in Chapter 1). Upon this consideration, a general retrosynthetic route is outlined in Scheme 2.1. The first step in the retrosynthesis leads to an aryl-DTF intermediate, which can be synthesized through a phosphite-promoted olefination reaction between thione **84** and a suitable arenecarbaldehyde.

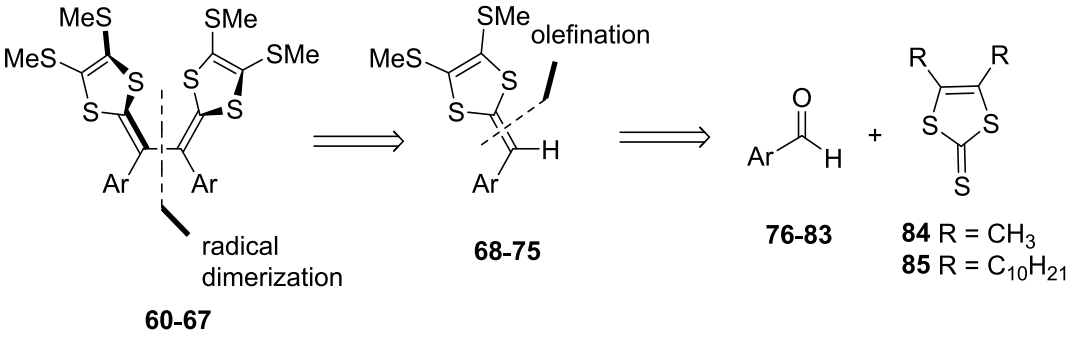

Scheme 2.1 Retrosynthetic analysis of aryl-substituted TTFVs.

2.2 Results and Discussion

As discussed in Scheme 2.1, to synthesize the target aryl-TTFV derivatives, two essential thione precursors **84** and **85** need to be prepared at first. The detailed synthesis of these compounds began with the preparation of zincate **86** through a radical reaction between sodium metal and CS_2, with DMF serving as both the activating agent and solvent.[17] The detailed mechanism of this reaction is discussed in Figure 1.7. The intermediate product of the radical reaction was a sodium dithiolate salt, which was coordinated with Zn(II) ion in the presence of Et_4NBr. The synthetic sequence eventually produced a red-colored zinc salt **86** in a relatively high yield of 64% (Scheme 2.2)

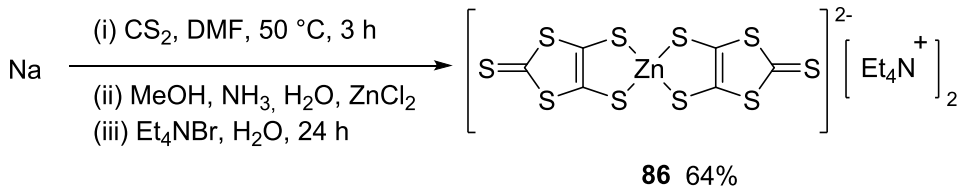

86 64%

Scheme 2.2 Synthesis of zincate **86**.

This zinc product **86** was then subjected to an S_N2-type alkylation reaction with CH_3I or $C_{10}H_{21}Br$ (Scheme 2.3) to afford thione precursors **84** in 73% yield and **85** in 68% yield. Depending on the individual workup and purification method used, different product colors were observed, especially in the case of the methylated thione **84**. The different colors are attributed to a very minute impurity which does not appear in the H-NMR spectra. However, the purity of the product is not affected by this alteration in color. Synthesis of the two thione precursors served two purposes: (1) the methylated thione **84** was intended for the preparation of aryl-TTFVs with good crystallinity, so that single crystals could be obtained for solid-state structural analysis; (2) the *n*-decylated thione **85** would be used in the synthetic cases where the solubility of the products in general organic solvents became an issue.

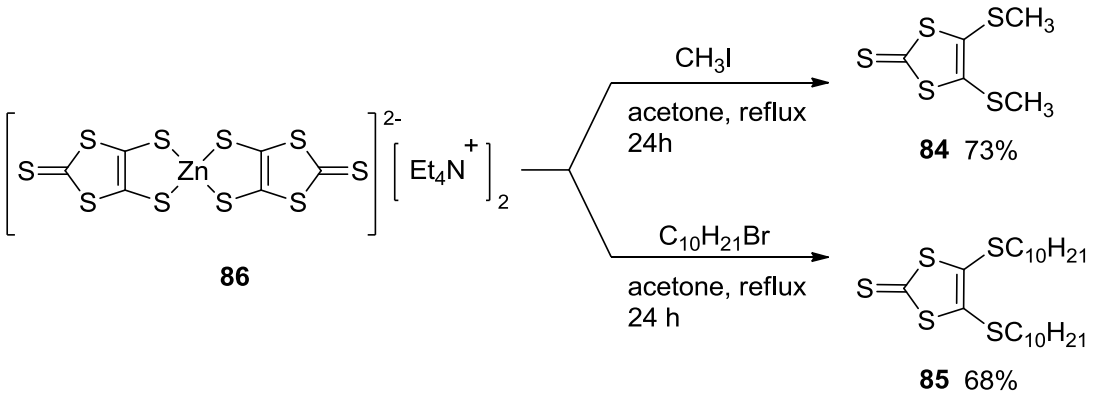

Scheme 2.3 Synthesis of methylated and *n*-deacylated thione precursors **84** and **85**.

With these two thiones in hand, construction of the target aryl-TTFV was next carried out. At first, 1-naphthaldehyde **76** and 2-naphthaldehyde **77** were respectively

subjected to an olefination reaction with thione **84**, promoted by $P(OMe)_3$ under heat (Scheme 2.4). The reactions afforded naphthyl-substituted DTFs **68** in 72% yield and **69** in 49% yield. Although the use a high-boiling aromatic solvent, such as toluene or xylene, was often mentioned in the literature methods, it was found that the olefination reactions in this work were more effective under the conditions of excess neat $P(OMe)_3$. $P(OMe)_3$ was a smelling reagent and not so easy to remove by solvent extraction or column chromatography during the purification step. The best way to remove it was through vacuum distillation.

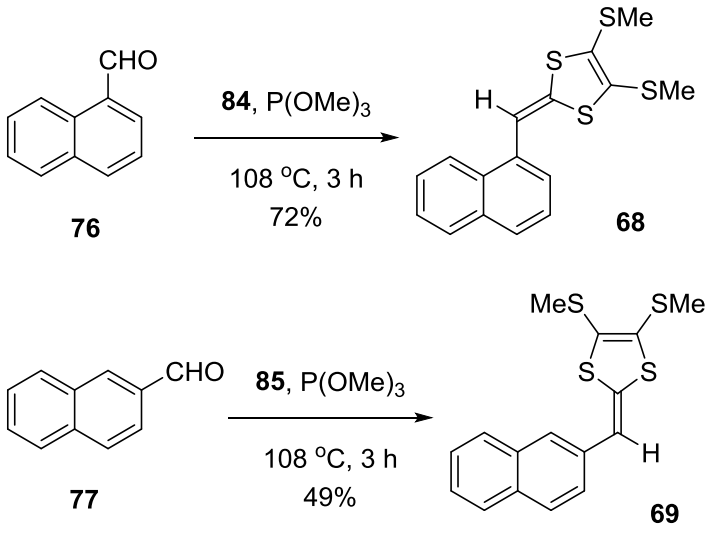

Scheme 2.4 Synthesis of naphthyl-substituted DTFs **68** and **69**.

Next, the two DTF products **68** and **69** were taken through an oxidative dimerization reaction using I_2 as oxidant to yield the naphthyl-TTFVs **60** and **61**. Both **60** and **61** were obtained in reasonable yields of 45% and 53% respectively as shown in

Scheme 2.5. Interestingly, 1-naphthyl-DTF **60** was quite challenging to purify by conventional flash column chromatography as it was found to decompose rapidly on silica gel. However, it was possible to precipitate out the product via the addition of diethyl ether to the reaction mixture. Furthermore, compound **60** exhibited poor solubility in most organic solvents, which in turn made its spectroscopic characterizations problematic. Comparatively, the solubility of 2-naphthyl-DTF **61** appeared to be much better than that of **60**. The very different solubility for the two isomers, **60** and **61**, may arise from their different molecular geometries, which in turn result in different intermolecular interactions (see the discussions on their X-ray structural properties in Chapter 3).

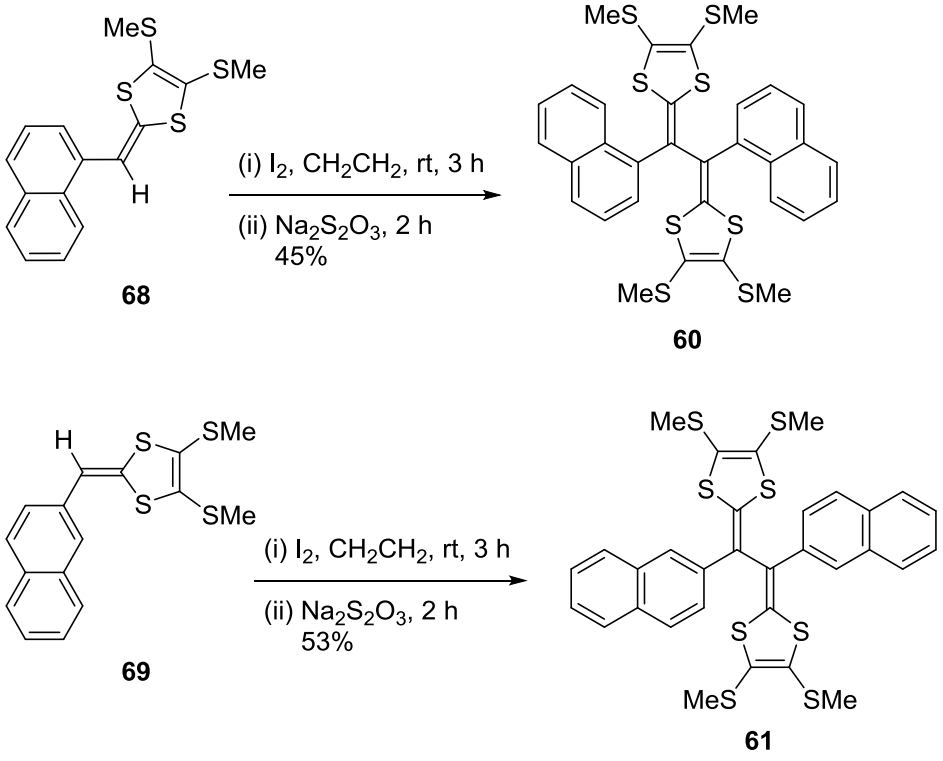

Scheme 2.5 Synthesis of naphthyl-substituted TTFVs **60** and **61**.

The second synthetic objective was aimed at the introduction of bromo-phenyl substituents on the TTFV skeleton. Three regioisomers of bromobenzaldehyde, **78**-**80**, were respectively reacted with thione **84** via the $P(OMe)_3$-promoted olefination to produce the desired DTFs **70**-**72** (see Scheme 2.6). Again neat $P(OMe)_3$ was used and the olefinated products were obtained in decent yields after heating at 108 °C for 3 h.

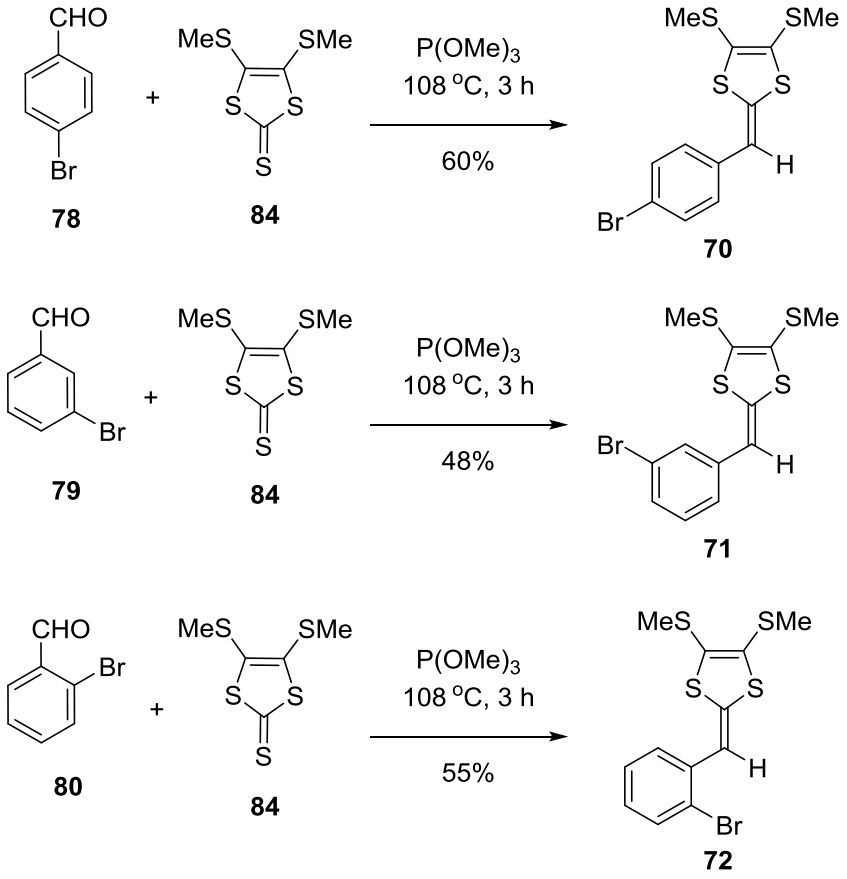

Scheme 2.6 Synthesis of bromophenyl-substituted DTFs **70**-**72**.

Compounds **70** and **71** were then brought through an oxidative dimerization reaction in the presence of I_2 to produce TTFVs **62** and **63** (Scheme 2.7). These reactions

proceeded well in CH_2Cl_2 at room temperature for 2 h. After the oxidative dimerization, the reaction mixtures were treated with $Na_2S_2O_3$ (aq) to reduce the resulting TTFVs to the neutral state, as well as to quench the excess I_2. Purification of the products, however, was not so easy and required very careful column chromatographic separation.

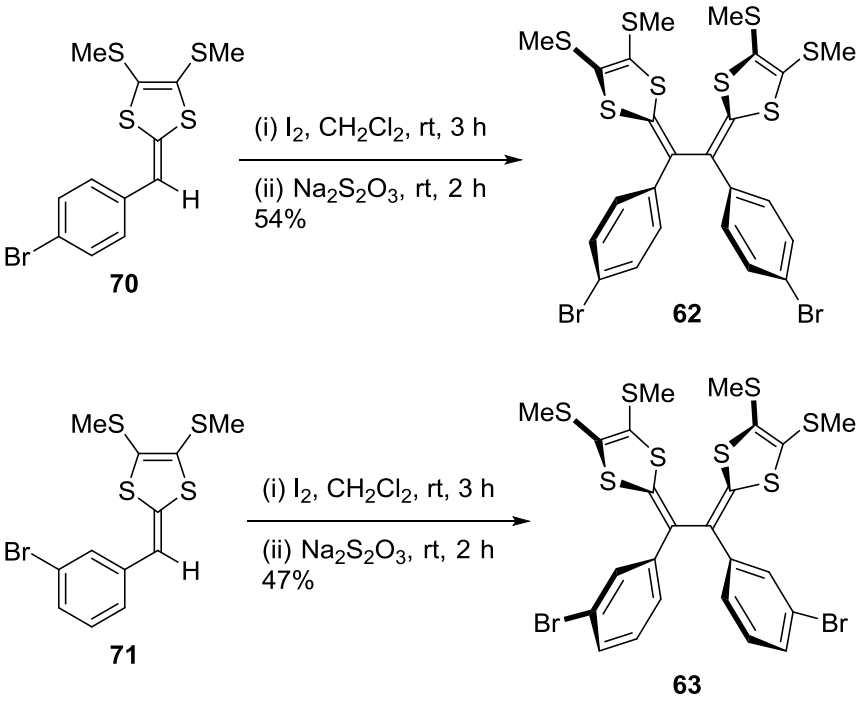

Scheme 2.7 Synthesis of bromophenyl-substituted TTFVs **62** and **63**.

In the case of the DTF **72**, its oxidative dimerization surprisingly yielded a bis-spiro compound **87** as the major product in an isolated yield of 55% after silica column chromatographic separation (Scheme 2.8). What may have been the expected TTFV product **64** was only observed as a minor product in a trace amount by TLC analysis under UV light. Furthermore its presence was postulated upon TLC oxidation with molecular iodine yielding a faint green spot. No meaningful amount of **64** could be

obtained after the column separation. The structure of 87 was convincingly characterized by NMR, IR, MS, and single crystal X-ray diffraction analysis.

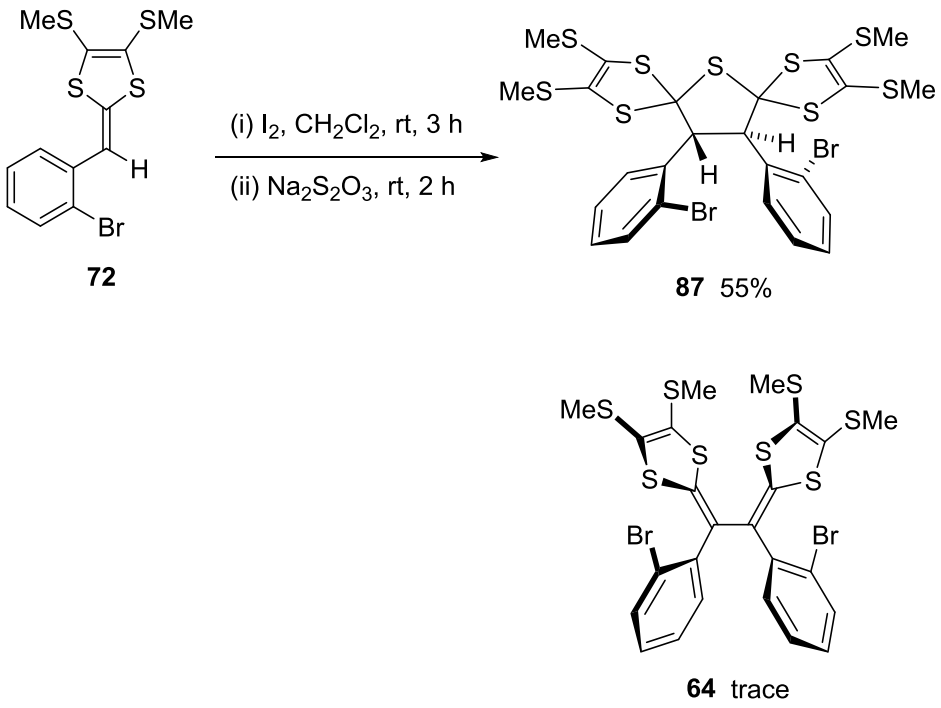

Scheme 2.8 Unexpected formation of bis-spiro **87** via oxidative dimerization of **72**.

A plausible mechanistic explanation for the formation of **87** is outlined in Figure 2.5. In contrast to the general oxidative dimerization mechanism (see Figure 1.14 in Chapter 1), the first dimerized intermediate 88 shows significant hydrogen bonding interactions between the *ortho*-bromo groups and the benzylic hydrogen atoms. Such an effect stabilizes the intermediate **88** and results in considerably slowed down deprotonation reactions. As such, intermediate **88** remains intact until the NaS2O3

workup step, wherein the thiosulfate ion acts as the nucleophile to attack the carbocation in the dithiolium ring, leading to bis-spiro intermediate **90**. Elimination of a molecule of SO_3 from **90** then gives the bis-spiro product **87**.

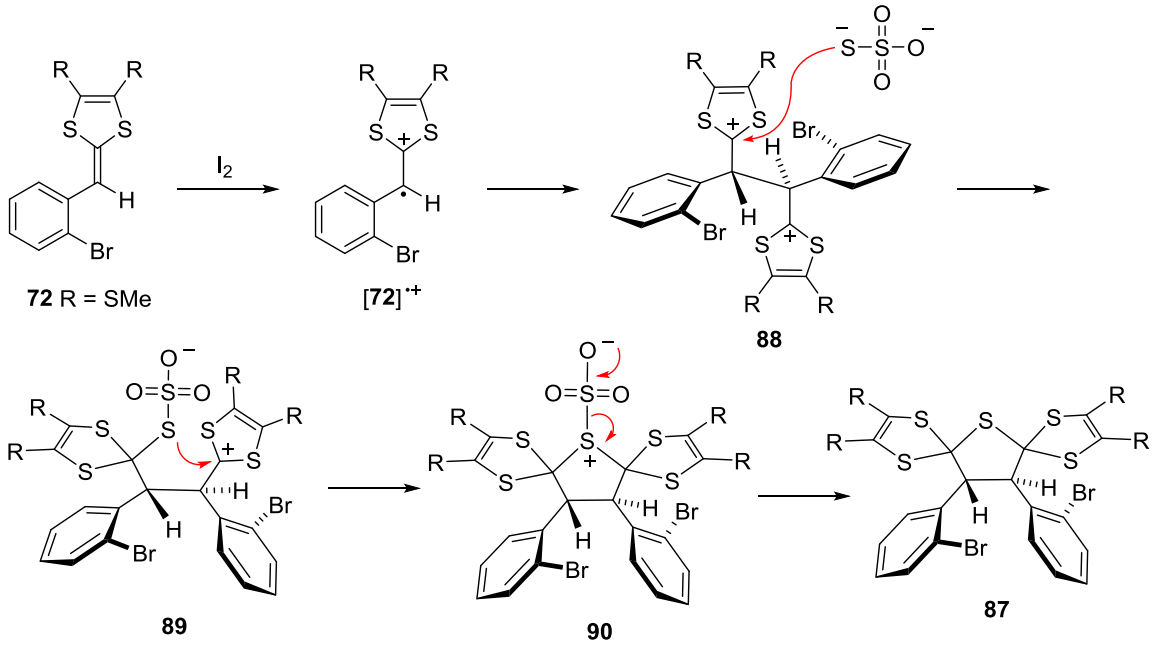

Figure 2.5 Proposed mechanism for the formation of bis-spiro product **87**.

The third synthetic objective in this chapter focused on alkynylphenyl substituted TTFV derivatives. In the synthesis, bromobenzaldehydes **78**-**80** were first converted into alkynylbenzaldehydes **81**-**82** through the Pd/Cu-catalyzed Sonogashira coupling reaction with trimethylsilylacetylene (TMSA) as shown in Scheme 2.9. The yields of the alkynylated compounds **81**-**83** are high (76-84%). Of all three of these products, the *meta*-substituted benzaldehyde **82** was found to decompose relatively quickly, indicating a low

chemical stability. This behavior was not observed in its *ortho* and *para* isomers, **81** and **83**.

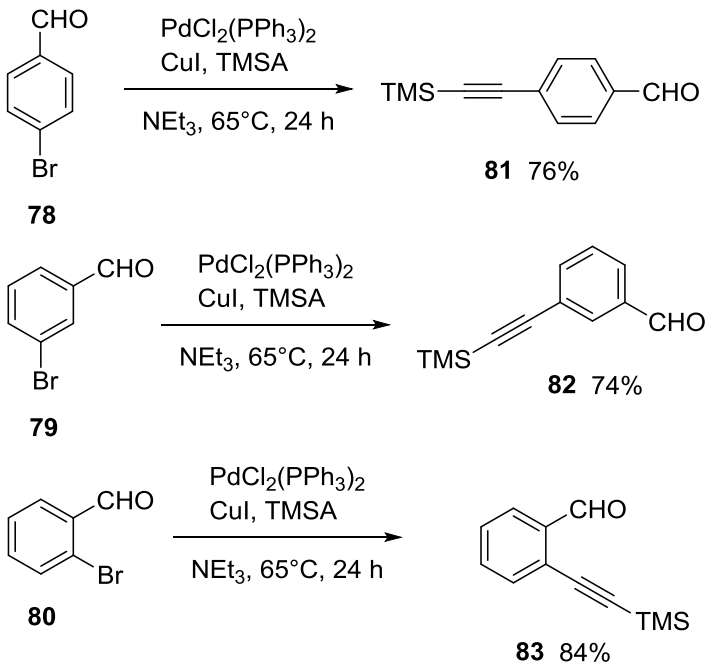

Scheme 2.9 Synthesis of alkynyl-benzaldehydes **81-83** via Sonogashira coupling.

The alkynlbenzaldehydes **81-83** were then subjected to the phosphite-promoted olefination reaction with the thione **84** to yield DTFs **73-75** respectively as shown Scheme 2.10. The isolated yields of these reactions were satisfactory, ranging from 47% to 57%.

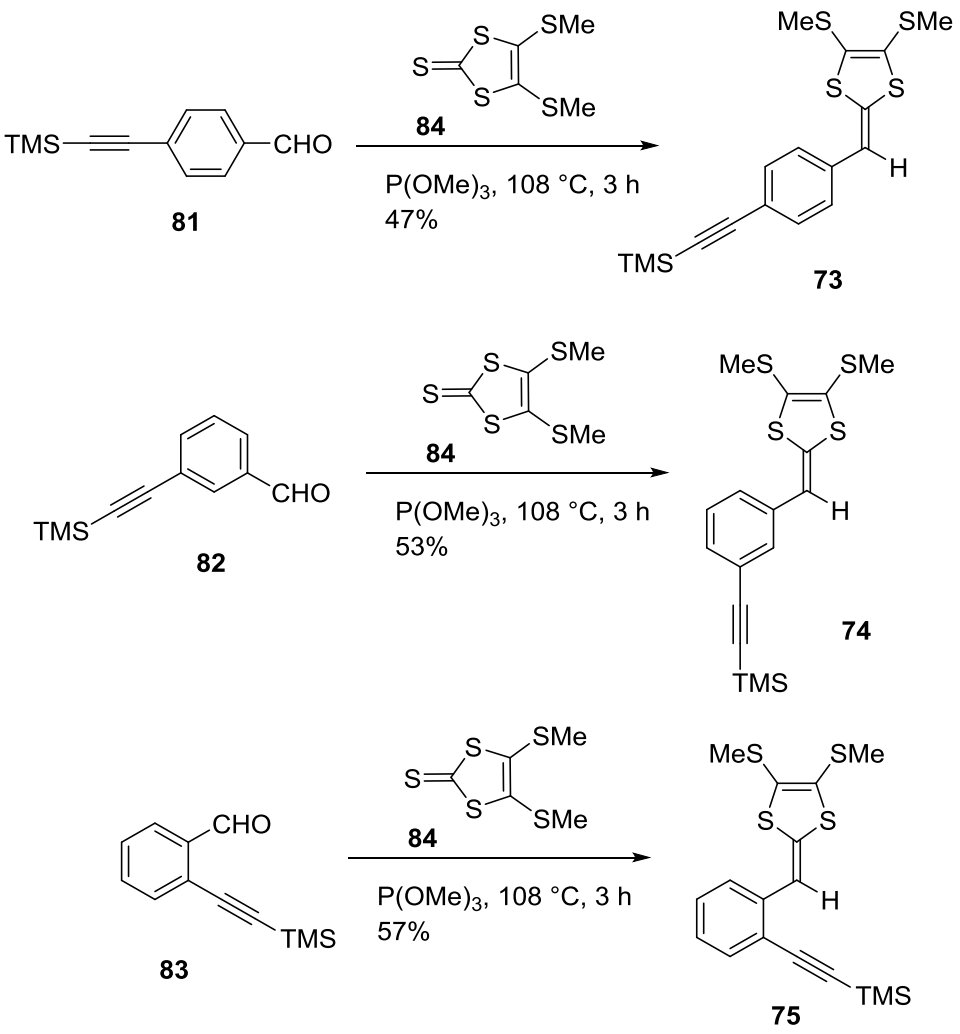

Scheme 2.10 Synthesis of alkynylphenyl-DTFs **73-75** via phosphite-promoted olefination reactions.

These three alkynylphenyl-DTFs **73-75** were then reacted via oxidative dimerization in the presence of I_2 to yield TTFVs **65-67** (Scheme 2.11). The meta-alkynylphenyl-TTFV **66** was isolated in a significantly lower yield than those of its other two isomers **65** and **67**. The low yield is ascribed mainly to its relatively poor chemical

stability. It may be that the *meta*-alkynyl groups have some unique effect on the stability of the TTFV derivative; however, the exact reason(s) still awaits further investigation.

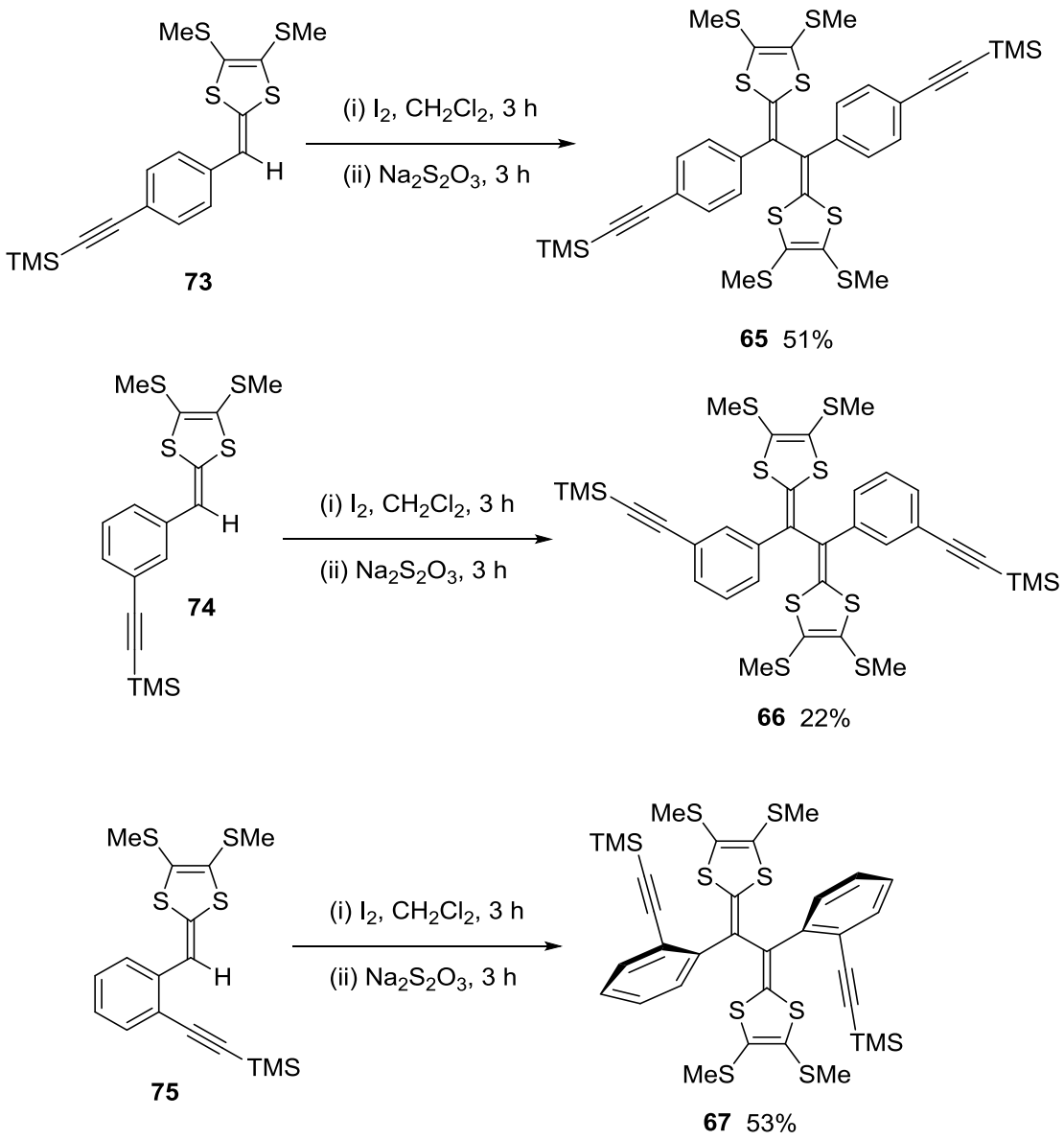

Scheme 2.11 Synthesis of alkynylphenyl-TTFVs **65**-**67** via oxidative dimerization reactions.

With all the target aryl-TTFVs synthesized, except the ortho-bromophenyl **64**, these compounds were then subjected to comparative studies based on various spectroscopic and electrochemical analyses. The detailed molecular properties and relevant structure-property/reactivity relationships are discussed in Chapter 3. In addition to the aryl-TTFVs, a new series of butadiyne-centered exTTFs **91**-**93** was constructed, taking advantage of the availability of the alkynylphenyl-DTFs **73**-**74**. Previously, a former group member, Guang Chen, synthesized and investigated the properties of exTTF **91**.[15, 16] With two more isomers **92** and **93** prepared in this work, the π-electron delocalization between the the butadiyne central π-bridge and the terminal DTF groups can be better understood via comparative analysis. In addition, the two exTTFs **92** and **93** can serve as building blocks to make some interesting π-extended macromolecular systems, such as polymer chains or macrocycles through oxidative coupling reactions.

As shown in Scheme 2.12, the synthesis of exTTFs **91**-93 was readily achieved by performing a Cu(I)-catalyzed alkynyl homocoupling reaction (i.e., Hay coupling)[15, 16] on the products resulting from *in situ* desilylation of **73**-**75**. The yields of the homocouplings were sufficiently high, affording few to no byproducts. This was an added benefit to the purification of exTTFs **91**-**93**.

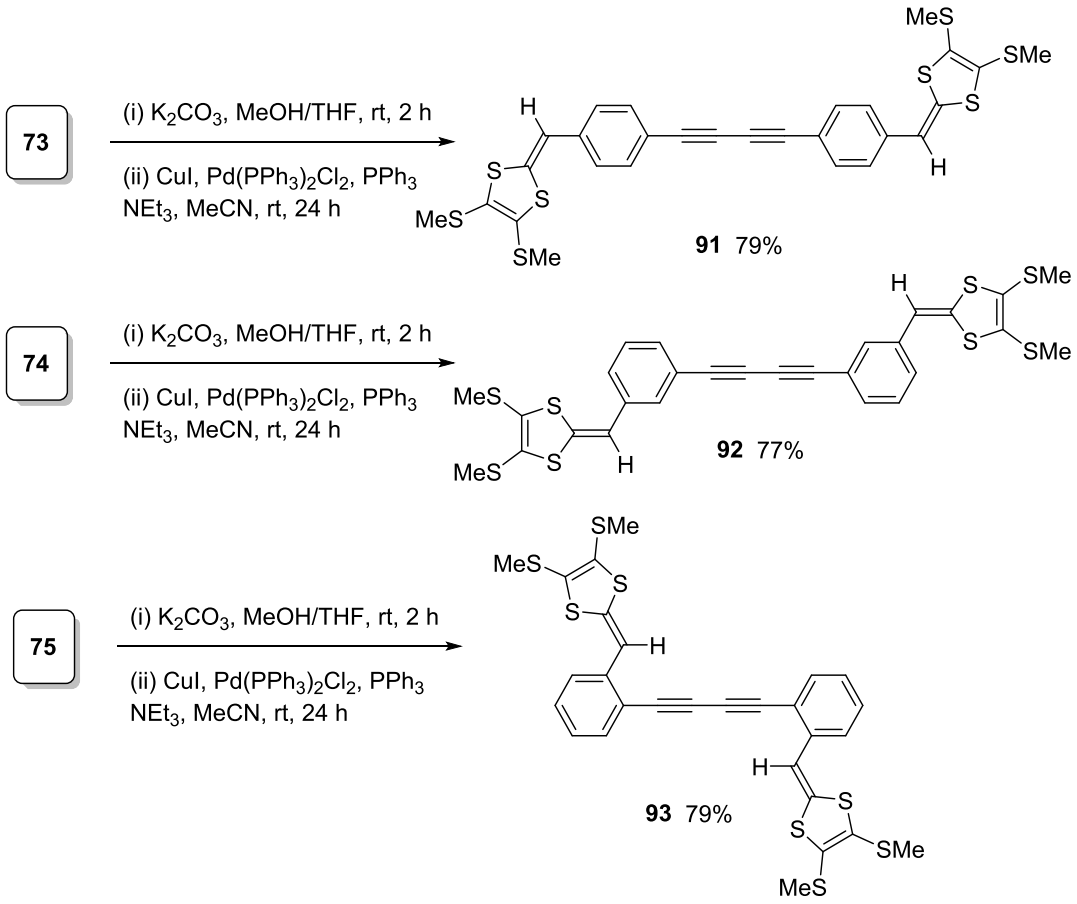

Scheme 2.12 Synthesis of butadiyne-centered exTTFs **91-93** via Hay coupling reactions.

2.3 Experimental

2.3.1 General

Chemicals and reagents were purchased from commercial suppliers and used without further purification. All reactions were performed in standard, dry glassware under an atmosphere of N_2. Evaporation and concentration were done at water-aspirator pressure. Flash column chromatography was carried out with silica gel 60 (230-400 mesh) from VWR International. Thin-layer chromatography (TLC) was carried out with silica gel 60

F254 covered on plastic sheets and visualized by UV light. ^{1}H and ^{13}C NMR spectra were measured on a Bruker Avance 500 MHz spectrometer or a Tecmag APOLLO 300 MHz spectrometer. Chemical shifts are reported in ppm downfield from the signal of the internal reference $SiMe_4$. Coupling constants (*J*) are given in Hz. Infrared spectra (IR) were recorded on a Bruker Tensor 27 spectrometer equipped with a ZnSe ATR module. High-resolution mass spectrometric (HRMS) analyses were performed on a GTC Premier Micromass instrument (MS Technology) using atmospheric pressure chemical ionization (APCI).

2.3.2 Synthetic Procedures

1-Naphthyl-DTF

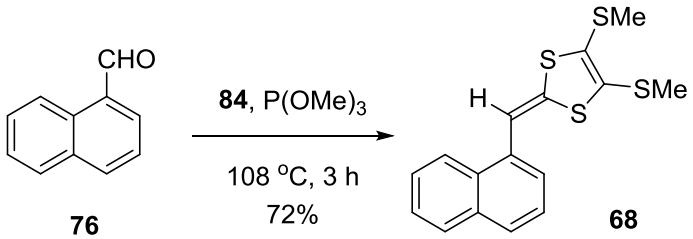

76 **68**

A mixture of 1-napthaldehyde **76** (0.17 mL, 0.19 g, 1.2 mmol) and thione **84** (287 mg, 1.27 mmol) in $P(OMe)_3$ (10 mL) was stirred at 108 °C for 3 h in an oil bath. The unreacted $P(OMe)_3$ was evaporated off under high vacuum, and the residue was subjected to column chromatography (CH_2Cl_2/hexanes 1:1) to afford compound **5a** (303 mg, 0.907 mmol, 72%) as a yellow crystalline solid. m.p.: 91–92 °C; ^{1}H NMR (500 MHz, $CDCl_3$): δ 8.01 (d, *J* = 8.0 Hz, 1H), 7.85 (d, *J* = 7.0 Hz, 1H), 7.74-7.73 (m, 1H), 7.54-7.46 (m, 4H), 7.07 (s, 1H), 2.46 (s, 3H), 2.35 (s, 3H); ^{13}C NMR (75 MHz, $CDCl_3$): δ 134.5, 133.70, 133.66, 130.7, 128.6, 127.4, 126.2, 126.1, 126.0, 125.4, 124.5, 124.2, 123.8, 112.4, 19.0,

18.9; FTIR (neat): 3041, 2992, 2914, 1941, 1559, 1494, 1422, 1310, 1253, 1076, 1012, 965, 878, 826 cm^{-1}; HRMS (APCI, positive) *m*/*z* calcd for $C_{16}H_{14}S_4$ 333.9973, found 333.9977 [M^+].

2-Naphthyl-DTF 69

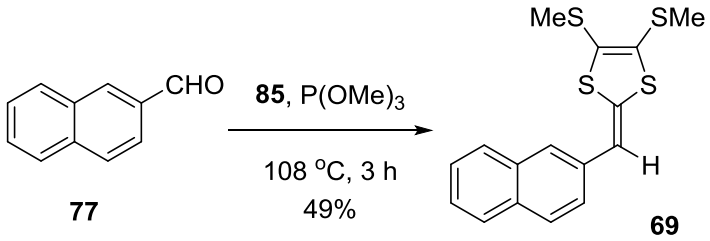

A mixture of 2-naphthaldehyde **77** (0.706 g, 4.52 mmol) and thione **85** (1.007 g, 6.448 mmol) in $P(OMe)_3$ (20 mL) was stirred at 108 °C for 3 h. The unreacted $P(OMe)_3$ was removed by vacuum distillation. The residue was subjected to column chromatography (CH_2Cl_2/hexanes 1:1) to afford compound **69** (0.739 g, 2.21 mmol, 49%) as a yellow crystalline solid. m.p.: 58–59 °C; ^{1}H NMR (500 MHz, $CDCl_3$): δ 7.83 (d, *J* = 8.0 Hz, 1H), 7.78 (d, *J* = 8.3 Hz, 1H), 7.62 (s, 1H), 7.49-7.40 (m, 2H), 7.35 (d, *J* = 8.6 Hz, 1H), 6.62 (s, 1H), 2.45 (s, 3H), 2.43 (s, 3H); ^{13}C NMR (75 MHz, $CDCl_3$): δ 133.9, 133.6, 132.6, 131.7, 128.1, 127.93, 127.91, 127.6, 126.4, 125.9, 125.7, 124.9, 124.2, 114.9, 19.1, 19.0; FTIR (neat): 3053, 2990, 2914, 1941, 1554, 1495, 1421, 1357, 1304, 1013, 959, 894, 857 cm^{-1}; HRMS (APCI, positive) *m*/*z* calcd for $C_{16}H_{14}S_4$ 333.9973, found 333.9979 [M^+].

Bis(1-naphthyl)-TTFV 60

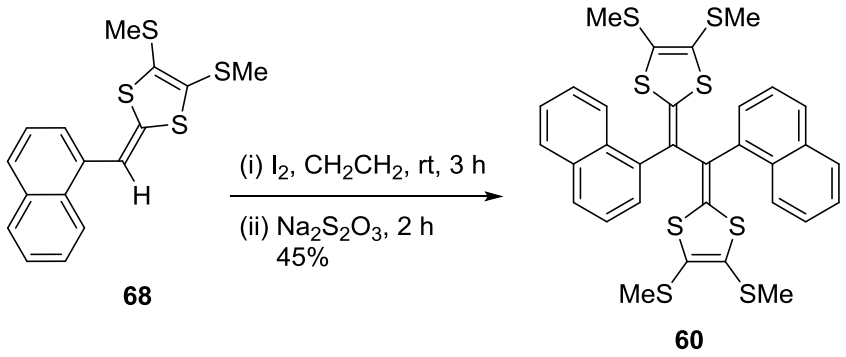

68 **60**

To a solution of 1-naphthyl-DTF **68** (0.502 g, 1.50 mmol) in CH_2Cl_2 (20 mL) was added I_2 (1.011 g, 3.98 mmol). The mixture was stirred for 3 h at rt. Then aqueous $Na_2S_2O_3$ (20 mL, satd.) was added and the mixture was stirred at rt for another 2 h. The organic layer was separated and dried over $MgSO_4$. Diethyl ether (30 mL) was then added, resulting in the precipitation of compound **60** which was collected by filtration as a bright orange powder (0.223 g, 0.335 mmol, 45%). m.p.: 251–252 ºC; ^{1}H NMR (500 MHz, $CDCl_3$): δ 7.77-7.67 (m, 4H), 7.62 (d, *J* = 8.3 Hz, 2H), 7.41-7.33 (m, 4H), 7.12 (br s, 2H), 2.46 (br s, 3H), 2.47 (s, 6H), 2.18 (s, 6H); ^{13}C NMR was not obtained due to poor solubility; FTIR (neat): 3045, 2914, 1584, 1506, 1465, 1421, 1309, 1163, 1013, 960, 859 cm^{-1}; HRMS (APCI, positive) *m*/*z* calcd for $C_{32}H_{26}S_8$ 665.9795, found 665.9800 [M^+].

Bis(2-naphthyl)-TTFV 61

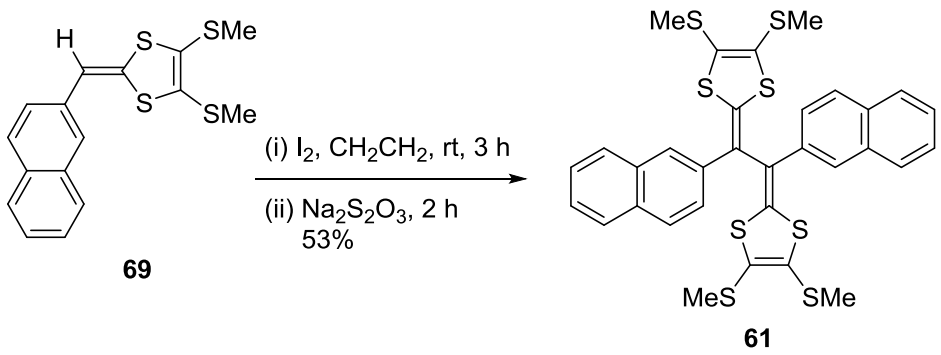

69 **61**

To a solution of 2-naphthyl-DTF **69** (0.508 g, 1.59 mmol) in CH_2Cl_2 (20 mL) was added I_2 (1.037 g, 4.09 mmol). The mixture was stirred for 3 h. Then aq. $Na_2S_2O_3$ (20 mL, satd.) was added and the mixture was stirred for 2 h. The organic layer was separated, dried over $MgSO_4$, and purified by column chromatography (CH_2Cl_2/hexanes 1:1) to afford product **61** as a yellow crystalline solid (279 mg, 0.419 mmol, 53%). m.p.: 189–190 °C; ^{1}H NMR (500 MHz, $CDCl_3$): δ 7.91 (s, 2H), 7.79 (d, *J* = 7.6 Hz, 2H), 7.75 (d, *J* = 8.6 Hz, 4H), 7.55 (d, *J* = 8.6 Hz, 2H), 7.45-7.38 (m, 4H), 2.43 (s, 6H), 2.39 (s, 6H); ^{13}C NMR (75 MHz, $CDCl_3$): δ 136.8, 135.0, 133.5, 132.3, 128.33, 128.32, 128.1, 128.0, 127.5, 126.2, 126.0, 125.7, 124.9, 124.8, 19.0, 18.9; FTIR (neat): 2913, 1591, 1532, 1491, 1421, 1308, 1133, 961, 892, 852, 811 cm^{-1}; HRMS (APCI, positive) *m*/*z* calcd for $C_{32}H_{26}S_8$ 665.9795, found 665.9785 $[M]^+$.

4-Bromophenyl-DTF 70

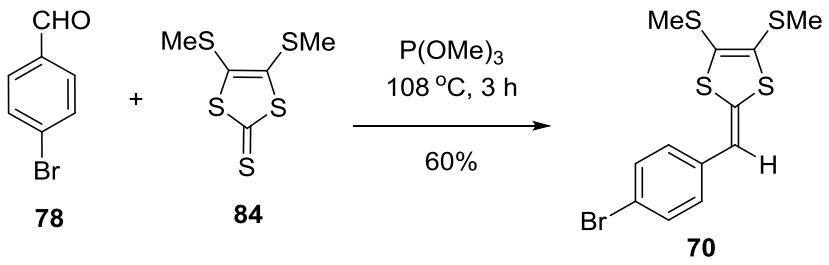

4-Bromobenzaldehyde **78** (1.03 g, 5.55 mmol) and thione **84** (1.45 g, 6.43 mmol) were placed in a round-bottomed flask. $P(OMe)_3$ (20 mL) was then added and the mixture was heated to 108 °C for 3 h with stirring. $P(OMe)_3$ was removed by vacuum distillation and the remaining mixture was purified by column chromatography with a 20% CH_2Cl_2/hexanes solvent system to yield **70** (1.20 g, 3.30 mmol, 60%) as a yellow crystalline solid. FTIR (neat): 3054, 2993, 2956, 2916, 1569, 1546, 1484, 1419, 586, 511 cm^{-1}; ^1H NMR (300 MHz, $CDCl_3$): δ 7.46 (d, *J* = 8.6 Hz, 2H), 7.07 (d, *J* = 8.4 Hz, 2H), 6.40 (s, 1H), 2.44 (s, 3H), 2.42 (s, 3H); ^{13}C NMR (75 MHz, $CDCl_3$): δ 135.1, 133.3, 131.6, 128.2, 127.5, 124.2, 119.3, 113.4, 19.0, 18.9; HRMS (APCI, positive) *m/z* calcd for $C_{12}H_{11}S_4{}^{79}Br$ 361.8927, found 361.8924 [M^+]. X-ray crystal data: $C_{12}H_{11}BrS_4$, *M* = 363.36, orthorhombic, *a* = 8.275(4) Å, *b* = 11.616(5) Å, *c* = 14.704(7) Å, α = 90.00°, β = 90.00°, γ = 90.00°, *V* = 1413.4(11) $Å^3$, *T* = 123(2) K, space group $P2_12_12_1$, *Z* = 4, μ(MoKα) = 3.482 mm^{-1}, 14131 reflections measured, 3206 independent reflections, 3151 with $I > 2\sigma(I)$ (R_{int} = 0.0444). R_1 = 0.0265 ($I > 2\sigma(I)$), $\omega R(F_2)$ = 0.0584 (all data). The goodness of fit on F_2 was 1.069. Flack parameter = 0.006(7). CCDC 936355.

Bis(4-bromophenyl)-TTFV 62

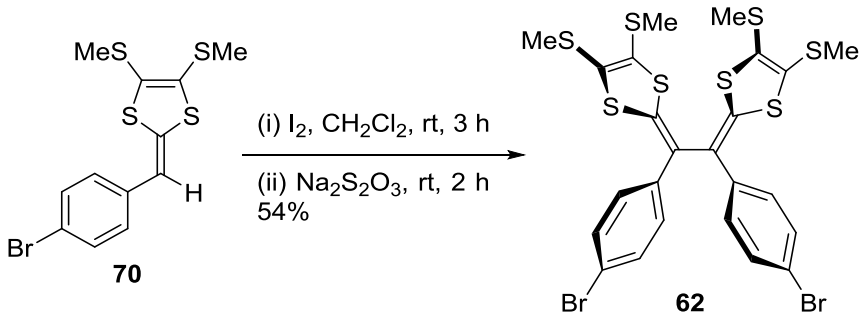

Compound **70** (1.12 g, 3.09 mmol) was placed in a round-bottomed flask with I_2 (2.59 g, 0.0102 mol) and CH_2Cl_2 (25 mL) and stirred for 3 h. $Na_2S_2O_3$ (satd aqueous solution, 20 mL) was then added to the flask and the mixture was stirred for another 3 h. The organic layer was then separated, dried over $MgSO_4$ and suction filtered. The filtrate was concentrated under vacuum and then purified by column chromatography with a 25% CH_2Cl_2/hexanes solvent system to yield **62** (0.608 g, 0.839 mmol, 54%) as an orange solid. FTIR (neat): 2954, 2915, 2859, 1533, 1483, 1420, 591, 502; ^{1}H NMR (300 MHz, $CDCl_3$): δ 7.42 (d, *J* = 8.6 Hz, 2H), 7.25 (d, *J* = 7.8 Hz, 2H), 2.42 (s, 3H), 2.40 (s, 3H); ^{13}C NMR (75 MHz, $CDCl_3$): δ 137.5, 135.8, 131.8, 128.3, 128.2, 125.1, 123.0, 120.5, 18.9, 18.9 cm^{-1}; HRMS (APCI, positive) *m/z* calcd for $C_{24}H_{20}S_8{}^{79}Br_2$ 721.7697, found 721.7704 [M^+].

3-Bromophenyl-DTF 71

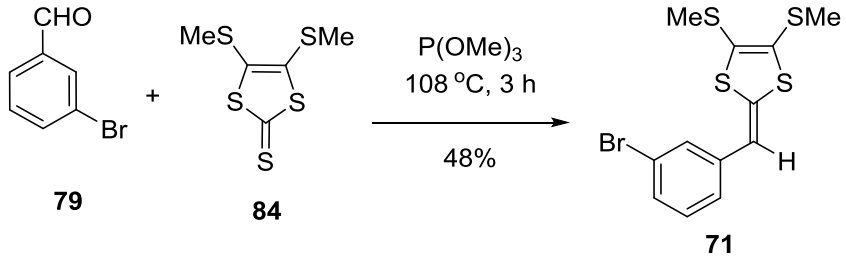

3-Bromobenzaldehyde **79** (1.03 g, 5.57 mmol) and thione **84** (1.41 g, 6.24 mmol) were placed in a round-bottomed flask. $P(OMe)_3$ (20 mL) was then added and the mixture was heated to 108 °C for 3 h with stirring. $P(OMe)_3$ was removed by vacuum distillation and the remaining mixture was purified by column chromatography with a 20% CH_2Cl_2/hexanes solvent system to yield **71** (0.986 g, 2.71 mmol, 48%) as an orange liquid. FTIR (neat): 3054, 2989, 2953, 2916, 1587, 1567, 1547, 1496, 1472, 1417, 1405 cm^{-1}; ^1H NMR (300 MHz, $CDCl_3$): δ 7.33 (s, 1H), 7.28 (t, *J* = 7.9 Hz, 1H), 7.20 (t, *J* = 7.7 Hz, 1H), 7.13 (d, *J* = 7.7 Hz, 1H), 6.38 (s, 1H), 2.44 (s, 3H), 2.42 (s, 3H); ^{13}C NMR (75 MHz, $CDCl_3$): δ 138.3, 134.5, 130.0, 129.5, 128.7, 127.8, 125.1, 124.1, 122.8, 112.9, 19.1, 18.9; HRMS (APCI, positive) *m/z* calcd for $C_{12}H_{11}S_4{}^{79}Br$ 361.8927, found 361.8930 [M^+].

Bis(3-bromophenyl)-TTFV 63

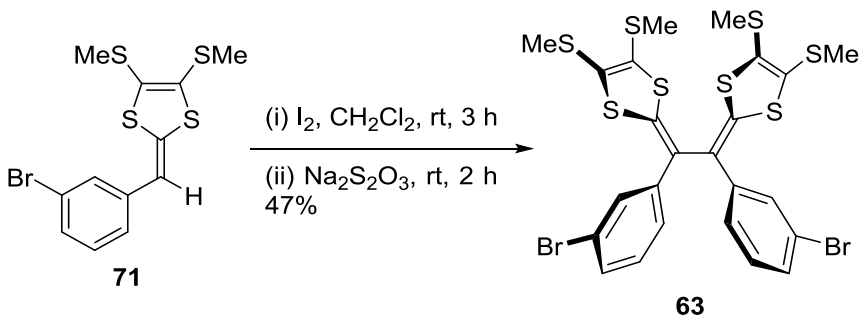

Compound **71** (1.09 g, 2.99 mmol) was placed in a round-bottomed flask with I_2 (2.42 g, 9.53 mmol) and CH_2Cl_2 (25 mL) and stirred for 3 h. $Na_2S_2O_3$ (satd aqueous solution, 20 mL) was then added to the flask and the mixture stirred for 3 h. The organic layer was then separated, dried over $MgSO_4$ and suction filtered. The filtrate was concentrated under vacuum and then purified by column chromatography with a 25% CH_2Cl_2/hexanes solvent system to yield **63** (0.517 g, 0.713 mmol, 47%) as an orange solid. FTIR (neat): 3053, 2956, 2914, 1579, 1550, 1521, 1482, 584, 515 cm^{-1}; ^1H NMR (300 MHz, $CDCl_3$): δ 7.51 (s, 2H), 7.31 (m, 4H), 7.17 (m, 2H), 2.44 (s, 6H), 2.41 (s, 6H); ^{13}C NMR (75 MHz, $CDCl_3$): δ 139.0, 138.7, 130.2, 129.95, 129.3, 128.4, 125.3, 125.2, 123.0, 122.2, 19.0, 18.9; HRMS (APCI, positive) *m/z* calcd for $C_{24}H_{20}S_8{}^{79}Br_2$ 721.7697, found 721.7695 [M^+].

2-Bromophenyl-DTF 72

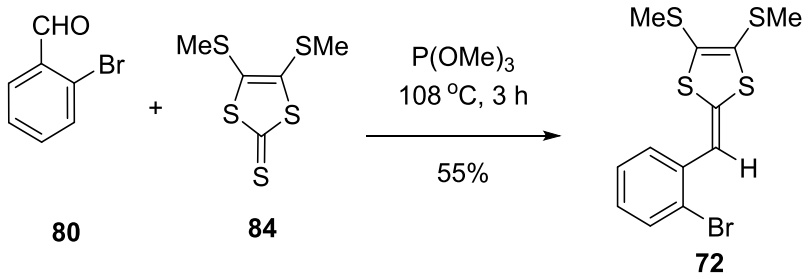

80 **84** **72**

2-Bromobenzaldehyde **80** (1.00 g, 5.40 mmol) and thione **84** (1.35 g, 7.30 mmol) were placed in a round-bottomed flask. $P(OMe)_3$ (20 mL) was then added and the mixture heated to 108 °C for 3 h with stirring. $P(OMe)_3$ was removed by vacuum distillation and the remaining mixture was purified by column chromatography with a 20% CH_2Cl_2/hexanes solvent system to yield **72** (1.08 g, 2.97 mmol, 55%) as a yellow solid. m.p.: 61.2-64.3 °C; FTIR (neat): 3053, 3012, 2914, 1575, 1551, 1493, 1457, 1424, 584, 527 cm^{-1}; ^1H NMR (300 MHz, $CDCl_3$): δ 7.56 (d, *J* = 8.0 Hz, 1H), 7.37 (d, *J* = 7.8 Hz, 1H), 7.31 (t, *J* = 7.7 Hz, 1H), 7.03 (t, *J* = 8.4 Hz, 1H), 6.70 (s, 1H), 2.44 (s, 3H), 2.39 (s, 3H); ^{13}C NMR (75 MHz, $CDCl_3$): δ 136.0, 135.5, 133.0, 127.6, 127.6, 127.4, 127.1, 123.7, 122.9, 113.8, 19.0, 18.9; HRMS (APCI, positive) *m/z* calcd for $C_{12}H_{11}S_4{}^{79}Br$ 362.9005, found 362.9010 $[M + H]^+$.

Compound 87

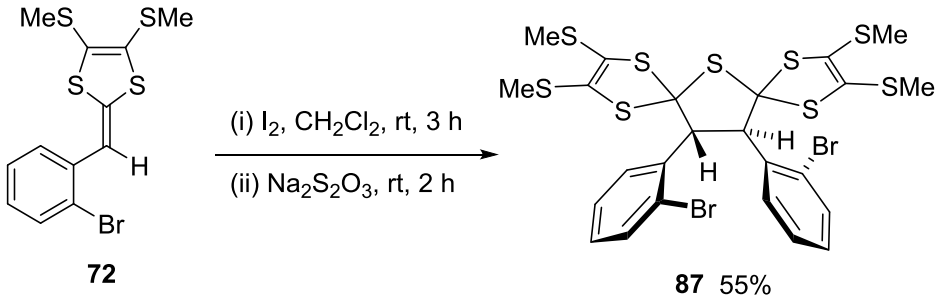

72 **87** 55%

Compound **72** (1.05 g, 2.90 mmol) was placed in a round-bottomed flask with I_2 (2.21 g, 8.76 mmol) and CH_2Cl_2 (25 mL) and stirred for 3 h. $Na_2S_2O_3$ (satd aqueous solution, 20 mL) was then added to the flask and the mixture stirred for 3 h. The organic layer was then separated, dried over $MgSO_4$ and suction filtered. The mixture was then subjected to column chromatography with a 25% CH_2Cl_2/hexanes solvent system. The product was then recrystallized from 20% ethyl acetate/hexanes to yield **10** (0.527 g, 0.694 mmol, 50%) as a yellow crystalline solid. m.p.: 153.3-164.6 °C; FTIR (neat); 3050, 2985, 2916, 1528, 1492, 1472, 1460, 1427, 1417, 591, 549 cm^{-1}; ^1H NMR (300 MHz, $CDCl_3$): δ 7.54 (dd, *J* = 7.9, 1.7 Hz, 2H), 7.44 (dd, *J* = 8.0, 1.3 Hz, 2H), 7.14 (td, *J* = 7.6, 1.3 Hz, 2H), 7.01 (td, *J* = 7.7, 1.6 Hz, 2H), 4.97 (s, 2H), 2.25 (s, 6H), 2.15 (s, 6H); ^{13}C NMR (75 MHz, $CDCl_3$): δ 133.2, 132.9, 131.2, 129.6, 127.1, 127.0, 126.9, 125.4, 62.2, 19.1, 19.0; HRMS (APCI, positive) *m/z* calcd for $C_{24}H_{22}S_9Br_2$ - 757.7554, found 723.7629 $[M - S]^+$; LCMS (APCI, positive) *m/z* calcd for $C_{24}H_{22}S_9{}^{79}Br_2$- 757.8, found 757.4 $[M^+]$. X-ray crystal data: $C_{24}H_{22}Br_2S_9$, *M* = 758.79, triclinic, *a* = 10.990(10) Å, *b* = 13.760(11) Å, *c* = 20.50(2) Å, α = 75.00(4)°, β = 88.43(5) °, γ = 73.35(4) °, *V* = 2865(4) $Å^3$, *T* = 123(2) K, space group $P\bar{1}$, *Z* = 4, μ(MoKα) = 3.509 mm^{-1}, 23751 reflections

measured, 1,714 independent reflections, 9071 with $I > 2\sigma(I)$ (R_{int} = 0.0773). R_1 = 0.0695 ($I > 2\sigma(I)$), $\omega R(F_2)$ = 0.2086 (all data). The goodness of fit on F_2 was 1.073. CCDC 936356.

4-(Trimetnylsilylethynyl)benzaldehyde 81

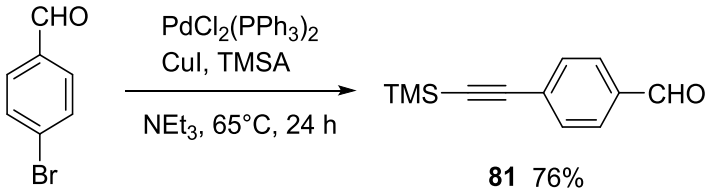

78 **81** 76%

4-Bromobenzaldehyde **78** (4.203 g, 20.72 mmol), CuI (0.220 g, 1.16 mmol), $PdCl_2(PPh_3)_2$ (0.487 g, 0.69 mmol) were placed in a round-bottomed flask with NEt_3 (50 ml). The mixture was then heated to 65 °C and then TMSA (10 mL, 71 mmol) added. The mixture was then stirred for 24 h. The crude mixture was passed through a silica column with a 20% CH_2Cl_2/hexanes solvent system then again with the same solvent system to yield **81** (3.49 g, 17.3 mmol, 76%) as a brown solid. FTIR (neat); 2957, 2897, 2830, 2737, 2156, 1697, 1599, 1562, 1248, 1204, 1161, 837, 758, 658, 535 cm^{-1}; ^1H NMR (300 MHz, $CDCl_3$): δ 10.00 (s, 1H), 7.83 (d, J = 8.5 Hz, 2H), 7.62 (d, J = 8.2 Hz, 2H), 0.27 (s, 9H); MS (APCI, positive) *m/z* calcd for $C_{12}H_{14}OSi$ 202.3, found 202.1 [M^+].

Compound 73

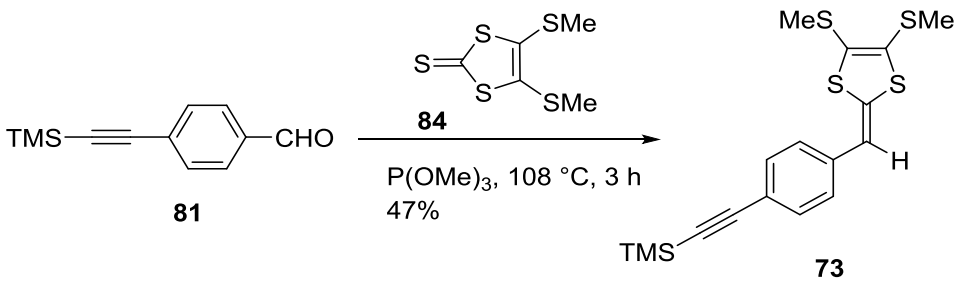

Compound **81** (2.43 g, 12.0 mmol) and thione **84** (2.72 g, 12.0 mmol) were placed in a round-bottomed flask. $P(OMe)_3$ (20 mL) was then added and the mixture was heated to 108 °C for 3 h with stirring. $P(OMe)_3$ was removed by vacuum distillation and the remaining mixture was purified by column chromatography with a 25% CH_2Cl_2/hexanes solvent system to yield **73** (2.15 g, 5.66 mmol, 47%) as a yellow/brown solid. FTIR (neat); 2949, 2147, 1561, 1538, 1497, 1427, 1245, 965, 840, 756 cm^{-1}; ^1H NMR (300 MHz, $CDCl_3$): δ 7.44 (d, *J* = 8.4 Hz, 2H), 7.14 (d, *J* = 8.2 Hz, 2H), 6.44 (s, 1H), 2.44 (s, 3H), 2.43 (s, 3H), 0.26 (s, 9H); MS (APCI, positive) *m/z* calcd for $C_{17}H_{20}S_4Si$ 380.0, found 381.1 $[M + H]^+$.

TTFV 65

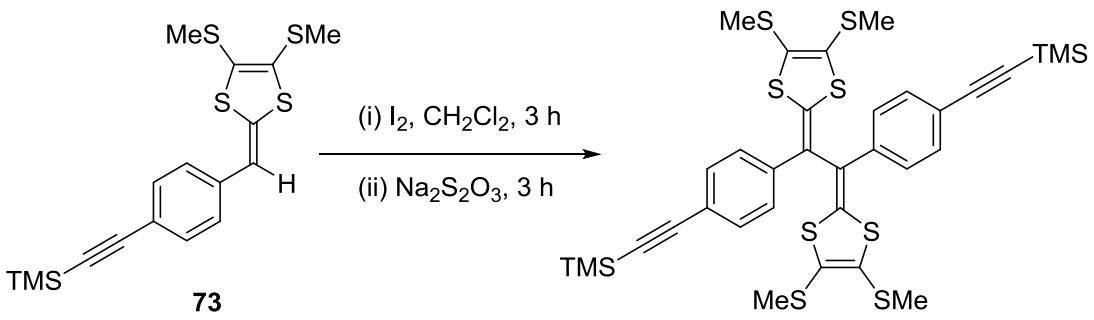

73 **65** 51%

Compound **73** (0.73 g, 1.94 mmol) was placed in a round-bottomed flask with I_2 (1.49 g, 5.89 mmol) and CH_2Cl_2 (25 mL) and stirred for 3 h. $Na_2S_2O_3$ (satd aqueous solution, 20 mL) was then added to the flask and the mixture stirred for 3 h. The organic layer was then separated, dried over $MgSO_4$ and suction filtered. The filtrate was concentrated under vacuum and then purified by column chromatography with a 20% CH_2Cl_2/hexanes solvent system to yield **65** (0.37 g, 0.49 mmol, 51%) as a yellow powder. FTIR (neat); 2955, 2919, 2152, 1500, 1246, 863, 839 cm^{-1}; ^1H NMR (300 MHz, $CDCl_3$): δ 7.39 (d, J = 8.6 Hz, 4H), 7.31 (d, J = 8.6 Hz, 4H), 2.42 (s, 6H), 2.38 (s, 6H), 0.23 (s, 18H); MS (APCI, positive) *m/z* calcd for $C_{34}H_{38}S_8Si_2$ 758.0, found 759.2 $[M + H]^+$. The spectroscopic data are consistent with those reported in the literature.[15, 16]

Compound 91

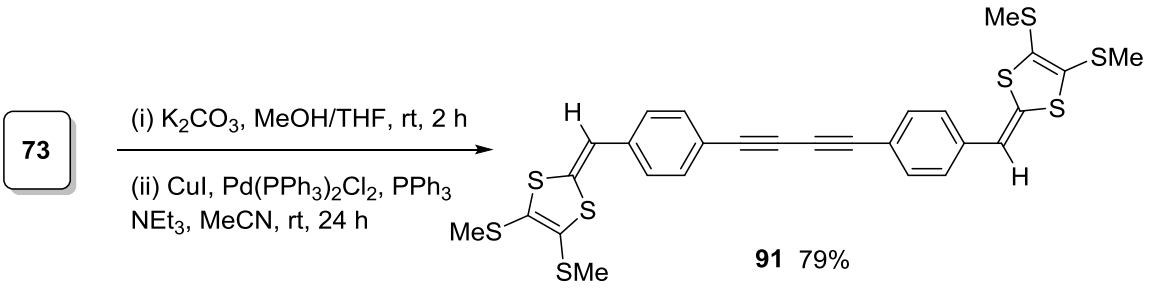

Compound **73** (0.860 g, 2.26 mmol) and K_2CO_3 (1.437 g, 10.41 mmol) were placed in a round-bottomed flask with 1:1 MeOH/THF (20 mL) and stirred for 2 h. The mixture was concentrated under vacuum, washed with NH_4Cl (satd aqueous solution, 3 × 25 mL), H_2O (3 × 25 mL), and dried over $MgSO_4$ and suction filtered. The mixture was then placed into a round-bottomed flask with CuI (0.0013 g, 0.0068 mmol), $PdCl_2(PPh_3)_2$ (0.0502 g, 0.715 mmol), PPh_3 (0.540 g, 0.206 mmol), and 1:1 MeCN /NEt_3 (40 mL). It was then stirred at rt for 24 h. It was then purified by column chromatography with a 25% CH_2Cl_2/hexanes solvent system to yield **91** (0.694 g, 1.13 mmol, 79%) as a yellow solid. FTIR (neat); 2918, 1568, 1538, 1498, 1417, 1404, 1171, 839, 534 cm^{-1}; ^1H NMR (300 MHz, $CDCl_3$): δ 7.51 (d, *J* = 8.4 Hz, 4H), 7.18 (d, *J* = 8.3 Hz, 4H), 6.46 (s, 2H), 2.45 (s, 6H), 2.44 (s, 6H); MS (APCI, positive) *m/z* calcd for $C_{28}H_{22}S_8$ 613.9, found 615.2 $[M + H]^+$. The spectroscopic data are consistent with those reported in the literature.[15, 16]

3-(Trimethnylsilylethynyl)benzaldehyde 82

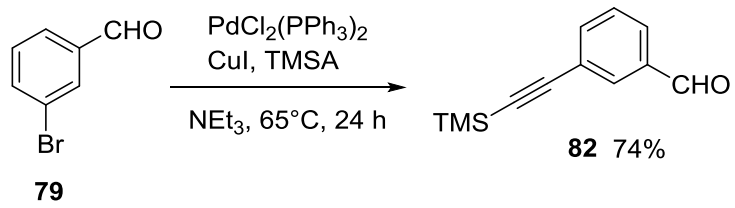

3-Bromobenzaldehyde 79 (5.212 g, 28.17 mmol), CuI (0.178 g, 0.937 mmol), $PdCl_2(PPh_3)_2$ (0.622 g, 0.886 mmol) were placed in a round-bottomed flask with NEt_3 (50 mL). The mixture was then heated to 65 °C and then TMSA (10 mL, 71 mmol) was added. The mixture was then stirred for 24 h. The crude mixture was passed through a silica column with a 20% CH_2Cl_2/hexanes solvent system then again with the same solvent system to yield **82** (4.250 g, 21.01 mmol, 74%) as a brown oil. FTIR (neat); 2959, 2156, 1698, 1598, 1575, 1472, 1433, 1381, 1248, 837, 759, 682, 642 cm^{-1}; ^1H NMR (300 MHz, $CDCl_3$): δ 9.99 (s, 1H), 7.97 (s, 1H), 7.84 (d, *J* = 7.7 Hz, 1H), 7.72 (d, *J* = 7.8 Hz, 1H), 7.50 (t, *J* = 7.7 Hz, 1H), 0.27 (s, 9H); ^{13}C NMR (75 MHz, $CDCl_3$): δ 191.6, 137.6, 136.5, 133.6, 129.2, 129.1, 124.5, 103.5, 96.4, 31.1; MS (APCI, positive) *m/z* calcd for $C_{15}H_{14}OSi$ 202.3, found 203.1 $[M + H]^+$.

Compound 74

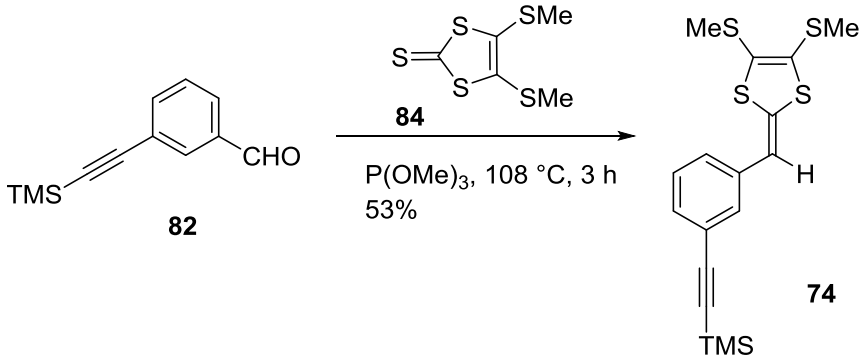

Compound **82** (3.026 g, 14.96 mmol) and thione **84** (3.431 g, 15.15 mmol) were placed in a round-bottomed flask. $P(OMe)_3$ (20 mL) was then added and the mixture was heated to 108 °C for 3 h with stirring. $P(OMe)_3$ was removed by vacuum distillation and the remaining mixture was purified by column chromatography with a 25% CH_2Cl_2/hexanes solvent system to yield **74** (3.017 g, 7.93 mmol, 53%) as an orange/red liquid. FTIR (neat); 2955, 2919, 2152, 1560, 1477, 1402, 1246, 837, 757, 683 cm^{-1}; ^1H NMR (300 MHz, $CDCl_3$): δ 7.28-7.26 (m, 3H), 7.19-7.18 (m, 1H), 2.44 (s, 6H), 0.26 (s, 9H); Meaningful ^{13}C NMR spectrum was not obtained due to poor stability; MS (APCI, positive) *m/z* calcd for $C_{17}H_{20}S_4Si$ 380.0, found 381.2 $[M + H]^+$.

TTFV 66

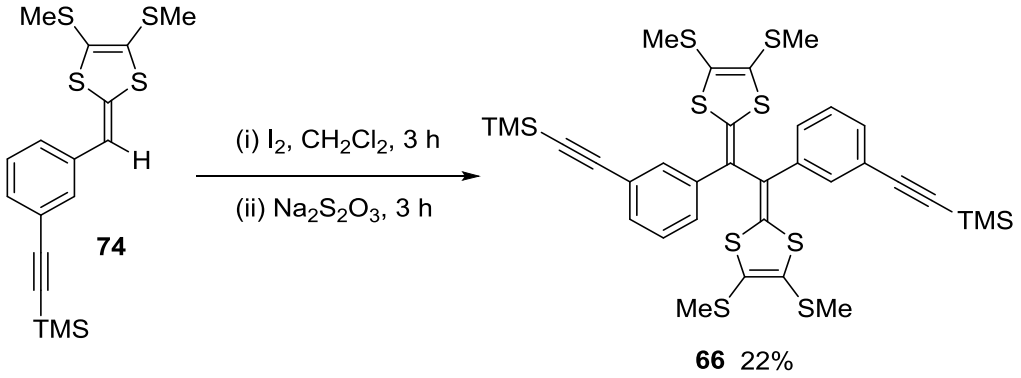

Compound **74** (0.945g, 2.48 mmol) was placed in a round-bottomed flask with I_2 (1.906 g, 7.510 mmol) and CH_2Cl_2 (25 mL) and stirred for 3 h. $Na_2S_2O_3$ (satd aqueous solution, 20 mL) was then added to the flask and the mixture stirred for 3 h. The organic layer was then separated, dried over $MgSO_4$ and suction filtered. The filtrate was concentrated under vacuum and then purified by column chromatography with a 20% CH_2Cl_2/hexanes solvent system to yield **66** (0.209 g, 0.275 mmol, 22%) as an orange oil.

FTIR (neat): 2953, 2918, 2153, 1524, 1489, 1420, 837, 693 cm^{-1}; ^{1}H NMR (300 MHz, $CDCl_3$): δ 7.63 (s, 2H), 7.50-7.49 (m, 6H), 2.58 (s, 6H), 2.56 (s, 6H), 0.41 (s, 18H); Meaningful ^{13}C NMR was not obtained due to poor stability; MS (APCI, positive) *m/z* calcd for $C_{34}H_{38}S_8Si_2$ 758.0, found 759.3 $[M + H]^+$.

Compound 92

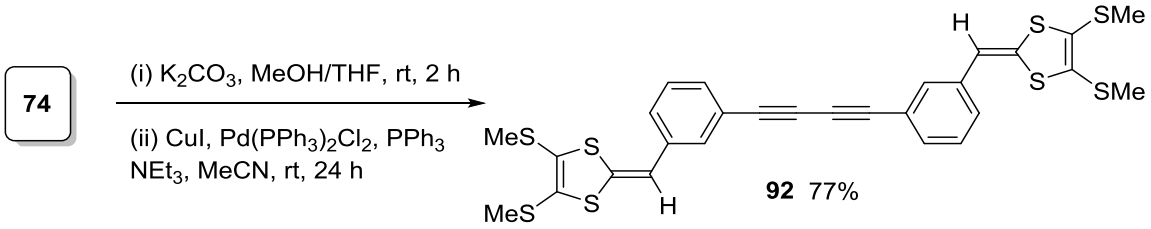

Compound **74** (1.165 g, 3.0595 mmol) and K_2CO_3 (1.735 g, 12.57 mmol) were placed in a round-bottomed flask with 1:1 MeOH/THF (40 mL) and stirred for 2 h. The mixture was concentrated under vacuum, washed with NH_4Cl (satd aqueous solution, 3 × 25 mL), H_2O (3 × 25 mL), and dried over $MgSO_4$ and suction filtered. The mixture was then placed into a round-bottomed flask with CuI (0.0021 g, 0.11 mmol), $PdCl_2(PPh_3)_2$ (0.0763 g, 0.109 mmol), PPh_3 (0.0773 g, 0.295 mmol), and 1:1 MeCN /NEt_3 (40 mL). It was then stirred at rt for 24 h. It was then purified by column chromatography with a 25% CH_2Cl_2/hexanes solvent system to yield **92** (0.732 g, 1.19 mmol, 77%) as an orange solid. FTIR (neat): 2914, 1569, 1493, 1416, 1311, 871, 807, 680, 488, 463 cm^{-1}; ^{1}H NMR (300 MHz, $CDCl_3$): δ 7.37-7.35 (m, 6H), 7.24-7.23 (m, 2H), 6.43 (s, 2H), 2.45 (s, 12H); ^{13}C NMR (75 MHz, $CDCl_3$): δ 136.6, 134.0, 130.4, 129.8, 128.7, 127.6, 124.3, 122.1, 113.3, 19.12, 18.93; MS (APCI, positive) *m/z* calcd for $C_{28}H_{22}S_8$ 613.9, found 615.2 $[M + H]^+$.

2-(Trimethylsilylethynyl)benzaldehyde 83

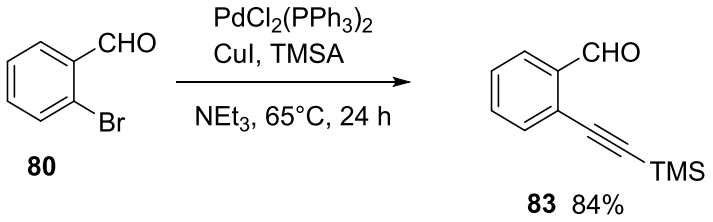

2-Bromobenzaldehyde **80** (4.691 g, 25.36 mmol), CuI (0.142 g, 0.749 mmol), $PdCl_2(PPh_3)_2$ (0.587 g, 0.836 mmol) were placed in a round bottom flask with NEt_3 (50 mL). The mixture was then heated to 65 °C and then TMSA (10 mL, 71 mmol) added. The mixture was then stirred for 24 h. The crude mixture was passed through a silica column with a 20% CH_2Cl_2/hexanes solvent system then again with the same solvent system to yield **83** (4.340 g, 21.45 mmol, 84%) as a brown solid. FTIR (neat); 2957, 2898, 2855, 2762, 2150, 1693, 1592, 1245, 809, 756, 652 cm^{-1}; ^1H NMR (300 MHz, $CDCl_3$): δ 10.56 (s, 1H), 7.92 (d, *J* = 7.2 Hz, 1H), 7.61-7.59 (m, 2H), 7.46-7.45 (m, 1H), 0.28 (s, 9H); ^{13}C NMR (75 MHz, $CDCl_3$): δ 192.1, 136.4, 133.9, 133.7, 129.1, 127.1, 127.0, 102.7, 100.3; MS (APCI, positive) *m/z* calcd for $C_{12}H_{15}OSi$ 202.3, found 202.1 [M + H]$^+$.

DTF 75

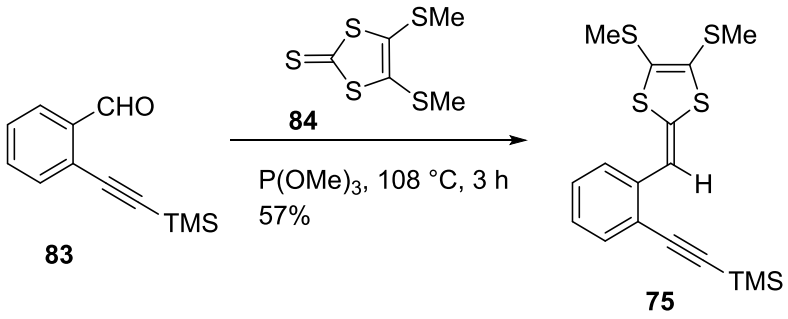

Compound **83** (3.519 g, 17.39 mmol) and thione **84** (4.005 g, 17.69 mmol) were placed in a round-bottomed flask. $P(OMe)_3$ (20 mL) was then added and the mixture was heated to 108 °C for 3 h with stirring. $P(OMe)_3$ was removed by vacuum distillation and the remaining mixture was purified by column chromatography with a 25% CH_2Cl_2/hexanes solvent system to yield **75** (3.801 g, 9.980 mmol, 57%) as a yellow oil. FTIR (neat): 2955, 2919, 2149, 1563, 1246, 864, 836, 748 cm^{-1}; ^1H NMR (300 MHz, $CDCl_3$): δ 7.47 (d, *J* = 7.5 Hz, 1H), 7.35-7.34 (m, 2H), 7.12-7.11 (m, 1H), 6.98 (s, 1H), 2.45 (s, 3H), 2.41 (s, 3H), 0.27 (s, 9H); ^{13}C NMR (75 MHz, $CDCl_3$): δ 137.9, 134.3, 132.8, 128.5, 127.6, 125.5, 125.0, 124.1, 121.0, 113.06, 100.0, 19.0, 18.9; MS (APCI, positive) *m/z* calcd for $C_{17}H_{20}S_4Si$ 380.0, found 381.1 $[M + H]^+$.

TTFV 67

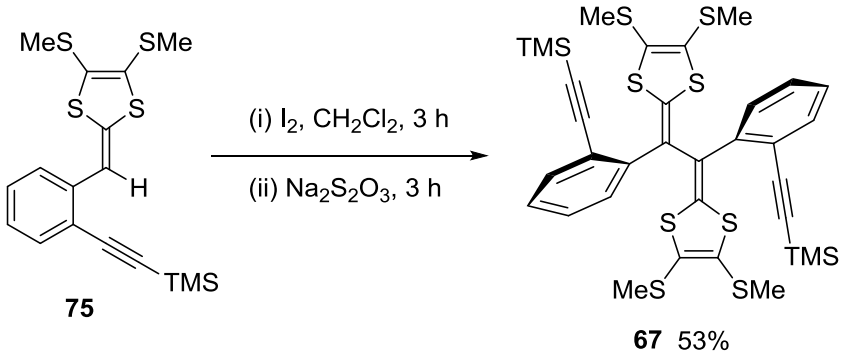

Compound **75** (0.865 g, 2.27 mmol) was placed in a round-bottomed flask with I_2 (1.91 g, 7.51 mmol) and CH_2Cl_2 (25 mL) and stirred for 3 h. $Na_2S_2O_3$ (satd aqueous solution, 20 mL) was then added to the flask and the mixture stirred for 3 h. The organic layer was then separated, dried over $MgSO_4$ and suction filtered. The filtrate was concentrated under vacuum and then purified by column chromatography with a 20%

CH_2Cl_2/hexanes solvent system to yield **67** (0.457 g, 0.602 mmol, 53%) as an orange oil. FTIR (neat): 2954, 2919, 2155, 1471, 1429, 1245, 837, 753 cm^{-1}; ^1H NMR (300 MHz, $CDCl_3$): δ 7.32-7.30 (m, 4H), 7.18-7.17 (m, 4H), 2.45 (s, 6H), 2.35 (s, 6H), 0.25 (s, 18H); Meaningful ^{13}C NMR spectrum was not obtained due to poor stability; MS (APCI, positive) *m/z* calcd for $C_{34}H_{38}S_8Si_2$ 758.0, found 759.2 $[M + H]^+$.

Compound 93

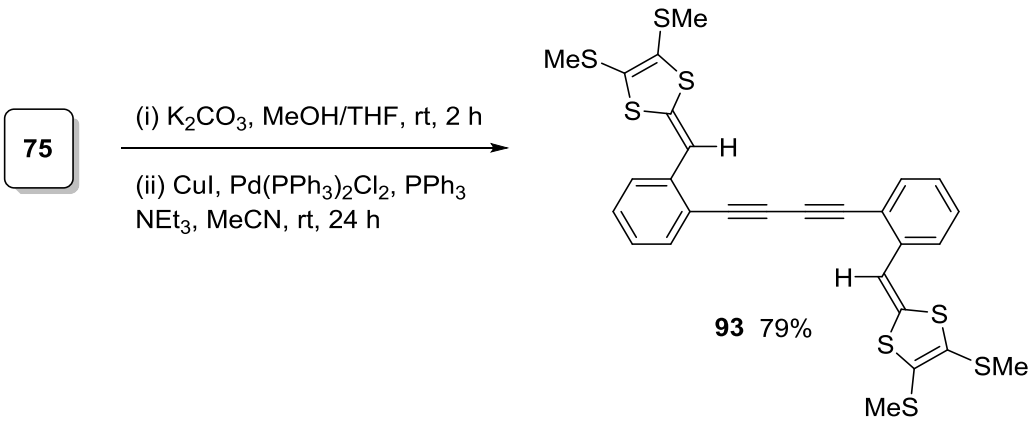

Compound **74** (1.165 g, 3.059 mmol) and K_2CO_3 (1.520 g, 11.01 mmol) were placed in a round-bottomed flask with 1:1 MeOH/THF (40 mL) and stirred for 2 h. The mixture was concentrated under vacuum, washed with NH_4Cl (satd aqueous solution, 3 × 25 mL), H_2O (3 × 25 mL), and dried over $MgSO_4$ and suction filtered. The mixture was then placed into a round-bottomed flask with CuI (0.0022 g, 0.12 mmol), $PdCl_2(PPh_3)_2$ (0.0715 g, 0.102 mmol), PPh_3 (0.0769 g, 0.293 mmol), and 1:1 MeCN /NEt_3 (40 mL). It was then stirred at rt for 24 h. The reaction mixture was then concentrated under vacuum and the residual was passed through a silica column with a 25% CH_2Cl_2/hexanes solvent system to yield **93** (0.747 g, 1.22 mmol, 79%) as a yellow powder. FTIR (neat): 2917,

1564, 1487, 1415, 1309, 875, 807, 680, 653, 490 cm^{-1}; ^{1}H NMR (300 MHz, $CDCl_3$): δ 7.56 (d, *J* = 7.5 Hz, 2H), 7.41-7.39 (m, 4H), 7.17-7.16 (m, 2H), 7.00 (s, 2H), 2.47 (s, 6H), 2.42 (s, 6H); ^{13}C NMR (75 MHz, $CDCl_3$): δ 139.0, 135.6, 133.8, 129.3, 128.1, 125.6, 125.2, 123.9, 119.7, 112.4, 19.1, 19.0; MS (APCI, positive) *m/z* calcd for $C_{28}H_{22}S_8$ 613.9, found 615.2 $[M + H]^+$.

2.4 Conclusions

In this chapter, a selection of aryl-substituted TTFV derivatives **60**-**67**, in which the aryl groups are naphthyl, bromophenyl, and alkynylphenyl units, has been successfully synthesized using phosphite-promoted olefination reactions and iodine-induced oxidative coupling reactions as the key steps, with an exception in the case of *ortho*-bromophenyl-TTFV **64**. The *ortho*-bromo group was found to divert the reaction mechanism to an unexpected cycloaddition, resulting in the formation of a bis-spiro product **87** rather than the desired TTFV structure. This synthetic outcome suggests that the *ortho*-substitution effect could be a very significant factor in the oxidative dimerization reaction. In the synthesis of alkynyl-substituted TTFVs **65**-**67** shows that meta-alkynyl substitution tends to reduce the chemical stability of TTFV. The exact reason for such a chemical behavior is unclear at this stage. Further investigation needs to conduct to carefully analyze the decomposition products as well as the mechanisms related. Finally, a group of butadiyne-centered exTTFs **91**-**93** was synthesized through alkynyl homocoupling reactions. The synthetic work reported in this chapter allows the properties of these TTFVs and related derivatives to be systematically characterized by

various spectroscopic analyses, the details of which will be subsequently described in Chapter 3.

2.5 References

1. Zhao, Y.; Chen, G.; Mulla, K.; Mahmud, I.; Liang, S.; Dongare, P.; Thompson, D. W.; Dawe, L. N.; Bouzan, S., Tetrathiafulvalene Vinylogues as Versatile Building Blocks for New Organic Materials. *Pure & Appl. Chem.* **2012**, *84*, 1005-1025.

2. Yoshida, Z.-i.; Kawase, T.; Awaji, H.; Sugimoto, I.; Sugimoto, T.; Yoneda, S., Synthesis and Properties of Ethanediylidene-2,2′-bis(1,3-dithiole). *Tetrahedron Lett.* **1983**, *24*, 3469-3472.

3. Sugimoto, T.; Awaji, H.; Sugimoto, I.; Misaki, Y.; Kawase, T.; Yoneda, S.; Yoshida, Z.; Kobayashi, T.; Anzai, H., Ethylene Analogs of Tetrathiafulvalene and Tetraselenafulvalene: New Donors for Organic Metals. *Chem. Mater.* **1989**, *1*, 535-547.

4. Bryce, M. R.; Chesney, A.; Yoshida, S.; J. Moore, A.; Batsanov, A. S.; A. K. Howard, J., Synthesis and X-ray Crystal Structure of a Vinylogue of Tetramethyltetraselenafulvalene. *J. Mater. Chem.* **1997**, *7*, 381-385.

5. Moore, A. J.; Bryce, M. R., Generation and Trapping of Phosphorus Stabilized 4,5-Ethylenedithio-1,3-dithiol-2-ide Carbanions: Synthesis of Ethylenedithio-1,3-dithiafulvalenes. *Synthesis* **1991**, *1991*, 26-28.

6. Misaki, Y.; Ohta, T.; Higuchi, N.; Fujiwara, H.; Yamabe, T.; Mori, T.; Mori, H.; Tanaka, S., A Vinylogue of Bis-fused Tetrathiafulvalene: Novel π-Electron Framework for Two-Dimensional Organic Metals. *J. Mater. Chem.* **1995**, *5*, 1571-1579.

7. Hansen, T. K.; Lakshmikantham, M. V.; Cava, M. P.; Metzger, R. M.; Becher, J., Synthesis and Properties of New π-Donor Sulfur Heterocycles. *J. Org. Chem.* **1991**, *56*, 2720-2722.

8. Bellec, N.; Boubekeur, K.; Carlier, R.; Hapiot, P.; Lorcy, D.; Tallec, A., Controlling the Conformation Changes Associated to Electron Transfer Steps through Chemical Substitution: Intriguing Redox Behavior of Substituted Vinylogous TTF. *J. Phys. Chem. A* **2000**, *104*, 9750-9759.

9. Yamashita, Y.; Tomura, M.; Tanaka, S.; Imaeda, K., Novel TTF Vinylogues Affording Stable Cation Radicals. *Synth. Met.* **1999**, *102*, 1730-1731.

10. Yamashita, Y.; Tomura, M.; Imaeda, K., Hydroxyphenyl Substituted Tetrathiafulvalene Vinylogues Affording Stable Cation Radical Salts with Unusual Crystal Structures. *Tetrahedron Lett.* **2001**, *42*, 4191-4193.

11. Yamashita, Y.; Tomura, M., Preparation and Structures of Dication Salts of Phenyl-Substituted TTF Vinylogues. *J. Solid State Chem.* **2002**, *168*, 427-432.

12. Yamashita, Y.; Tomura, M.; Badruz Zaman, M., Synthesis and Properties of Novel Tetrathiafulvalene Vinylogues. *Chem. Commun.* **1998**, 1657-1658.

13. Rimbaud, C.; Le Magueres, P.; Ouahab, L.; Lorcy, D.; Robert, A., 1,2-Bis(5-methyl-4-methylthio-1,3-dithiolium-2-ylidene)-1,2-diphenylethane Bis(triiodide) and 1,2-

Bis(4-methoxyphenyl)-1,2-bis(5-methyl-4-methylthio-1,3-dithiolium-2-ylidene)ethane Diperchlorate. *Acta Cryst.* **1998**, *C54*, 679-681.

14. Massue, J.; Bellec, N.; Guerro, M.; Bergamini, J.-F.; Hapiot, P.; Lorcy, D., Crown Ether Vinylogous Tetrathiafulvalene Receptors: Complexation Interference on the Molecular Movements Triggered by Electron Transfer. *J. Org. Chem.* **2007**, *72*, 4655-4662.

15. Chen, G.; Mahmud, I.; Dawe, L. N.; Zhao, Y., Acetylenic Phenyldithiafulvene: A Versatile Synthon for TTFV-Based Macromolecules. *Org. Lett.* **2010**, *12*, 704-707.

16. Chen, G.; Mahmud, I.; Dawe, L. N.; Daniels, L. M.; Zhao, Y., Synthesis and Properties of Conjugated Oligoyne-Centered π-Extended Tetrathiafulvalene Analogues and Related Macromolecular Systems. *J. Org. Chem.* **2011**, *76*, 2701-2715.

17. Moltzen, K.G.; Senniy, A.; Hazell, R. G.; Lund, H.; The Role of Carbon Monosulfide in the Electrochemical Preparation of 4,5-Bis(methylthio)-1,3-dithiole-2-thione, *Acta Chem. Scand. B*, **1986**, 40, 593-597.

Chapter 3 Analysis of the Structure-Property Relationships for Aryl-Substituted TTFVs

3.1 Introduction

As discussed in the previous chapters, TTFV derivatives exhibit rich redox activity and conformational switching properties associated with the redox processes. In the cases of aryl-substituted TTFVs, the electronic properties, such as HOMO-LUMO gap, ionization potentials, and vertical excitation energies, can be readily modified by the substitution effects imposed on the aryl rings. This is because different substituents on the aryl groups can not only change the π-electron density of the central TTFV moiety through resonance and inductive effects, but also alter the conformation of the TTFV framework through steric, dipole-dipole, or hydrogen bonding interactions. The synthetic access to the various TTFV derivatives established in Chapter 2 thus allows for a comprehensive investigation on the structural, electronic, and redox properties of these compounds. This chapter describes the detailed characterization results and tries to reasonably correlate the properties with the effects of substituents. The ultimate goal of this study is to gain a better understanding on the structure-property relationships involved in various TTFV containing systems, so as to make the acquired knowledge useful in the design of TTFV-based functional molecular materials and devices. It is worth mentioning that parts of the characterization results have been recently published.[1, 2]

3.2 Results and Discussion

3.2.1 Substitution Effects on the Solid-State Structural Properties

The single crystal structure of bis(1-naphthyl)-TTFV **60** was determined by single-crystal X-ray diffraction analysis. Figure 3.2 shows the molecular geometry and solid-state packing of compound **60**. As predicted by the steric hindrance argument made previously, **60** possesses an almost planar, *s-trans* TTFV conformation, in which the torsion angle between the two vinyl units (C1-C4-C5-C6) deviates from planarity slightly by ca. 3° (Figure 3.1 A and B). The two 1-naphthyl rings are oriented perpendicular to the central TTFV plane to avoid significant allylic interaction. In the solid-state packing diagram (Figure 3.1 C), intimate face-to-edge stacking of the naphthyl groups (d = 3.36 Å) at adjacent molecules can be seen. This kind of interactions yield the so-called "brick and mortar" packing motif,[3-6] which is beneficial for the crystal engineering of organic semiconductors with enhanced properties such as high charge mobility.

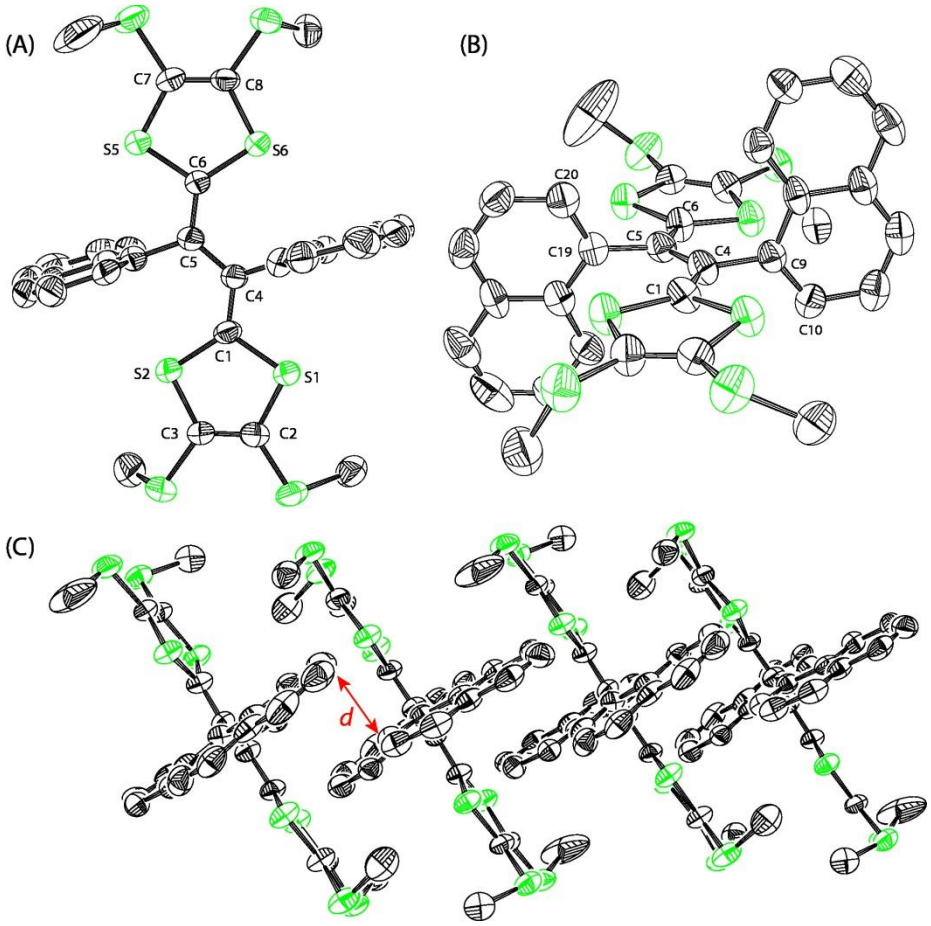

Figure 3.1 ORTEP plots of **60** at 50% ellipsoid probability. (A) Front view, (B) side view, and (C) crystal packing diagram. Selected bond distances (Å): C(1)-C(4) 1.393(7), C(4)-C(5) 1.428(8), C(5)-C(6) 1.396(8), C(1)-S(1) 1.777(6), C(1)-S(2) 1.746(6), S(1)-C(2) 1.752(6), S(2)-C(3) 1.769(6), C(2)-C(3) 1.342(9). Selected bond angles (°): S(1)-C(1)-S(2) 112.4(3), C(1)-C(4)-C(5) 124.2(5), C(1)-C(4)-C(9) 115.1(5), C(4)-C(5)-C(6) 124.1(5). Selected torsion angles (°): C(1)-S(1)-C(2)-C(3) -2.6(5), S(1)-C(1)-C(4)-C(9) -1.8(7), C(1)-C(4)-C(5)-C(19) 4.0(9), C(1)-C(4)-C(9)-C(10) 85.7(7), C(1)-C(4)-C(9)-C(18) -91.1(6). CCDC 888258.

Unlike **60**, bis(2-naphthyl)-TTFV **61** assumes a non-planar, twisted TTFV conformation (Figure 3.2 A and B), in which the torsion angle between the two vinyl

groups is 112°. This angle is much greater than those observed in the crystal structures of typical phenyl-substituted TTFV derivatives (usually from 40-75°), indicating that the bulkiness of the naphthyl substituent plays an important role in dictating conformation. Also of note is that each naphthyl group rotates away from the adjacent dithiole ring by 36°, and such a highly distorted conformation results in less intimate intermolecular π-contact than that of **60**. The loosely packed crystal structure of **61** can reasonably account for its much lower melting point (190 °C) than that of **60** (251 °C).

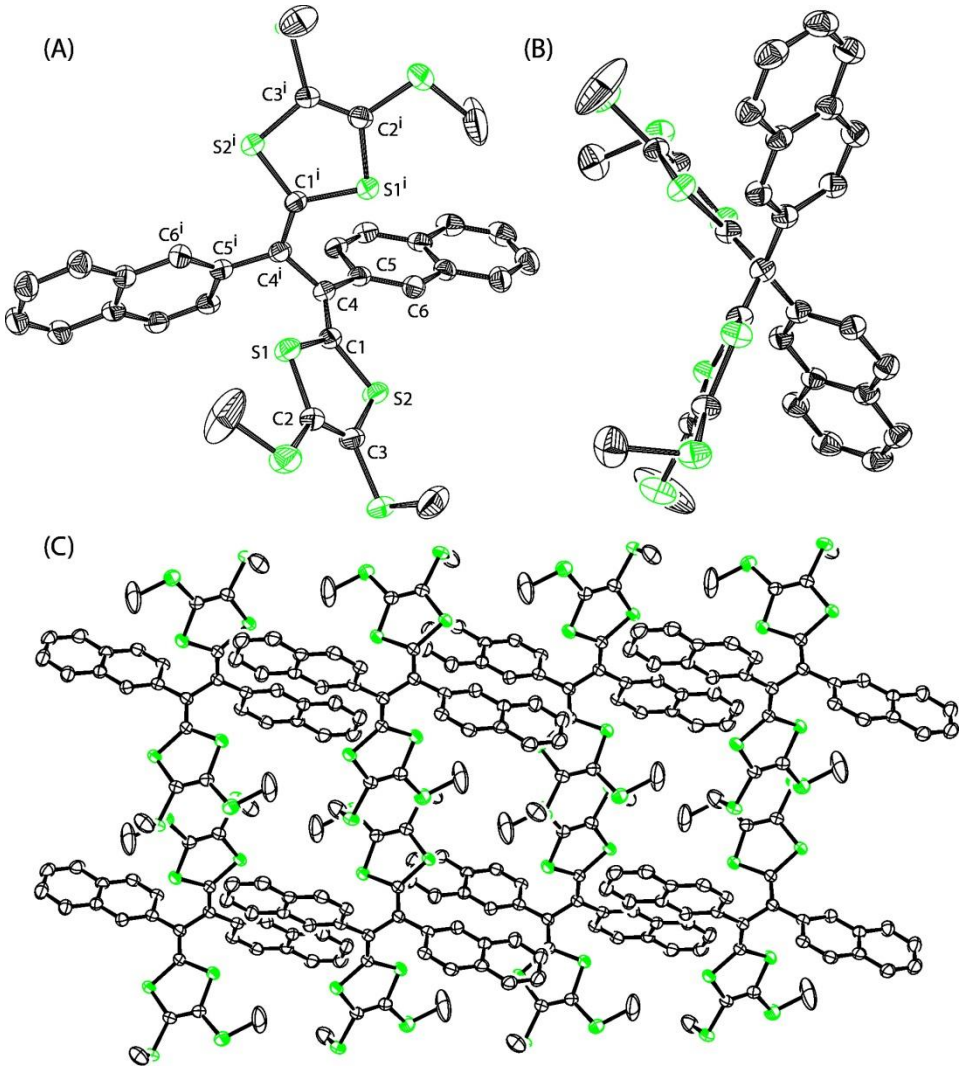

Figure 3.2 ORTEP plots of **61** at 50% ellipsoid probability. (A) Front view, (B) side view, and (C) crystal packing diagram. Selected bond distances (Å): S(1)-C(1) 1.763(2), S(1)-C(2) 1.745(2), S(2)-C(1) 1.756(2), S(2)-C(3) 1.749(2), C(1)-C(4) 1.351(3), C(2)-C(3) 1.344(3), C(4)-C(4i) 1.4994(4). Selected bond angles (°):S(1)-C(1)-S(2) 113.20(13), C(1)-C(4)-C(5) 124.00(20), C(4)-C(5)-C(6) 122.9(2). Selected torsion angles (°):C(1)-S(1)-C(2)-C(3) 1.00(18), S(1)-C(1)-C(4)-C(4i) -3.57(19), C(1)-C(4)-C(4i)-C(1i) 111.78(2), C(1)-C(4)-C(5)-C(6) -36.3(3). i = 1-x, y,1/2-z. CCDC 888259.

The single crystal structures of **70** and **87** were also determined by X-ray structural analysis (Figure 3.3). The molecular structure of dithiafulvene precursor **70** assumes a slightly twisted conformation along the π-conjugated framework, with the torsion angle between the phenyl and vinylene units being 19.4°. It is noteworthy that the C-S-C bond angles in the dithiole ring are around 95°, which is consistent with the known fact that sulfur atom prefers to adopt a 90° bond angle.[7] The relatively small C-S-C bond angle hence drives the dithiole five-membered ring to take a non-planar structure as can be clearly seen in Figure 3.3 B.

Of great interest is the unusual bis-spiro motif in compound **87**. Compound **87** crystallized with two chemically identical molecules in the asymmetric unit, but for simplicity only one is shown in Figure 3.3. As a result of the significant steric hindrance in **87**, the two dithiole and two phenyl rings surrounding the central tetrahydrothiophene unit are in a nearly perpendicular orientation. The two bromo groups are positioned in a *trans* orientation so as to reduce the net molecular dipole moment. This orientation possibly enables the bromine atoms to form intramolecular hydrogen bonds, stabilizing its dicationic form and preventing the benzylic protons from deprotonation. On the other, steric effects or dipole interactions may contribute to the stabilization. The exact physical origin has not been experimentally confirmed and certainly warrants continued investigation in future work. The crystal structure hence indicates that the formation of the bis-spiro compound **87** can be reasonably correlated to the *ortho*-bromo substitution effect.

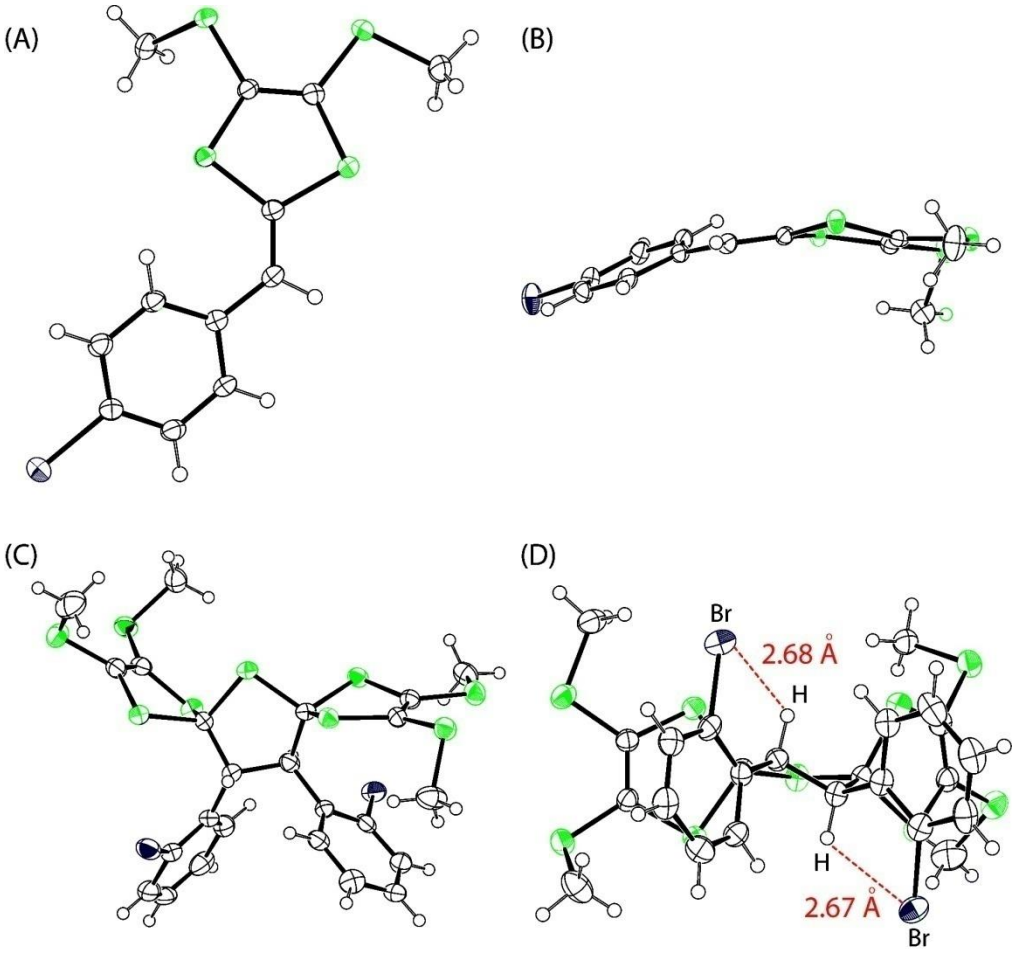

Figure 3.3 ORTEP plots (50% ellipsoid probability) of compounds **70** (CCDC 936355) and **87** (CCDC 936356): (A) front view of **70**, (B) side view of **70**, (C) front view of **87**, and (D) side view of **87**. Atomic color code: Grey = C, Green = S, Blue = Br, H represented by spheres.

3.2.2 Electrochemical Properties

The redox properties of naphthyl-substituted TTFVs **60** and **61** were investigated by cyclic voltammetry (CV) and differential pulse voltammetry (DPV). The CV of **60** reveals two reversible wave pairs (E_{pa}^{1} = +0.44 V, E_{pc}^{1} = +0.33 V, E_{pa}^{2} = +0.68 V, E_{pc}^{2} =

+0.57 V) corresponding to two single-electron transfers. This is consistent with the DPV results which show two oxidation peaks at +0.36 V and +0.60 V with equal intensity. The CV of **61** shows a quasi-reversible redox wave pair at E_{pa} = +0.64 V, E_{pc} = +0.44 V which is substantially shifted towards the positive direction in comparison to **60**. This reversible wave pair is attributed to a concerted two-electron transfer reaction as a result of potential inversion in the molecule. This CV data depicts two very different redox patterns for the two bis(naphthyl)-TTFV isomers, corroborating the hypothesis by Yamashita of the *ortho* steric effects on conformation and redox behaviour. [8]

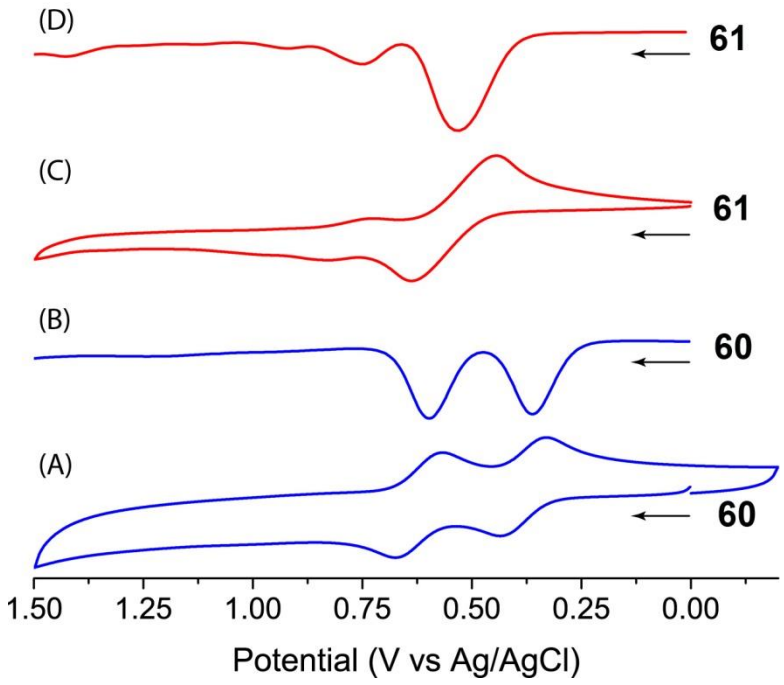

Figure 3.4 (A) Cyclic voltammogram and (B) differential pulse voltammogram of **60**. (C) Cyclic voltammogram and (D) differential pulse voltammogram of **61**. Supporting electrolyte, Bu_4NBF_4 (0.1 M); solvent, CH_2Cl_2; working electrode, glassy carbon; counter electrode, Pt; reference electrode, Ag/AgCl; For CV measurements: scan rate: 200 mV/s. For DPV measurements: step: 4 mV, pulse width: 50 ms, pulse period: 200 ms, scan rate: 20 mV/s.

The cyclic voltammetric properties of bromophenyl-substituted DTFs and TTFVs are shown in Figure 3.5. In Figure 3.5 A, compound **70** exhibits a pair of redox peaks at +0.78 V and +0.46 V, which are attributed to a single-electron oxidation process on the dithiafulvene unit and reduction of the resulting TTFV dication. The voltammogram of **71** shows very similar patterns to those of **70**, with the redox peaks slightly shifted to the positive potential direction. The voltammogram of the *ortho*-bromo isomer **72** shows a similar anodic peak at +0.80 V, but the profile of the reverse scan appears to be very complex, with a number of weak anodic peaks observable. Such a feature is indicative of chemical irreversibility and is likely due to some electrochemical (EC) reaction mechanisms (e.g. electrochemical hydrodehalogenation[9]). The exact mechanisms still await further investigations to clarify.

The voltammograms of bis(bromophenyl)-TTFV isomers **62** and **63** feature a similar pair of reversible redox peaks that can be assigned to the known simultaneous two-electron transfer on the TTFV unit. Unlike their dithiafulvene precursors, the different bromo-substitution positions in **62** and **63** result in noticeable differences in the redox potentials. As shown in Figure 3.5 B, the redox peaks of *meta*-bromo isomer **63** are shifted to the negative potential direction by ca. 40 mV relative to **62**. The redox properties of **87** appear to be complex. Two anodic peaks are clearly seen at +0.63 V and +1.05 V in the positive scan. On the reverse scan, several cathodic peaks emerge. Clearly, the *ortho*-bromo substitution induces some kinds of electrochemical reactions to give rise to such electrochemical behaviour.

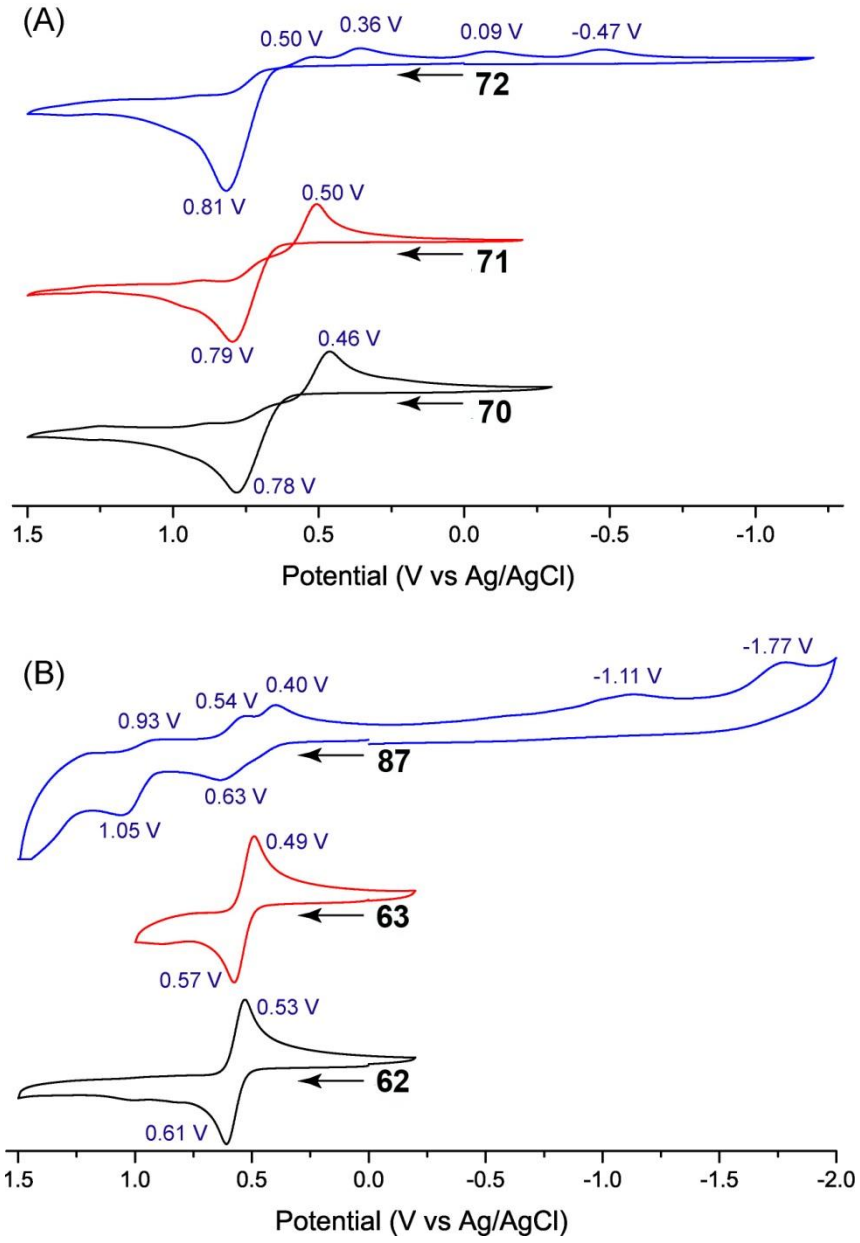

Figure 3.5 Cyclic voltammograms for (A) bromophenyl-DTFs **70**-**72**, and (B) TTFVs **62**-**63** and bis-spiro compound **87**. Supporting electrolyte, Bu_4NBF_4 (0.1 M); solvent, CH_2Cl_2; working electrode, glassy carbon; counter electrode, Pt; reference electrode, Ag/AgCl; scan rate: 200 mV/s.

The electrochemical properties of alkynylphenyl-DTF **73-75** were also investigated by cyclic voltammetry (Figure 3.6). In the cyclic voltammograms, *para*-alkynyl derivative **73** shows the lowest oxidation potential at E_{pa} = +0.90 V. This can be explained by that the *para*-alkynyl provides a resonance effect to stabilize the oxidized product, DTF radical cation. Similarly, the *ortho*-alkynyl derivative **75** shows an oxidation potential at E_{pa} = +0.98 V, which is slightly shifted anodically relative to that of **73**. The *meta*-alkynyl derivative **74** gives the highest oxidation potentials at +1.19 V, which is due to the lack of resonance effect by the *meta*-substitution. In the reverse scan, **73** shows a cathodic peak at +0.53 V, which can be assigned to the TTFV product arising from the oxidative dimerization of **73** on the surface of working electrode. In addition to this peak, two cathodic peaks appear in the negative potential region (-0.13 V and -0.44 V). These peaks are tentatively assigned to some products other than TTFV during the oxidation processes. For compound **74**, one cathodic peak can be observed in the positive window at +0.44 V, along with two others (-0.20 V and -0.56 V) in the negative potential region. For compound **75**, two cathodic peaks appear in the positive window (+0.64 and +0.37 V). Most likely, they are associated with a two-step reduction of the TTFV product (see Figure. 3.4 A and B). In addition, one cathodic peak is seen in the negative window at -0.46 V.

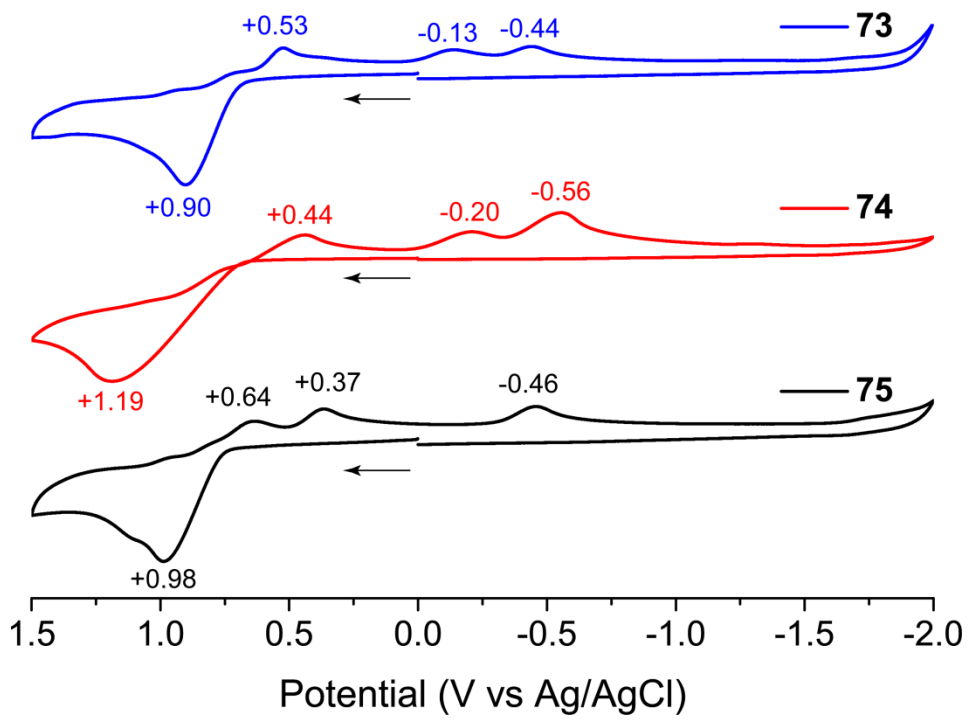

Figure 3.6 Cyclic voltammograms for alkynylphenyl-DTFs **73**-**75**. Supporting electrolyte, Bu_4NBF_4 (0.1 M); solvent, CH_2Cl_2; working electrode, glassy carbon; counter electrode, Pt; reference electrode, Ag/AgCl; scan rate: 200 mV/s.

The cyclic voltammograms of bis(alkynylphenyl)-TTFVs **65**-**67** are compared in Figure 3.7. Both the *para* (**65**) and *meta* (**66**) show a typical pattern of chemically reversible simultaneous two-electron transfer in their voltammograms. However, the redox peaks are slightly different. For compound **65**, the redox wave pair is observed to have a narrower gap (E_{pa} = +0.68 V, E_{pc} = +0.50 V, ΔE = 0.18 V), while for compound **66** the redox feature is more close to a quasi-reversible pattern (E_{pa} = +0.75 V, E_{pc} = +0.44 V, ΔE = 0.31 V). Of great interest is the dramatically different redox pattern observed for the *ortho*-alkynyl-substituted TTFV **67**. Its voltammogram clearly shows two reversible

redox wave pairs at E_{pa}^{1} = +0.50 V, E_{pa}^{2} = +0.78 V, E_{pc}^{1} = +0.34 V, E_{pc}^{2} = +0.62 V. These features resemble those observed in the *trans*-bis(1-naphthyl)-TTFV **60** (Figure 3.4), suggesting that the conformation of **67** could also be *trans*, due to the steric bulkiness imposed by the *ortho*-alkynyl groups.

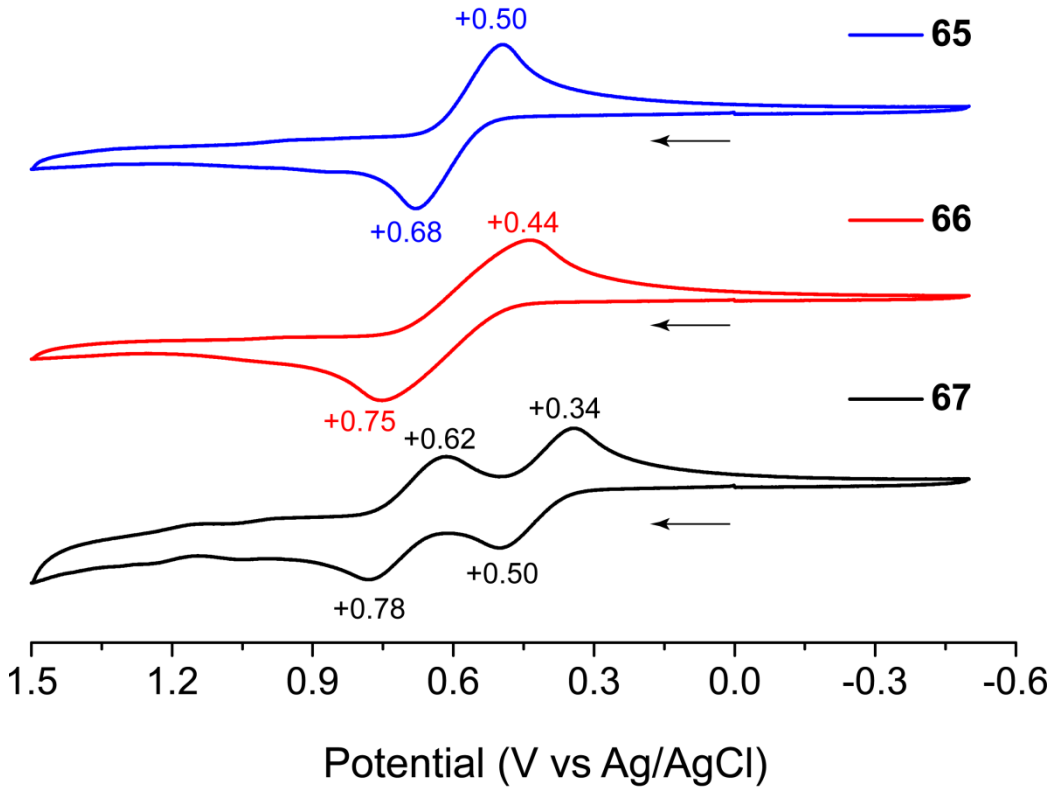

Figure 3.7 Cyclic voltammograms for alkynylphenyl-TTFVs **65**-**67**. Supporting electrolyte, Bu_4NBF_4 (0.1 M); solvent, CH_2Cl_2; working electrode, glassy carbon; counter electrode, Pt; reference electrode, Ag/AgCl; scan rate: 200 mV/s.

The cyclic voltammograms of bis(DTF)-endcapped butadiynes **91**-**93** are shown in Figure 3.8. Of these three isomers, it is interesting to see an increasing trend of the oxidation potentials of the DTF moieties from *para* **91** (+0.90 V) to *meta* **92** (+0,98 V) to

ortho **93** (+1.02 V). The trend can be reasonably correlated with the conjugation degree between the DTF moiety and the phenyl ring. In the reverse scans, a cathodic peak due to the reduction of TTFV can be seen in each of the voltammograms for **91** and **92**, indicating that the two compounds can undergo electrochemically-induced oxidative DTF dimerization on the electrode surface. For compound **93**, in which the DTF unit is *ortho* to the butadiyne group, such a feature is not observable. This can be explained by the increased steric hindrance that impedes the DTF dimerization pathway. In all the three voltammograms, several anodic peaks in the negative potential region can be seen. These peaks are similar to those observed in alkynylphenyl-DTFs (see Figure 2.6), and their origins are tentatively attributed to the reduction of some electrochemical byproducts in the oxidation process.

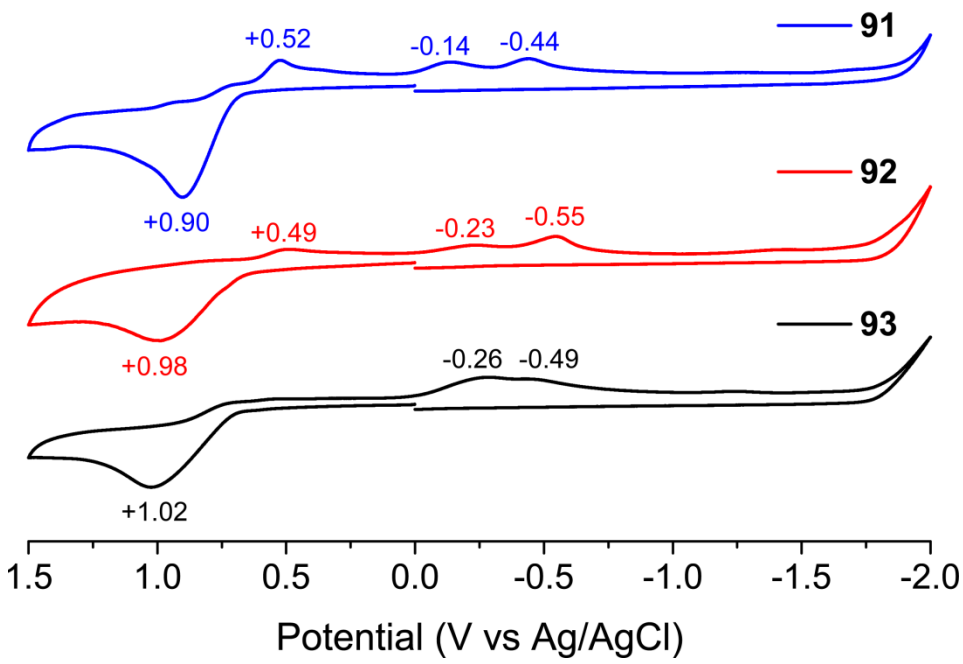

Figure 3.8 Cyclic voltammograms for exTTFs **91-93**. Supporting electrolyte, Bu_4NBF_4 (0.1 M); solvent, CH_2Cl_2; working electrode, glassy carbon; counter electrode, Pt; reference electrode, Ag/AgCl; scan rate: 200 mV/s.

3.2.3 Electronic Absorption Properties

The electronic absorption properties of naphthyl-TTFVs **60** and **61** as well as their naphthyl dithiafulvene precursors **68** and **69** were studied by UV-Vis spectroscopic analysis (Figure 3.9). Interestingly, planar TTFV **60** shows very different absorption features in the low-energy region compared with the others. In the spectrum of **60**, an absorption peak at 288 nm and two shoulders at 329 and 387 nm are seen, while for **61**, **68** and **69** a broad absorption band from 330 to 425 nm dominates the low-energy absorption features. It is noted that the cut-off energy of the lowest-energy band for **60** is redshifted relative to that for **61**. This observation concurs with the results of X-ray

structural analysis, which indicates that **60** is more planar and hence possesses a higher degree of π-delocalization than **61**. In the crystal structures, the bond length alternation (BLA) of the central vinyl π-bridge in **60** is smaller than that of **61** (**60**: C=C 1.39 Å and C-C 1.43 Å; **61**: C=C 1.35 Å, C-C 1.50 Å), and DFT calculations predict that the HOMO-LUMO gap of **60** (3.0 eV) is smaller than that of **61** (3.5 eV).[2]

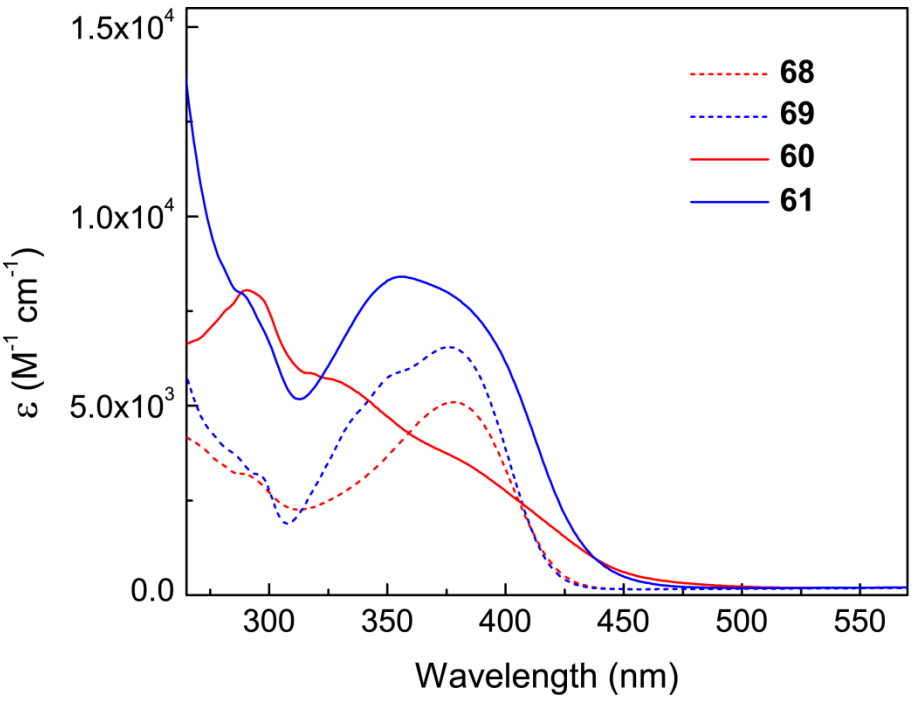

Figure 3.9 UV-Vis absorption spectra of naphthyl-substituted TTFVs and DTFs **60**, **61**, **68** and **69** measured in CH_2Cl_2 at room temperature.

The normalized UV-Vis absorption spectra of bromophenyl-substituted DTFs **70**-**72** and TTFVs **62**, **63**, and spiro-compound **87** are shown in Figure 3.10. It can be clearly seen that the absorption spectra of bromophenyl-DTFs **70**-**72** are nearly superimposable, and so are the spectra of TTFVs **62** and **63**, suggesting that changing the bromo-

substitution position has little effect on the electronic absorption properties. The UV-Vis spectrum of bis-spiro **87** shows a maximum absorption peak at 311 nm, which is considerably blueshifted in comparison with those of the other compounds at ca. 357 nm. It is also notable that there is a significantly long absorption tail extending to ca. 470 nm in the spectrum of **87**.

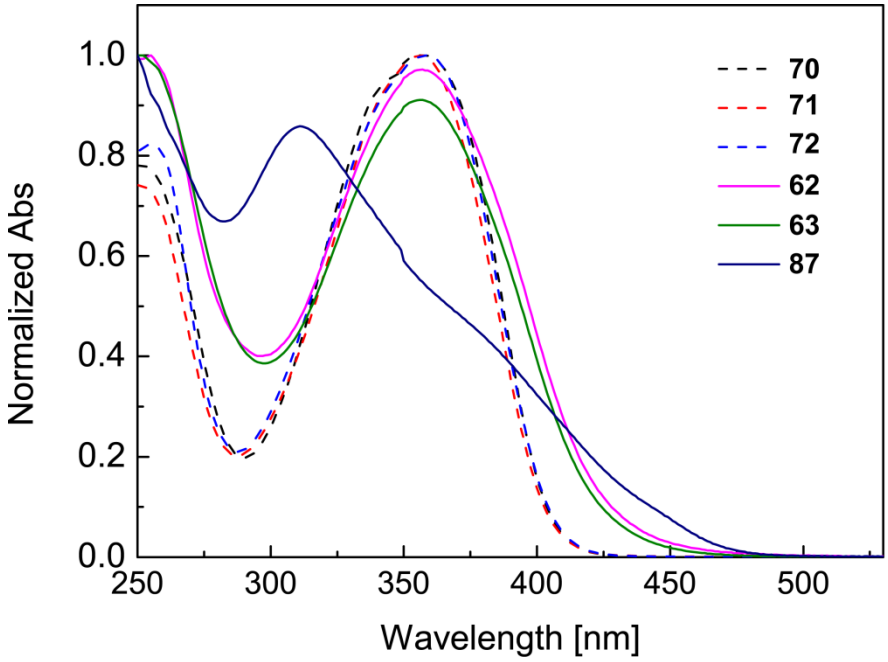

Figure 3.10 Normalized UV-Vis absorption spectra of bromophenyl-substituted DTFs, **70**-**72**, and TTFVs **62** and **63**, and bis-spiro compound **87** measured in CH_2Cl_2 at room temperature.

The electronic absorption properties of alkynylphenyl-substituted DTFs **73**-**74** are compared in Figure 3.11. The three isomers all show very similar absorption spectral patterns, with a nearly identical maximum absorption wavelength at ca. 377 nm in each of the spectra. The UV-Vis results suggests that alkynyl-substitution does not affect the

electronic absorption behaviour of the three compounds, and in reference to the spectra of bromophenyl-DTFs in Figure 3.10 the low-energy bands in Figure 3.11 can be reasonably assigned to the electronic transitions on the dithiafulvenyl moiety.

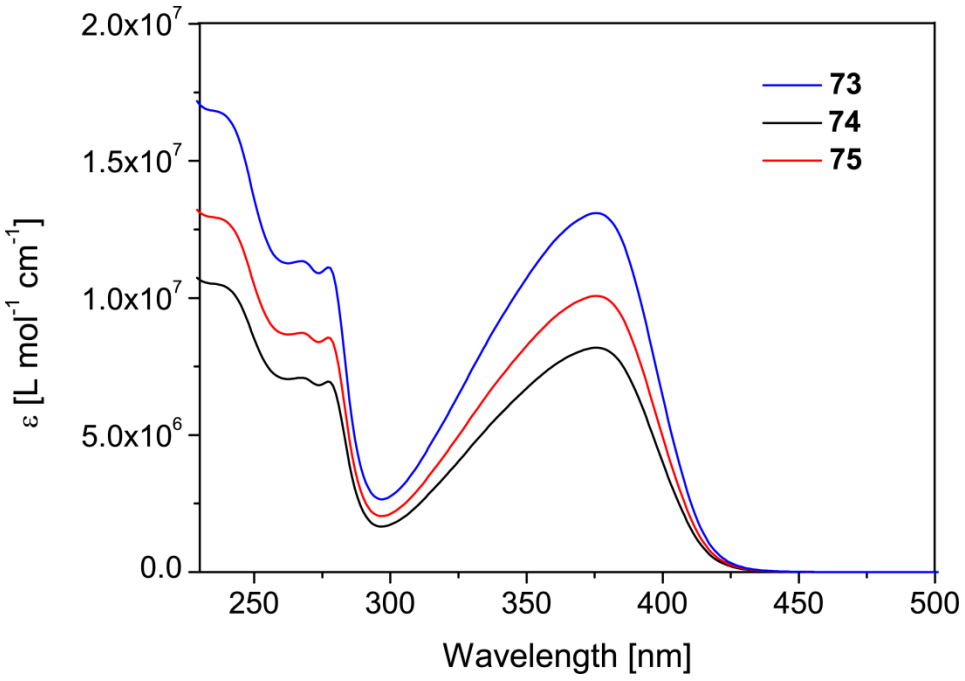

Figure 3.11 UV-Vis absorption spectra of alkynylphenyl-substituted DTFs **73-75** measured in CH_2Cl_2 at room temperature.

The UV-Vis spectra of alkynylphenyl-substituted TTFVs **65-67** are given in Figure 3.12. Similar to the series of alkynyl-DTFs **73-75**, no significant differences in the maximum absorption wavelengths can be found among these TTFV isomers. In each spectrum, the low-energy absorption band shows a peak at ca. 377 nm, which is also similar to those in the spectra of alkynyl-DTFs **73-75**. Nevertheless, the molar absorptivities for the three compounds appear to be dramatically different. A decreasing

trend for molar absorptivity (or extinction coefficient, ε) goes as: *para* **65** > *meta* **66** > *ortho* **67**. In principle, the extinction coefficient is proportional to the square of transition dipole moment (μ_T); therefore, it is likely that the three bis(alkynylphenyl)-TTFV isomers have very different transition dipole moments due to their different substitution motifs.

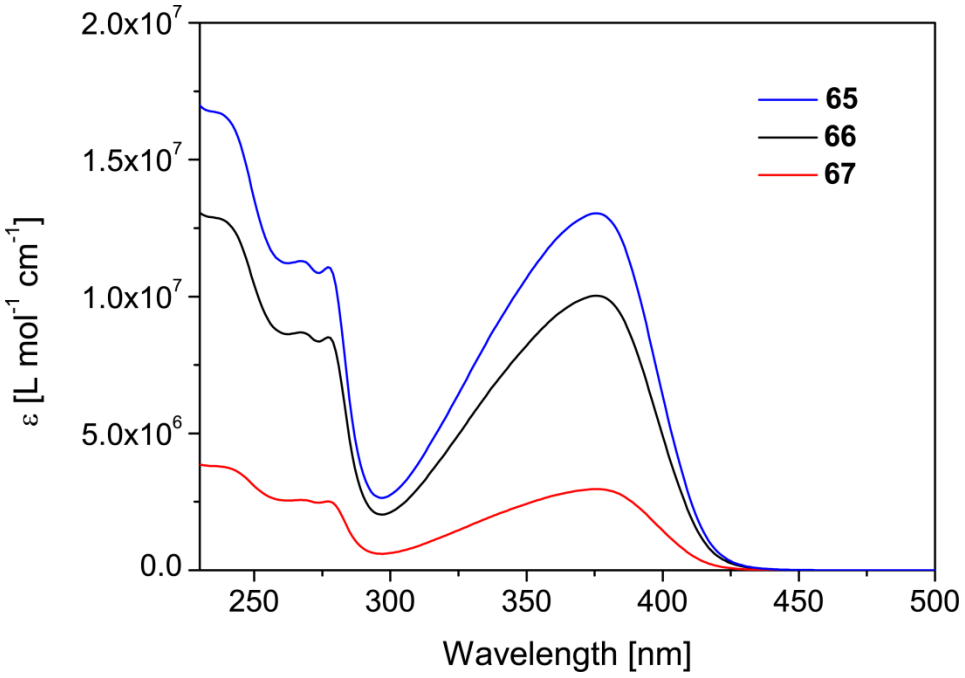

Figure 3.12 UV-Vis absorption spectra of alkynylphenyl-substituted TTFVs **65-67** measured in CH_2Cl_2 at room temperature.

The UV-Vis absorption spectra of bis(DTF)-endcapped butadiynes **91-93** are shown in Figure 3.13. Of these three isomers, the absorption spectra of *para* **91** and *meta* **92** show similarities with respect to their maximum absorption wavelengths being the same at 376 nm. For *ortho* isomer **93**, the absorption spectral patterns are dramatically altered, with two low-energy absorption bands observed at 400 nm and 334 nm,

respectively. The unusually large redshift of the lowest-energy absorption band to 400 nm from the typical 376 nm appears to be a quite complex and challenging issue to address. According to the cyclic voltammetric study (see Figure 3.8), the *ortho* isomer **93** possesses the highest oxidation potential than the other two, suggesting a relatively low HOMO energy and large HOMO-LUMO gap. Therefore, the significantly redshited low-energy absorption band should not be attributed to the HOMO to LUMO transition. At this moment, tentative explanations can be made based on either a strong aggregation effect or intramolecular charge-transfer interactions in the ground state. In any event, understanding this phenomenon needs more investigations through both experimental and theoretical approaches in the future work.

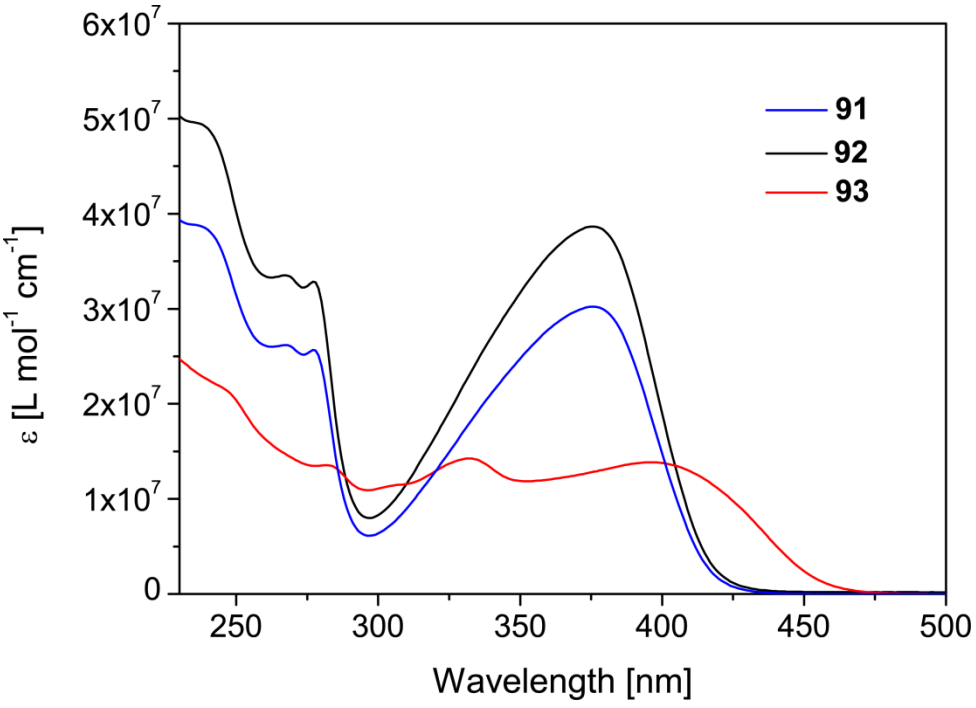

Figure 3.13 UV-Vis absorption spectra of bis(DTF)-endcapped butadiynes **91-93** measured in CH_2Cl_2 at room temperature.

3.3 Conclusion

This chapter reports the solid-state structural, electrochemical, and electronic absorption properties of various phenyl- and naphthyl-substituted DTFs, TTFVs, and related exTTF structures. Comparative analyses of the characterized data highlight that the *ortho*-substitution effect tends to bring about the most significantly altered molecular properties. Presently, modulation of the electrochemical properties is heavily based on either strong electronic (inductive or field) or resonance effect. Understanding of the interplay between the electronic nature and substitution position of various functional groups with the electronic, photophysical, and structural properties of DTF and TTFV π-analogues is of great value to the future work in developing practically useful molecular electronic and optoelectronic materials and devices. In the meantime, with the DTFs and TTFVs in hand and their fundamental properties understood, the current work sets up a foundation for further design and synthesis of DTF-/TTFV-containing molecular and macromolecular systems, where the compounds reported in this thesis can be applied as the active functional building blocks.

3.4 References

1. Bouzan, S.; Dawe, L. N.; Zhao, Y., Bromophenyl Substituted Dithiafulvenes and Tetrathiafulvalene Vinylogues: Synthesis, Structure, and Electronic Properties. *Tetrahedron Lett.* **2013**, *54*, 4666-4669.

2. Bouzan, S.; Chen, G.; Mulla, K.; Dawe, L. N.; Zhao, Y., Conformational Control of TTFV π-Frameworks through Naphthyl Substituents. *Org. Biomol. Chem.* **2012**, *10*, 7673-7676.

3. Anthony, J. E.; Eaton, D. L.; Parkin, S. R., A Road Map to Stable, Soluble, Easily Crystallized Pentacene Derivatives. *Org. Lett.* **2001**, *4*, 15-18.

4. Rose, B. D.; Chase, D. T.; Weber, C. D.; Zakharov, L. N.; Lonergan, M. C.; Haley, M. M., Synthesis, Crystal Structures, and Photophysical Properties of Electron-Accepting Diethynylindenofluorenediones. *Org. Lett.* **2011**, *13*, 2106-2109.

5. Anthony, J. E.; Brooks, J. S.; Eaton, D. L.; Parkin, S. R., Functionalized Pentacene: Improved Electronic Properties from Control of Solid-State Order. *J. Am. Chem. Soc.* **2001**, *123*, 9482-9483.

6. Wu, Y.; Liu, K.; Liu, H.; Zhang, Y.; Zhang, H.; Yao, J.; Fu, H., Impact of Intermolecular Distance on Singlet Fission in a Series of TIPS Pentacene Compounds. *J. Phys. Chem. Lett.* **2014**, *5*, 3451-3455.

7. Demiralp, E.; Goddard, W. A., Structures and Energetics Study of Tetrathiafulvalene-Based Donors of Organic Superconductors. *J. Phys. Chem. A* **1997**, *101*, 8128-8131.

8. Yamashita, Y.; Tomura, M.; Badruz Zaman, M., Synthesis and Properties of Novel Tetrathiafulvalene Vinylogues. *Chem. Commun.* **1998**, 1657-1658.

9. Cheng, H.; Scott, K.; Christensen, P. A., Feasibility Study of Electrochemical Hydrodehalogenation of 2,4-Dibromophenol in a Paraffin Oil. *Electrochim. Acta* **2004**, *49*, 729-735.

Chapter 4 Conclusion and Future Work

4.1 Conclusion

The synthetic work of this thesis has shed light on the nature of TTFV substitution effects. In general substituents that impose steric hindrance in TTFV structures are able to alter and modify the electronic and structural properties of the TTFV. Specifically, this research has found that the use of allylic strain provides an effective way to produce an unprecedented neutral *trans* aryl-substituted TTFV framework. Furthermore, bulky substituents prevent aryl-DTFs to form corresponding TTFV products via the oxidative dimerization reaction. Together, these two discoveries have contributed to a beter understanding of the structure-property relationships of various aryl-substituted TTFV derivatives. This is important as TTFV is a promising candidate for electroactive materials, especially those relating to molecular switch functions. Future work should focus on developing more derivatives with functional groups attached to aryl substituents, so that not only greater insight into the structure-property relationship of aryl-substituted TTFVs can be gained, but novel TTFV-based molecular materials and devices may be generated.

4.2 Suggested Future Research Directions

In the future work, a number of new π-conjugated systems are envisioned on the basis of the aryl-TTFVs developed in this thesis work. The first direction can be aimed at

synthesizing a new type of naphthyl-TTFV polymers **94** (see Figure 4.1). The *trans* TTFV moiety in **94** will not only allow a linear-shaped polymer backbone to be constructed, but also engender highly ordered intermolecular π-stacking to form semiconducting solids. Doping of these polymers by oxidant, on the other hand, may lead to intriguing organic conductors. The synthesis of polymers such as **94** can be undertaken by metal-catalyzed coupling reactions (e.g. Sonogashira and Stille).

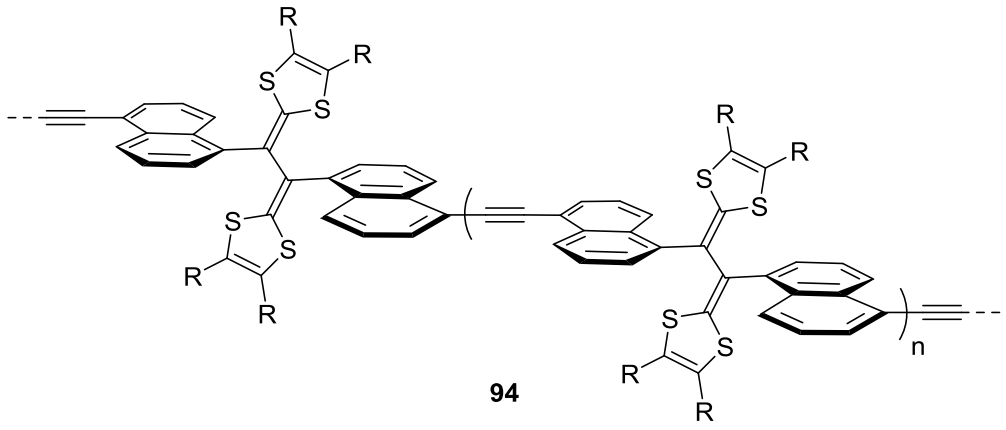

94

Figure 4.1 Proposed poly(naphthylene-TTFV-ethynylene)s **94**.

Another interesting synthetic target arises from the bis(DTF)-endcapped butadiyne. Previously, the Zhao group reported the preparation of TTFV-butadiyne polymers by chemically or electrochemically induced oxidative coupling of bis(DTF)-butadiyne **91**. Adopting the same oxidative polymerization strategy, the *meta* isomer of **91**, such as compound **95** in Figure. 4.2, is expected to undergo similar polymerization processes under oxidative conditions. In view of the non-linear shape of compound **95**, the resulting polymer **96** is envisioned to possess a highly folded conformation in the neutral state. The

folded structure will in turn generate some inner cavities with certain dimensions. Upon oxidation, the conformation of polymer **96** should be dramatically changed as a result of the conformational changes on the TTFV units. This should to a large extent unfold the polymer backbone and remove the cavities in the polymer matrix. In this sense, polymer **96** may function as an intelligent microscopic porous material, the porosity of which can be readily controlled by applied redox potentials. The applications of these materials can be found in such fields as chemical vapour sensing, gas adsorption and separation.

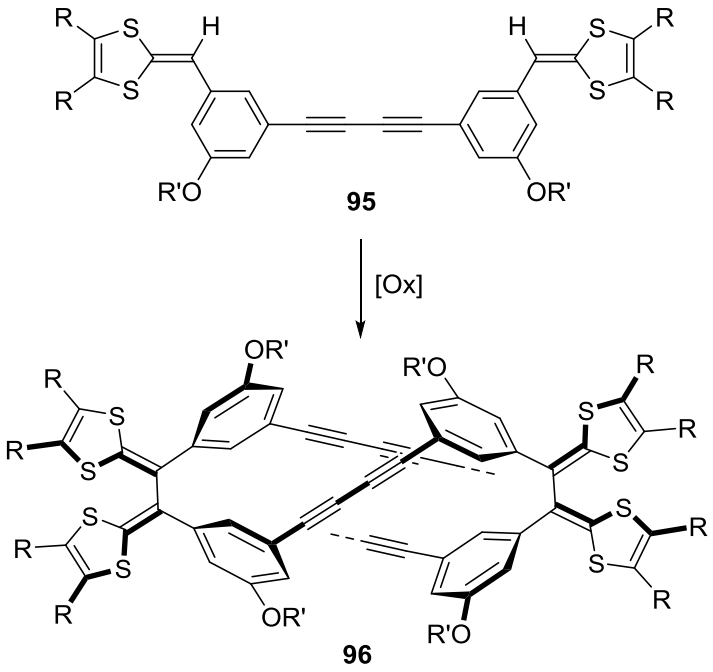

Figure 4.2 Proposed poly(TTFV-phenylenebutadiynylene)s **96**.

In a long-term perspective, continued study of various aryl-substituted TTFV derivatives will foster more new and exciting chemistry that could potentially lead to the

discovery of practically useful materials and technologies for modern organic materials chemistry and nanoscience.

Appendix: NMR Spectra for New Compounds

A.1 ^{1}H NMR Spectra

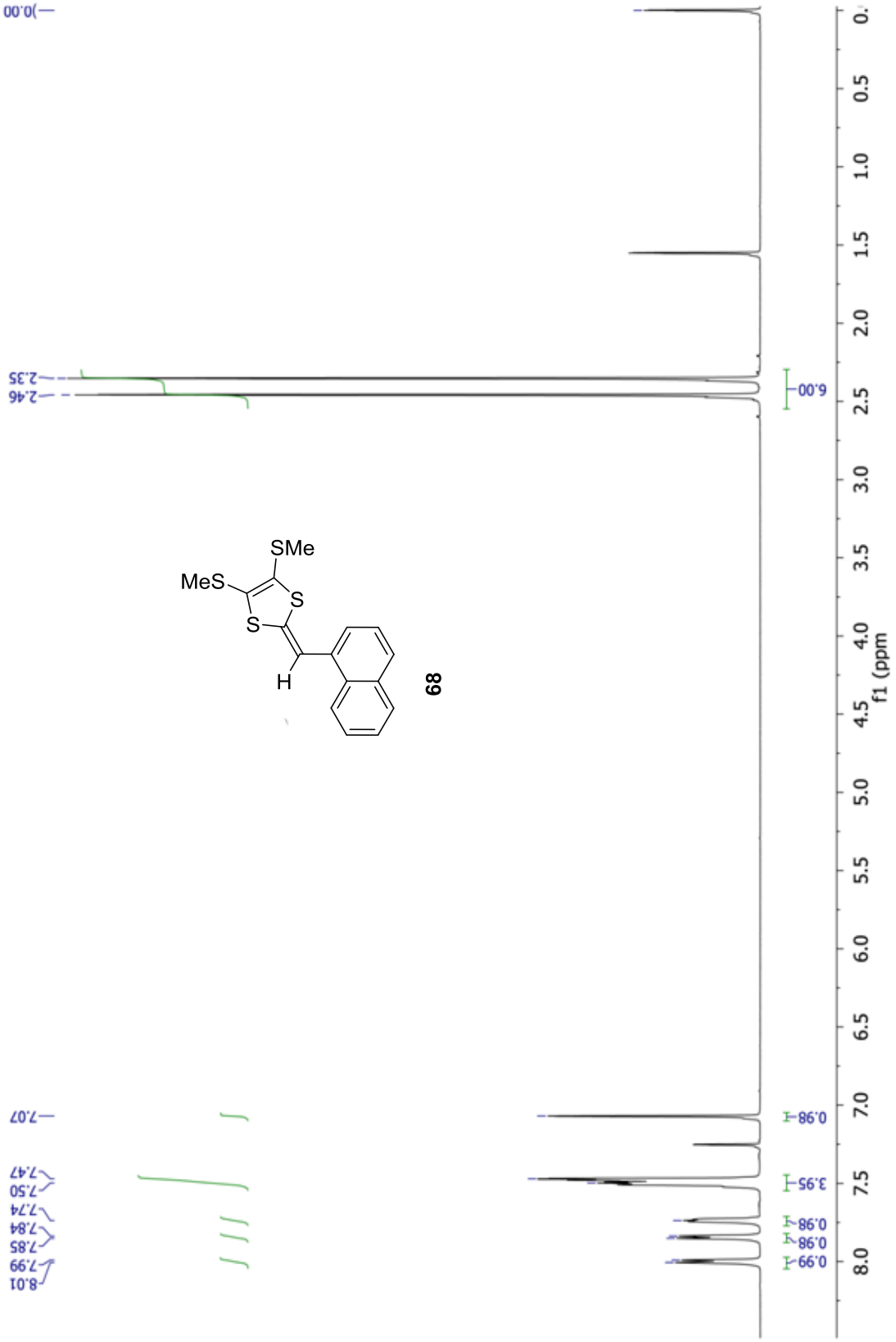
SMe
MeS
S
S
H
68
f1 (ppm)

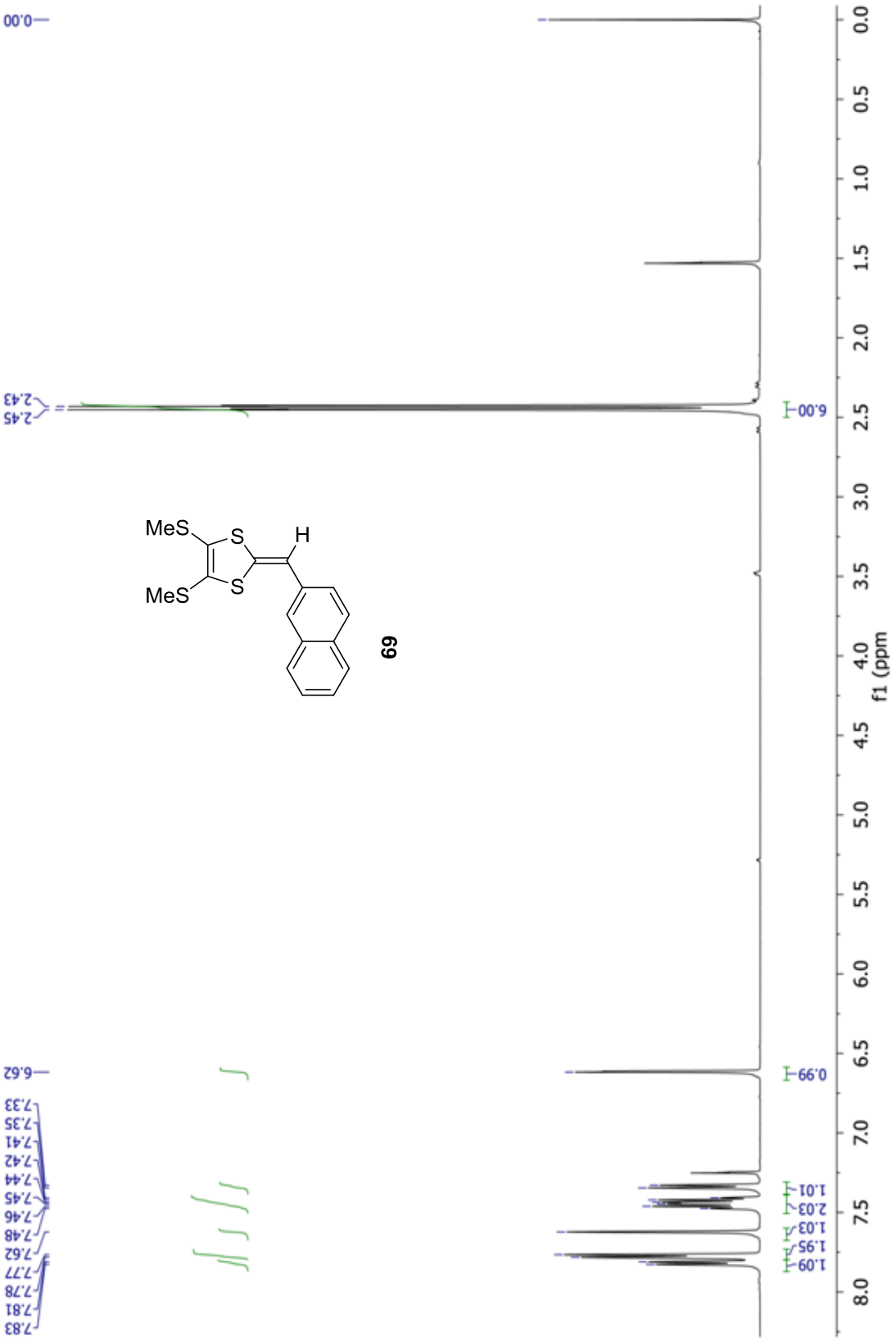
MeS
S
H
MeS
S
69
f1 (ppm)

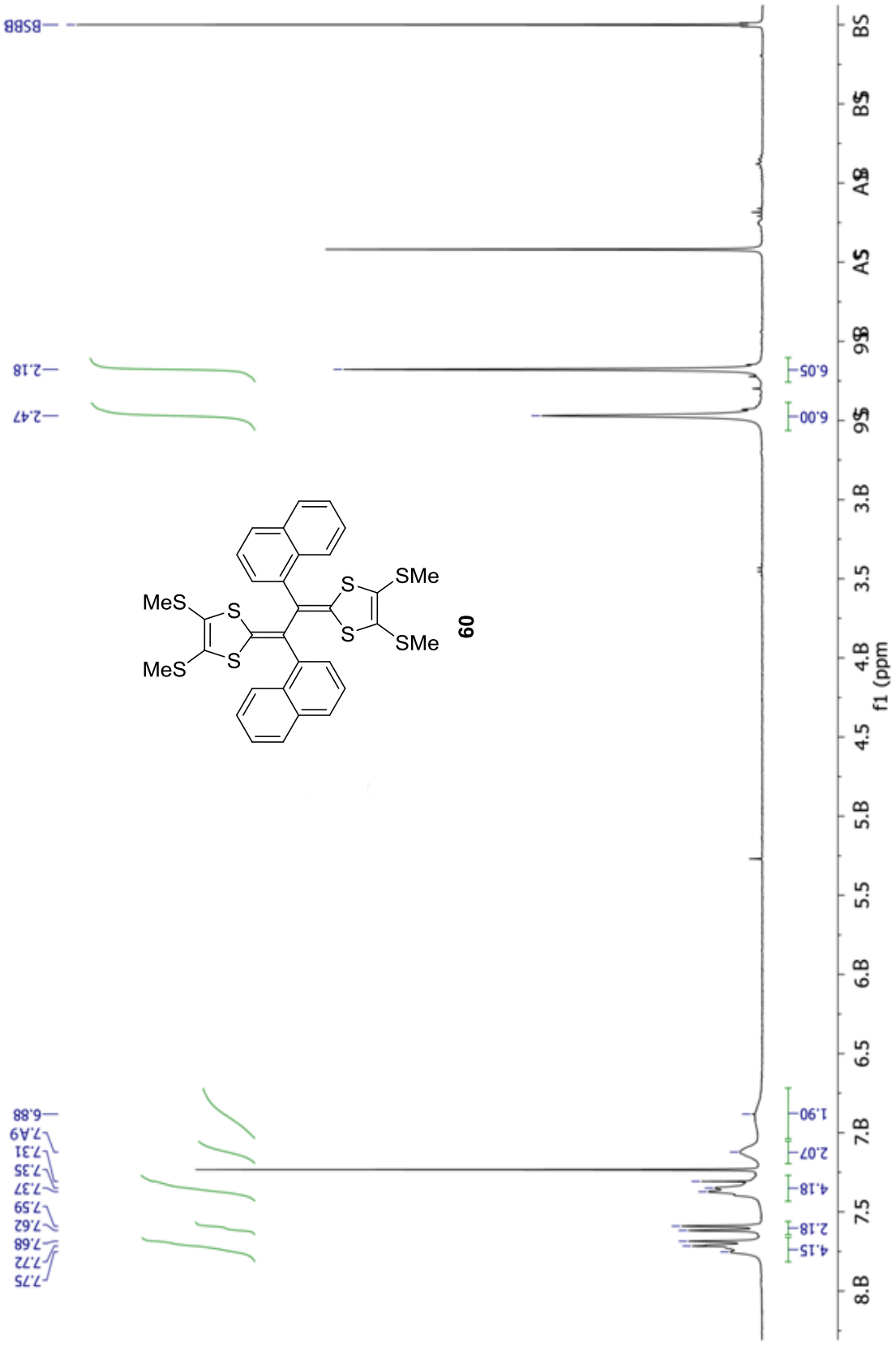
MeS
S
S
SMe
MeS
S
S
SMe
60
f1 (ppm)

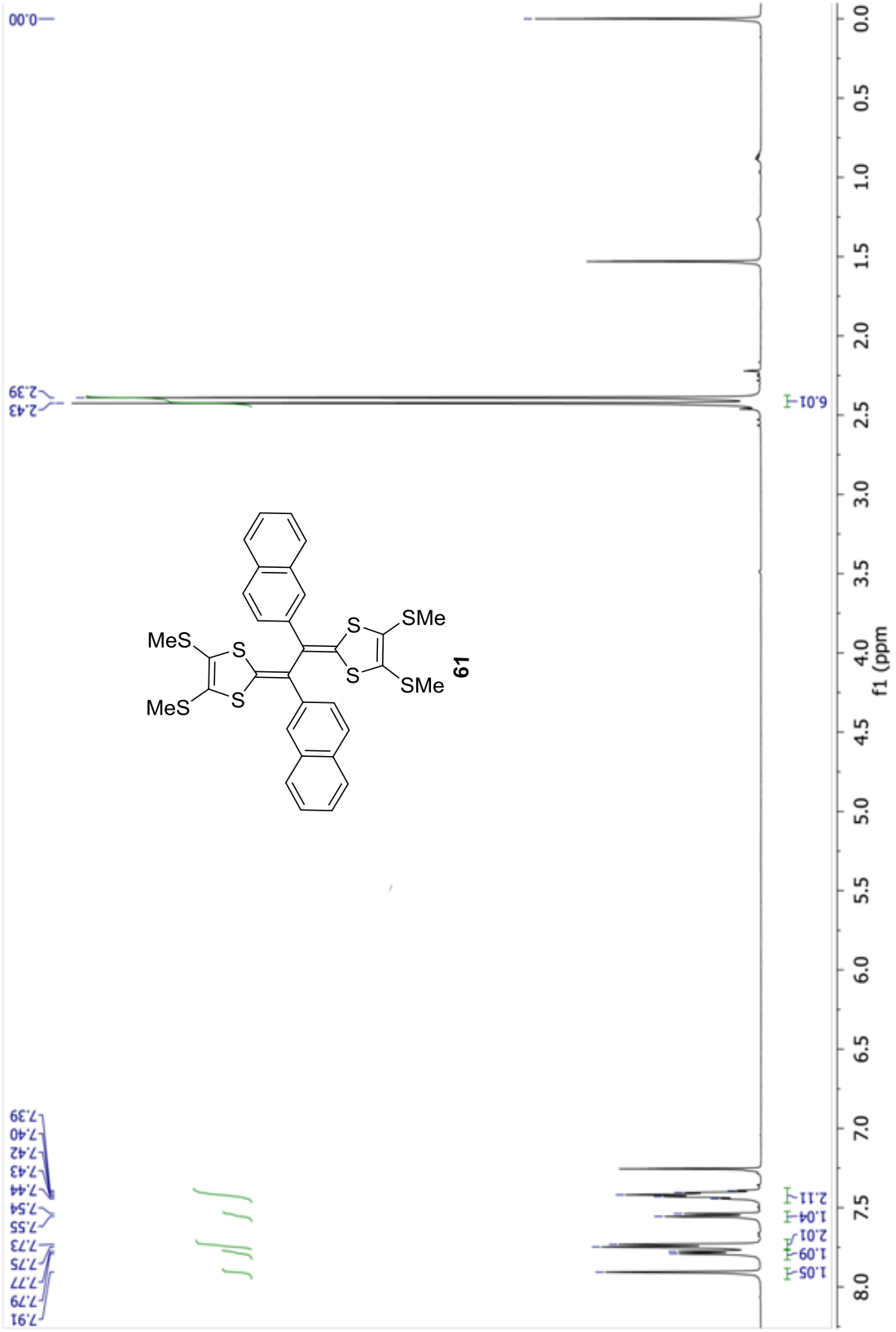
MeS
S
S
MeS
S
S
SMe
SMe
61
0.00
2.43
2.39
6.01
7.91
7.79
7.77
7.75
7.73
7.55
7.54
7.44
7.43
7.42
7.40
7.39
1.05
1.09
2.01
1.04
2.11
f1 (ppm)

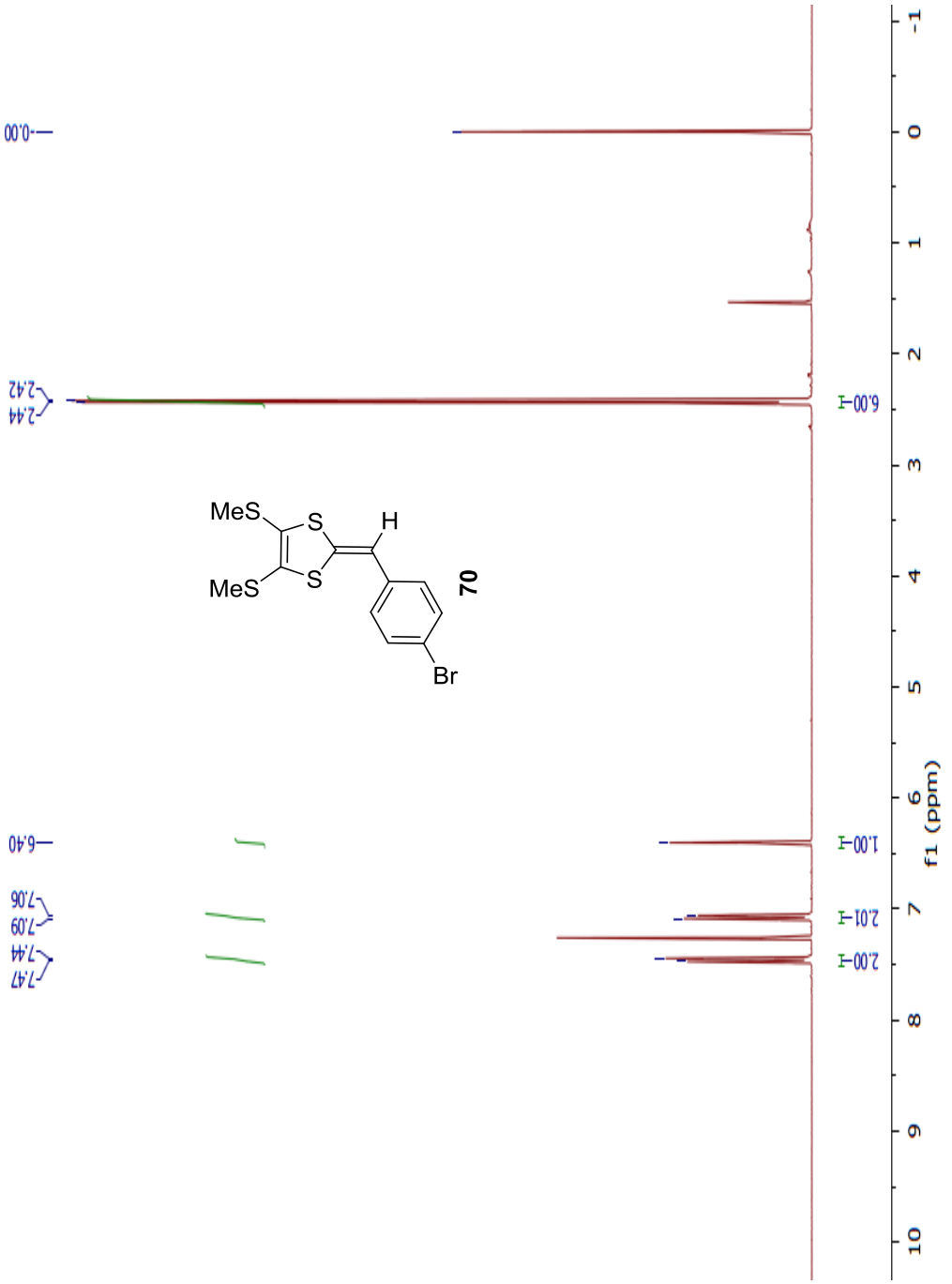
0.00
2.44
2.42
6.40
7.47
7.44
7.09
7.06
MeS
MeS
S
S
H
Br
70
6.00
1.00
2.01
2.00
f1 (ppm)

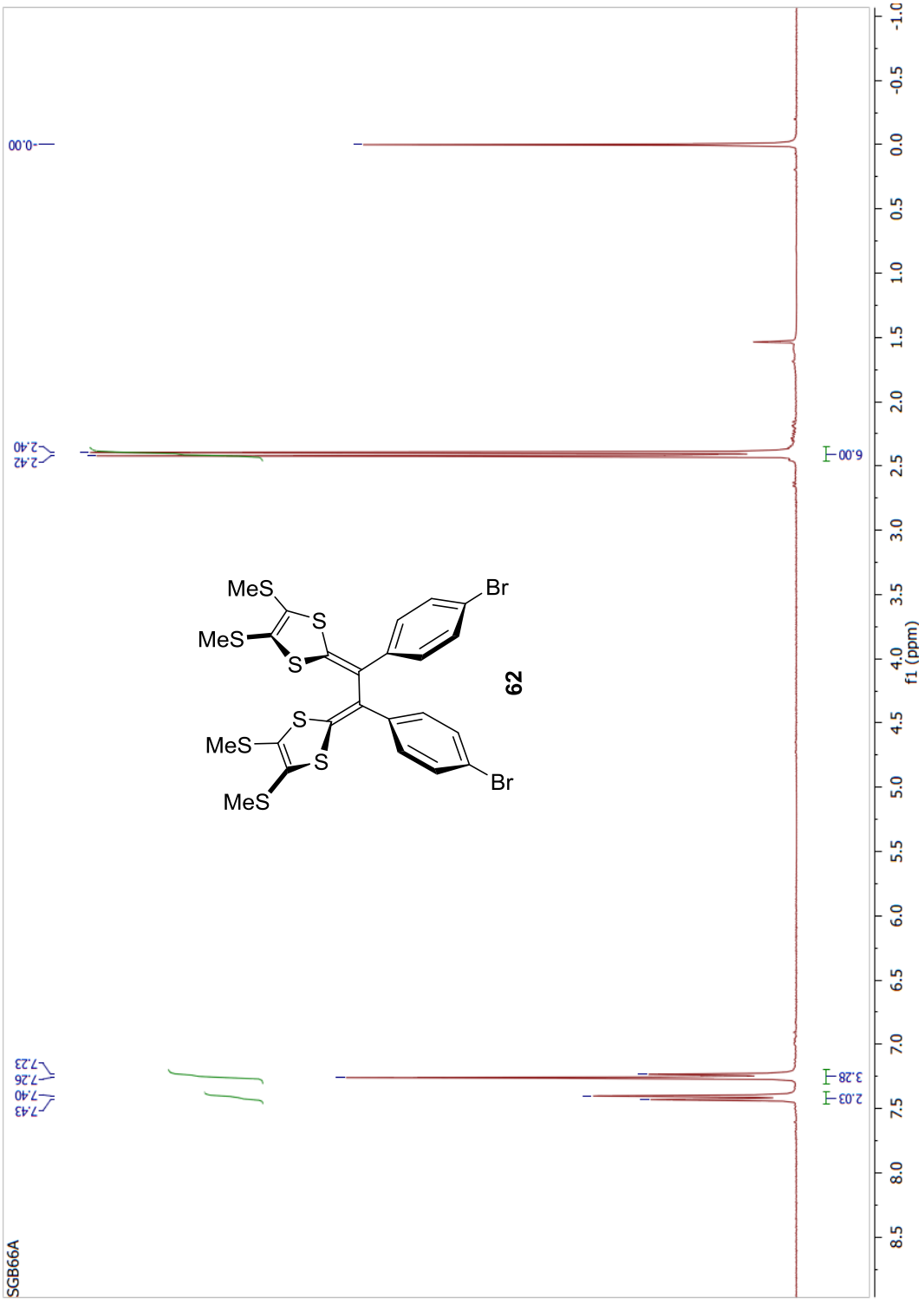
0.00
2.40
2.42
7.23
7.26
7.40
7.43
6.00
3.28
2.03
SGB66A
f1 (ppm)
MeS
MeS
MeS
MeS
S
S
S
S
Br
Br
62

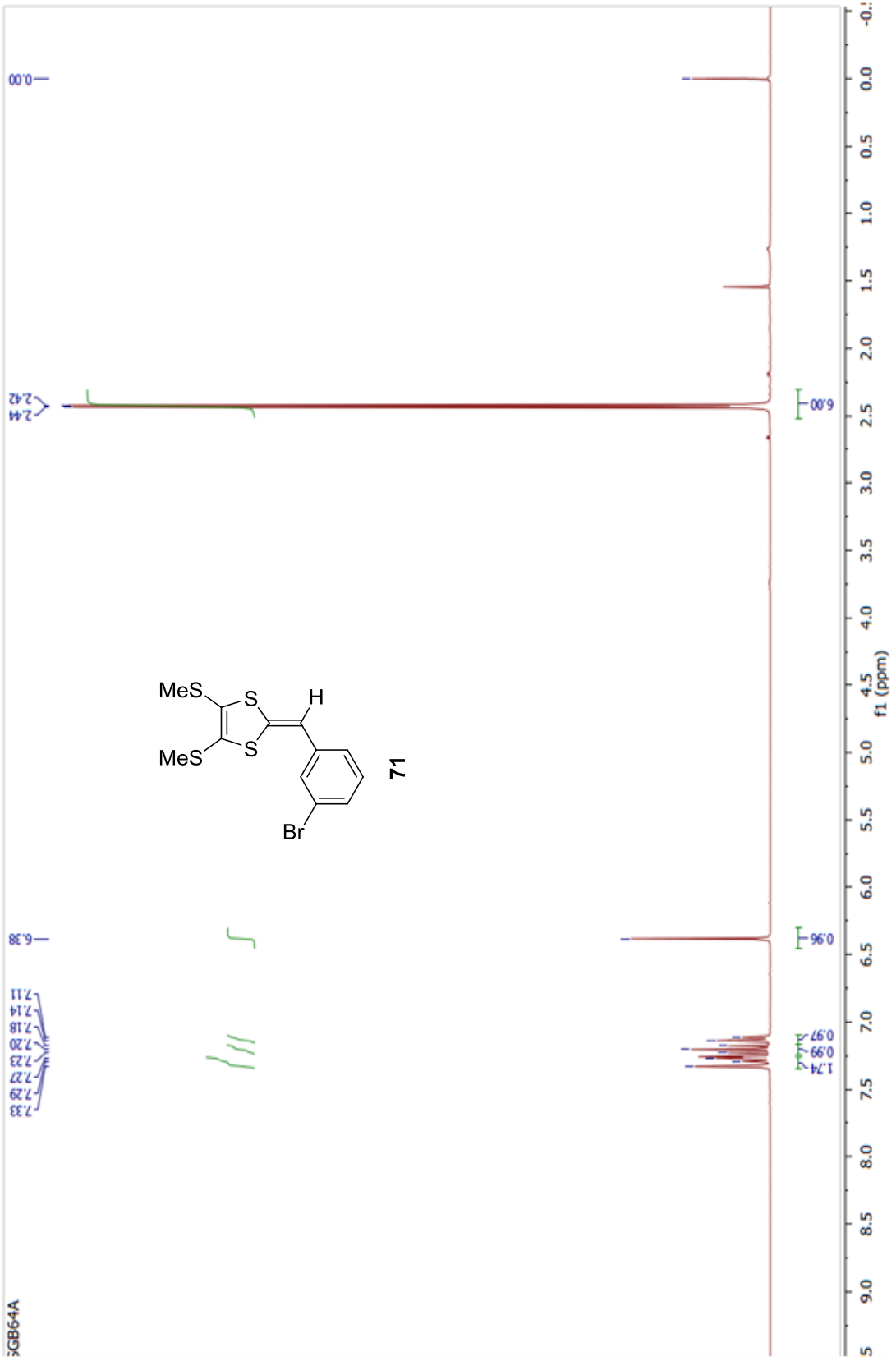
MeS
MeS
S
S
H
Br
71
f1 (ppm)

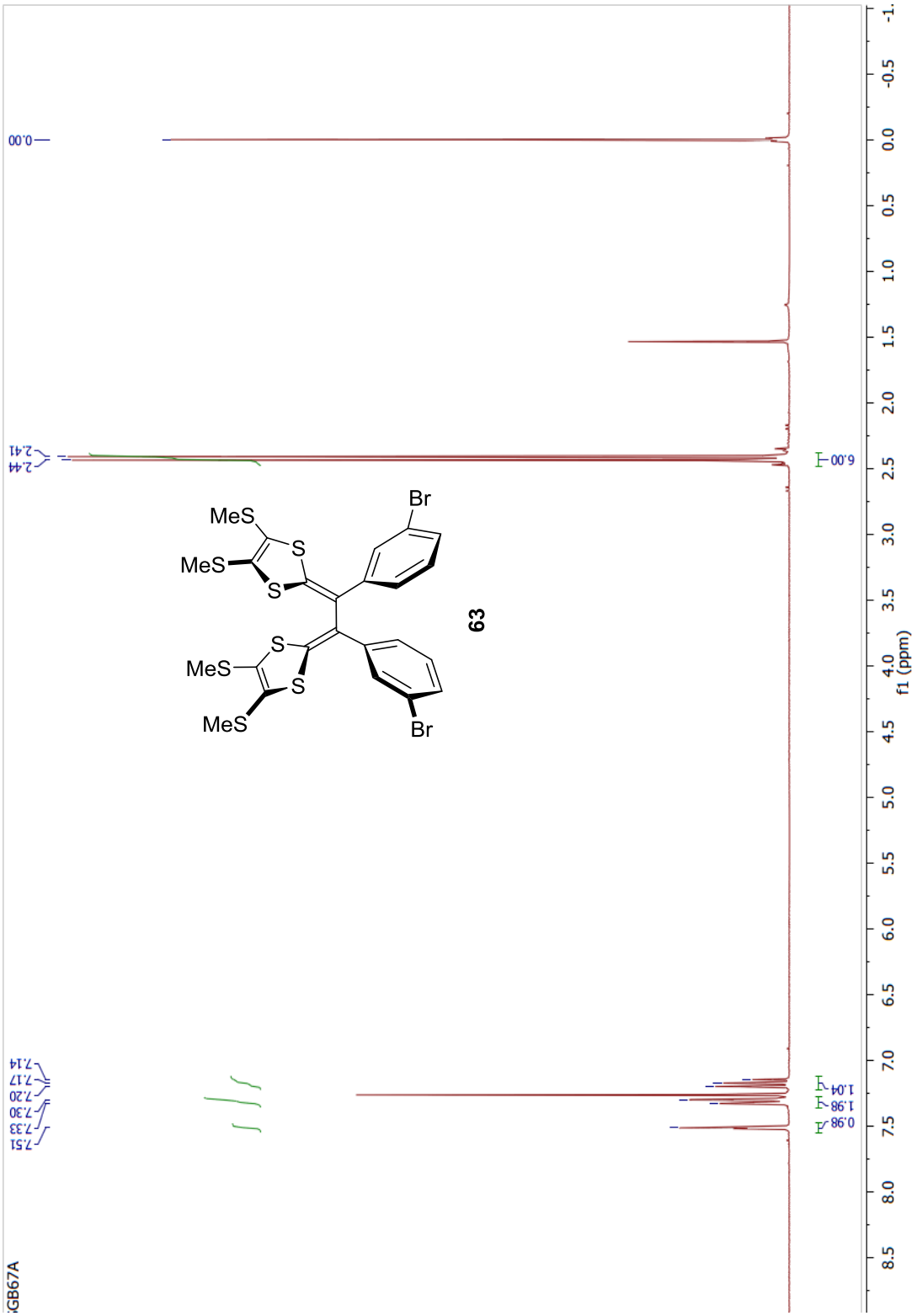
MeS
MeS
S
S
Br
S
MeS
S
MeS
Br
63
f1 (ppm)

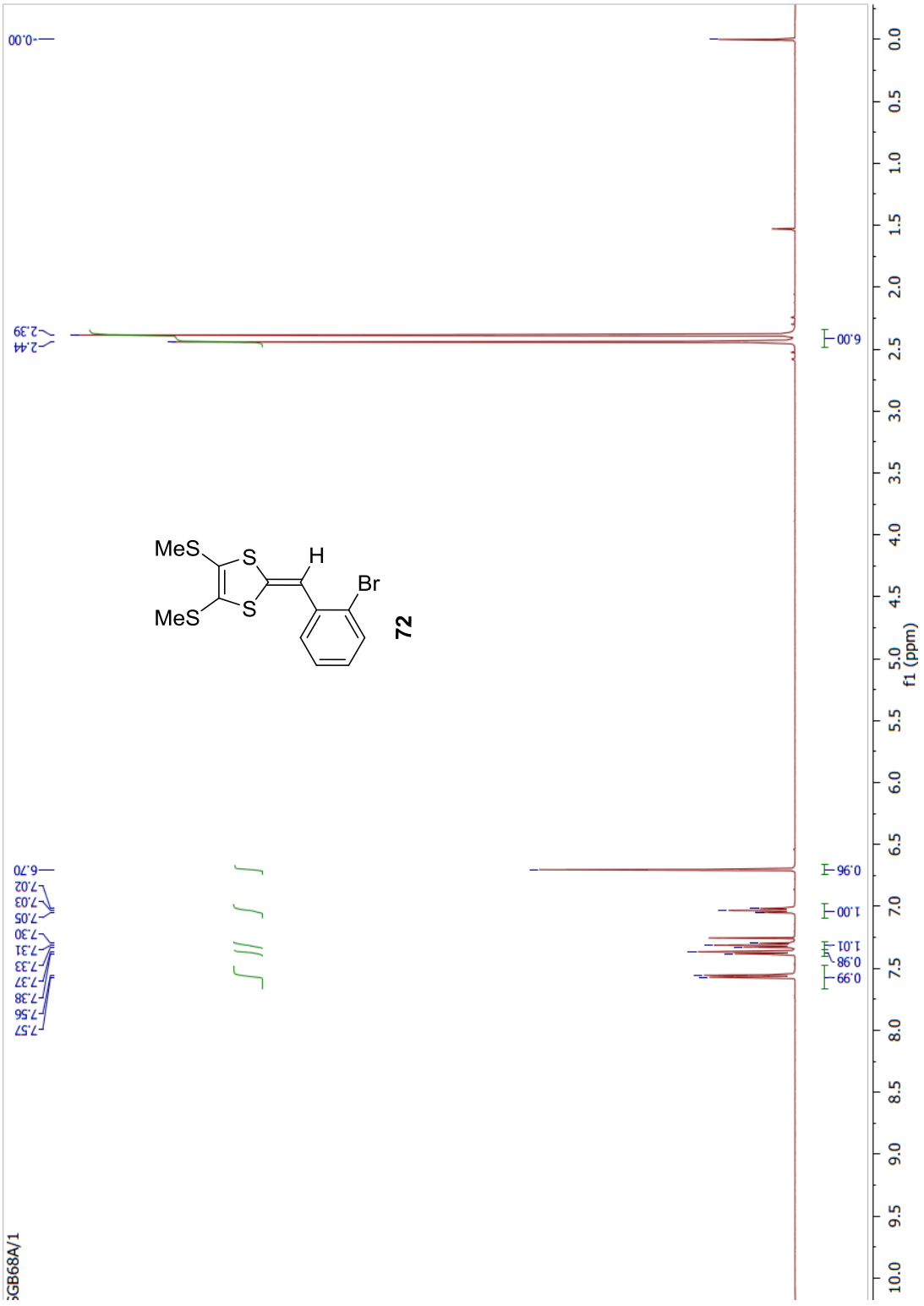
MeS
S
H
Br
MeS
S
72
f1 (ppm)

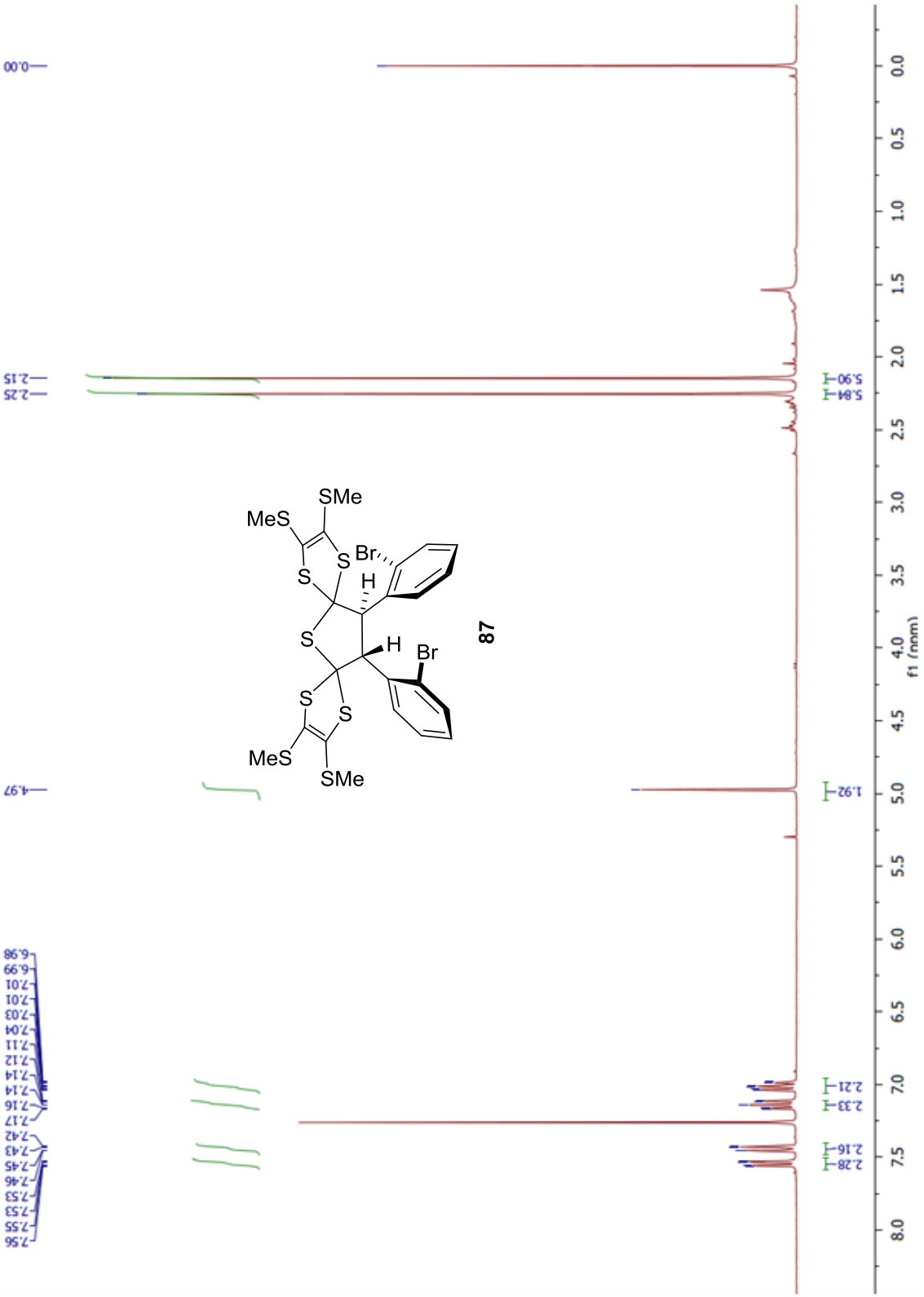
SMe
MeS
S
S
Br
H
S
H
Br
S
S
MeS
SMe
87
f1 (ppm)

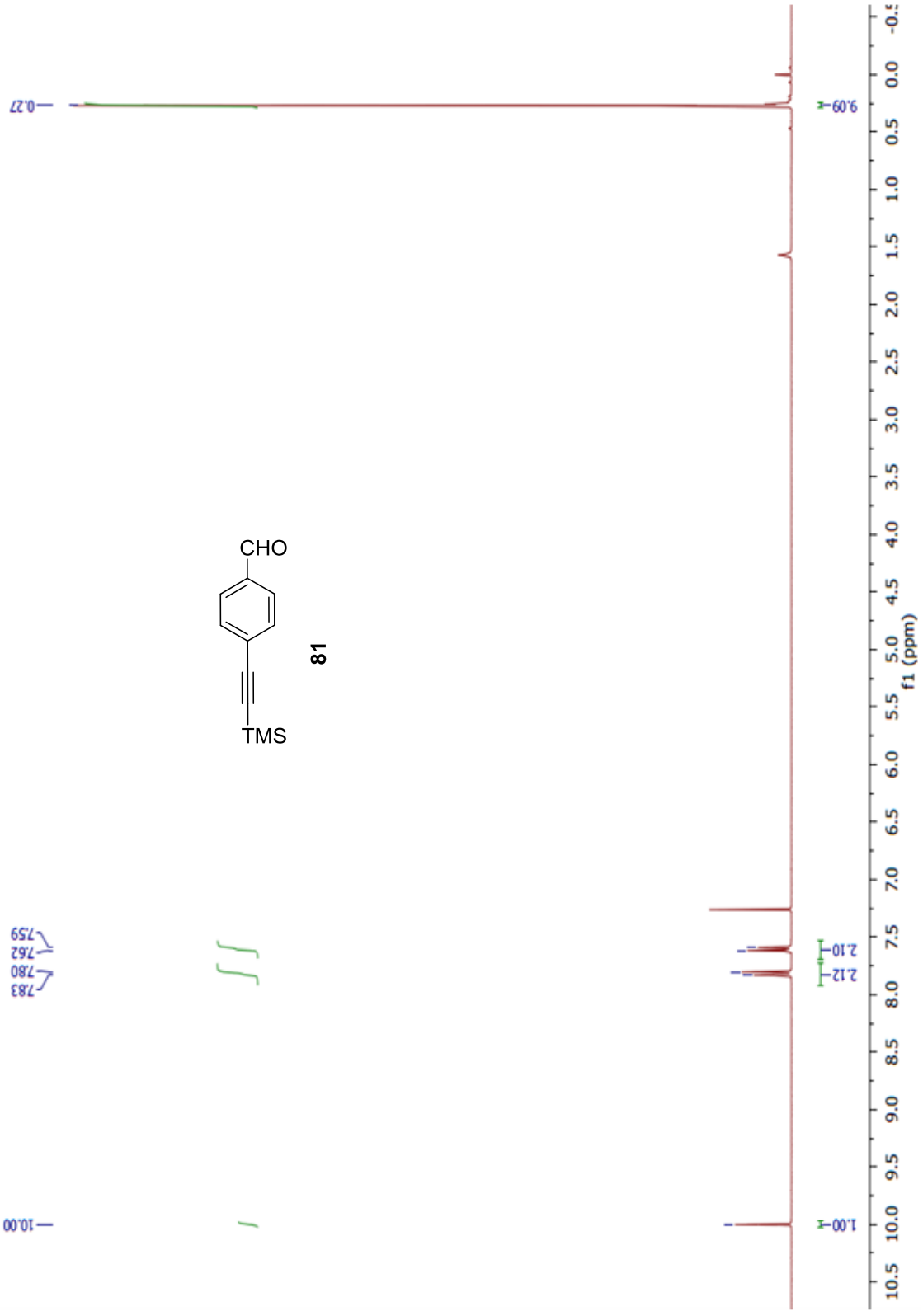
CHO
TMS
81
0.27
9.09
7.83
7.80
7.62
7.59
2.10
2.12
10.00
1.00
f1 (ppm)

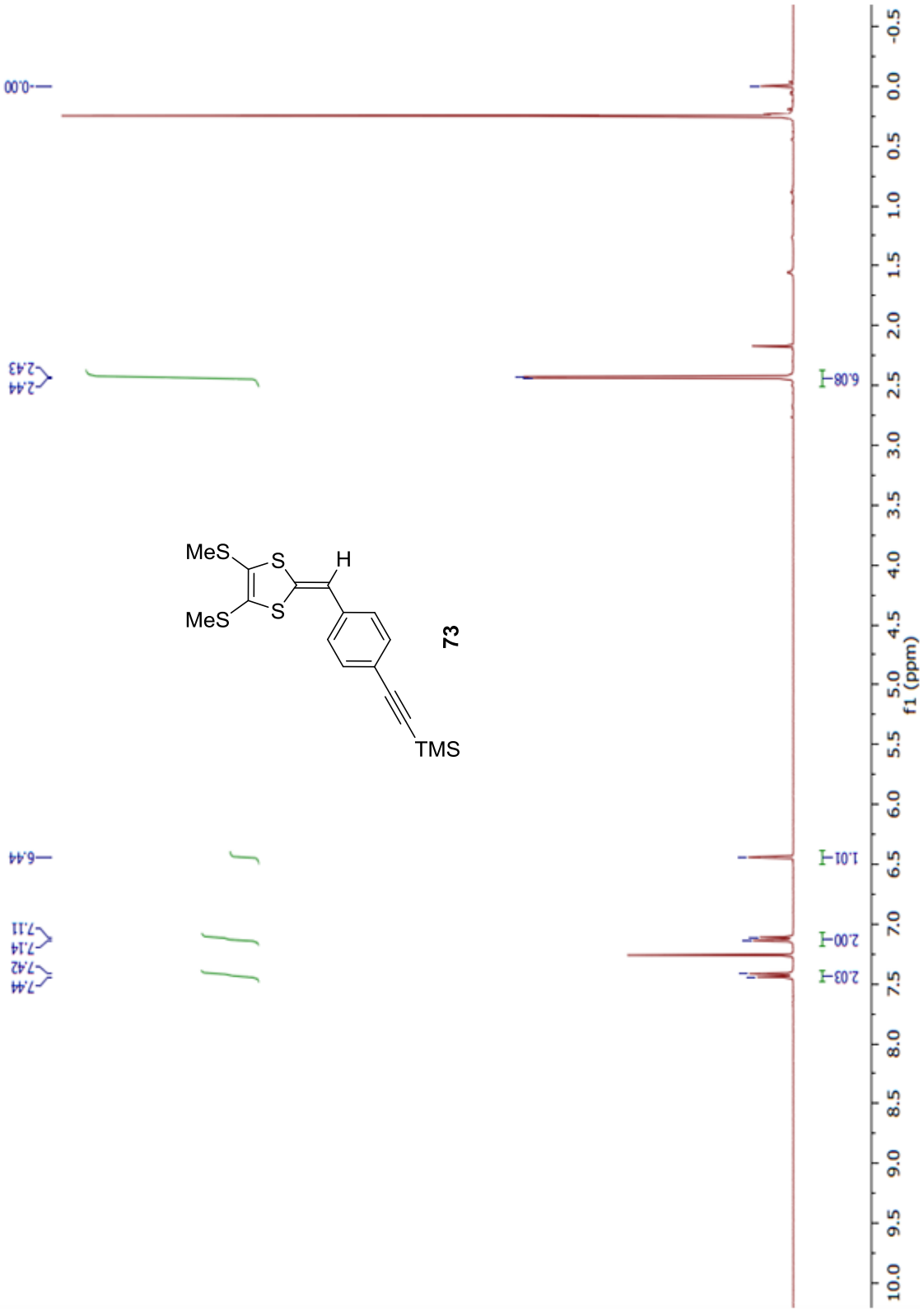
0.00
2.43
2.44
6.08
6.44
1.01
7.11
7.14
7.42
7.44
2.00
2.03
MeS
MeS
S
S
H
TMS
73
f1 (ppm)

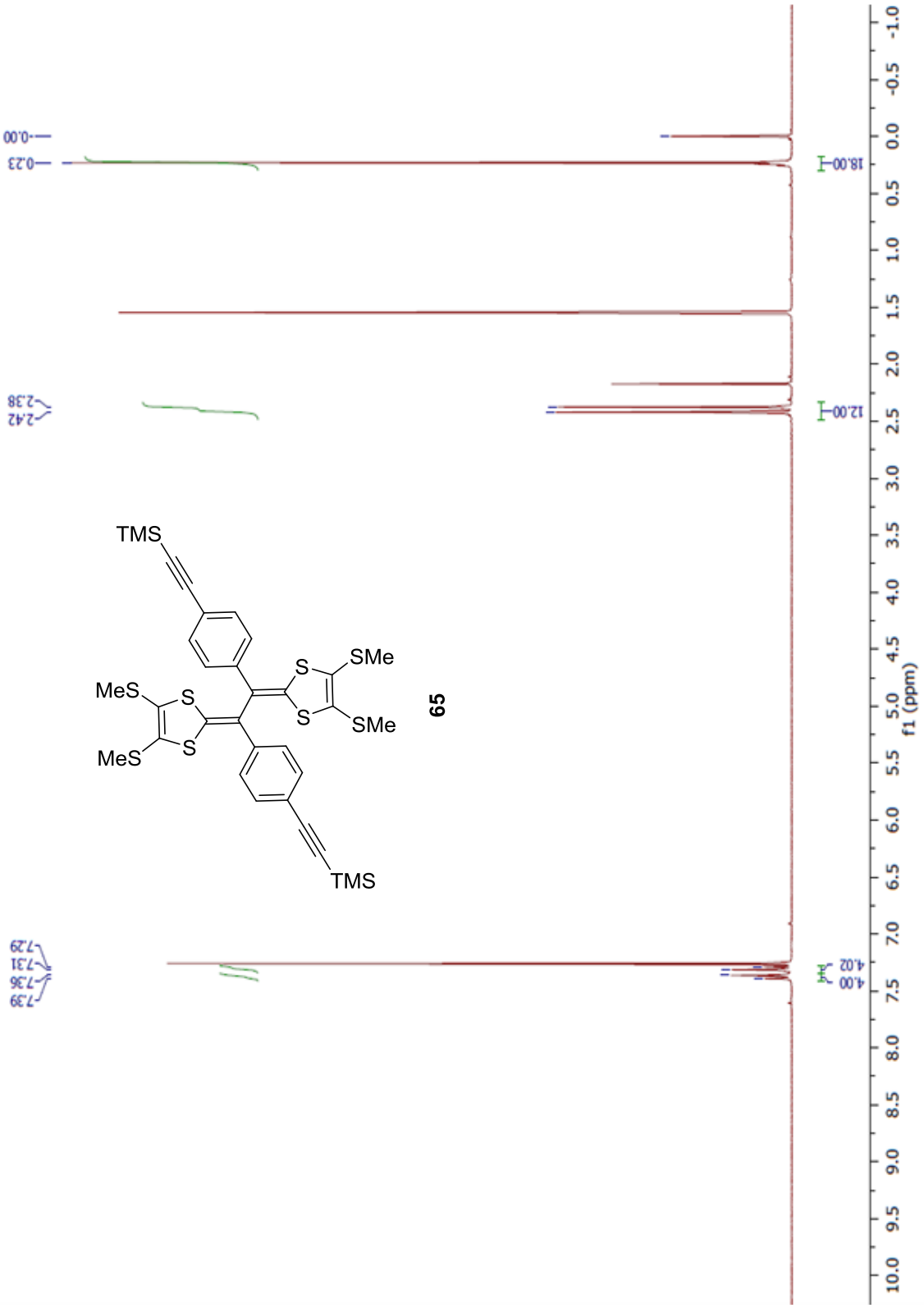
TMS
SMe
MeS
S
SMe
MeS
TMS
65
0.00
0.23
2.38
2.42
7.29
7.31
7.36
7.39
18.00
12.00
4.00
4.02
f1 (ppm)

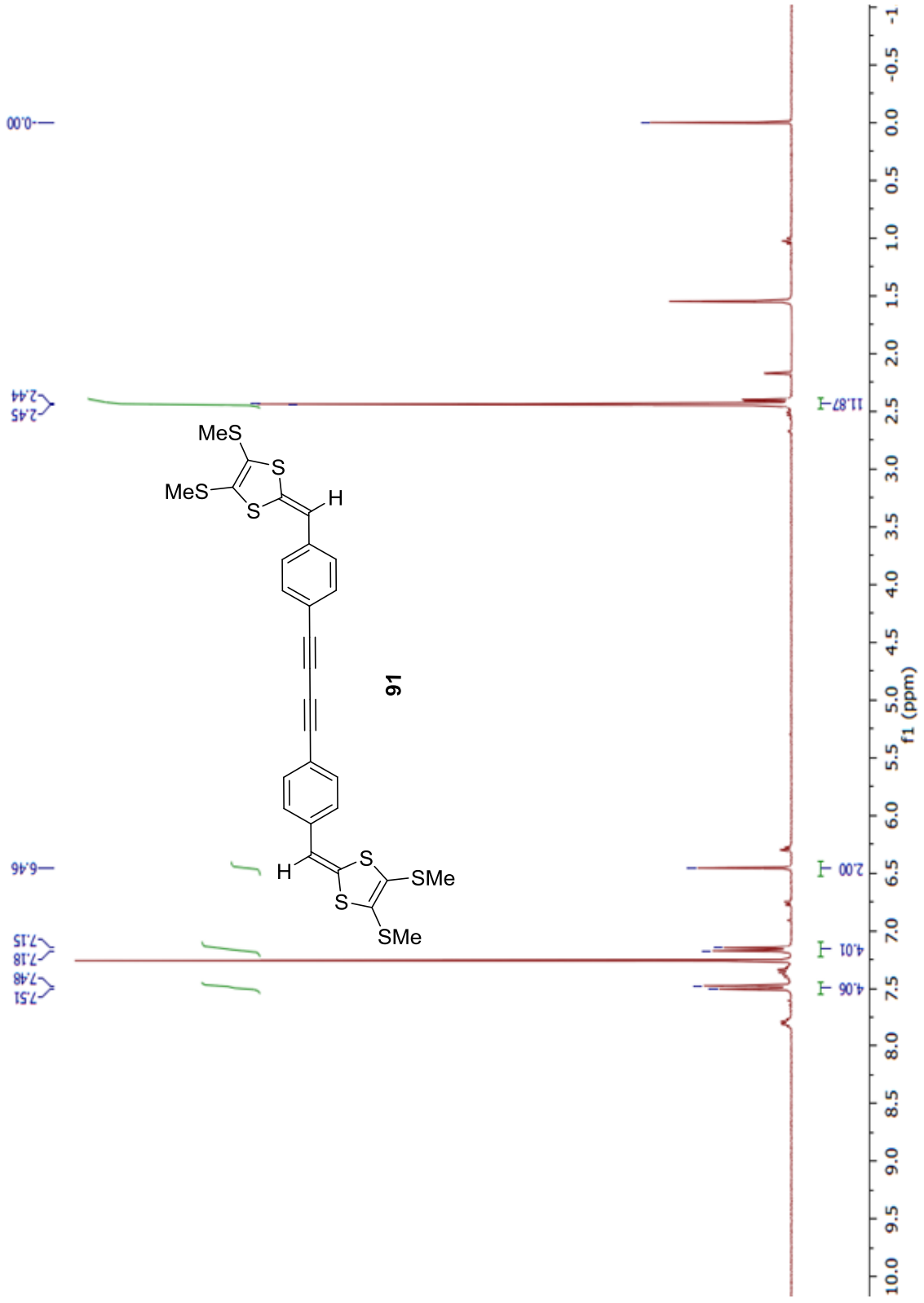
MeS
S
MeS
S
H
H
S
SMe
S
SMe
91
0.00
2.44
2.45
6.46
7.15
7.18
7.48
7.51
11.87
2.00
4.01
4.06
f1 (ppm)

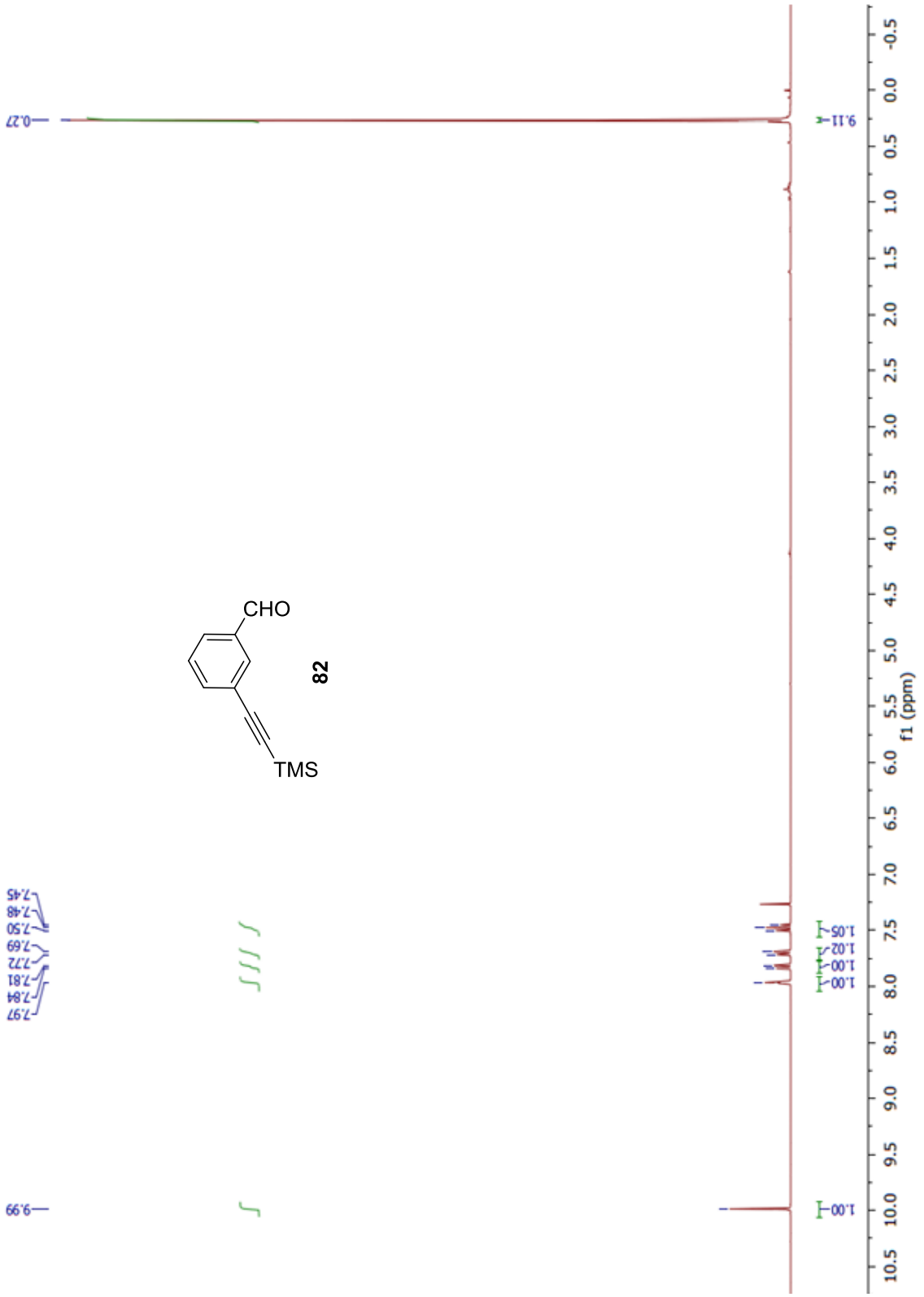
CHO
TMS
82
f1 (ppm)

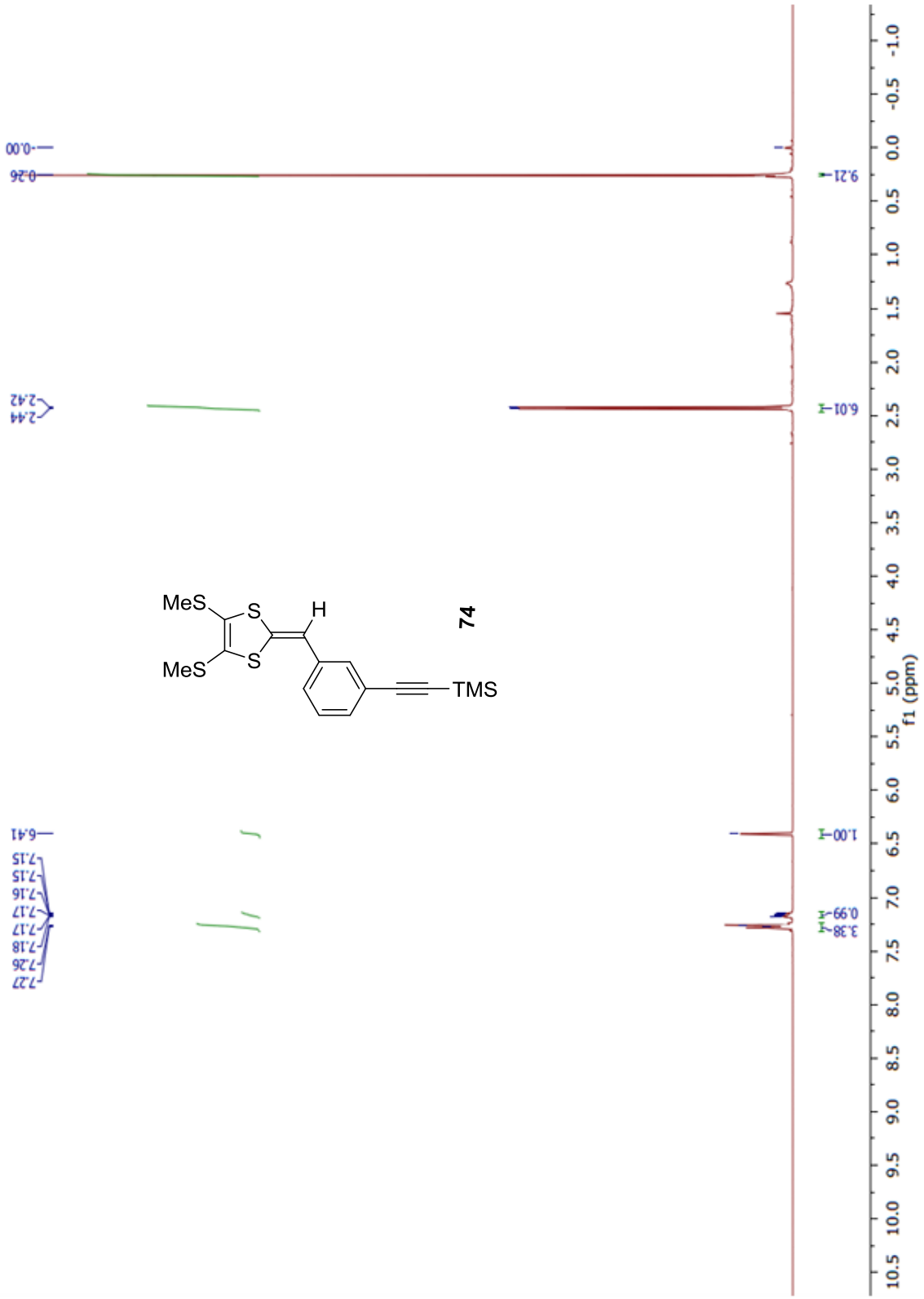
MeS
S
H
MeS
S
TMS
74
f1 (ppm)

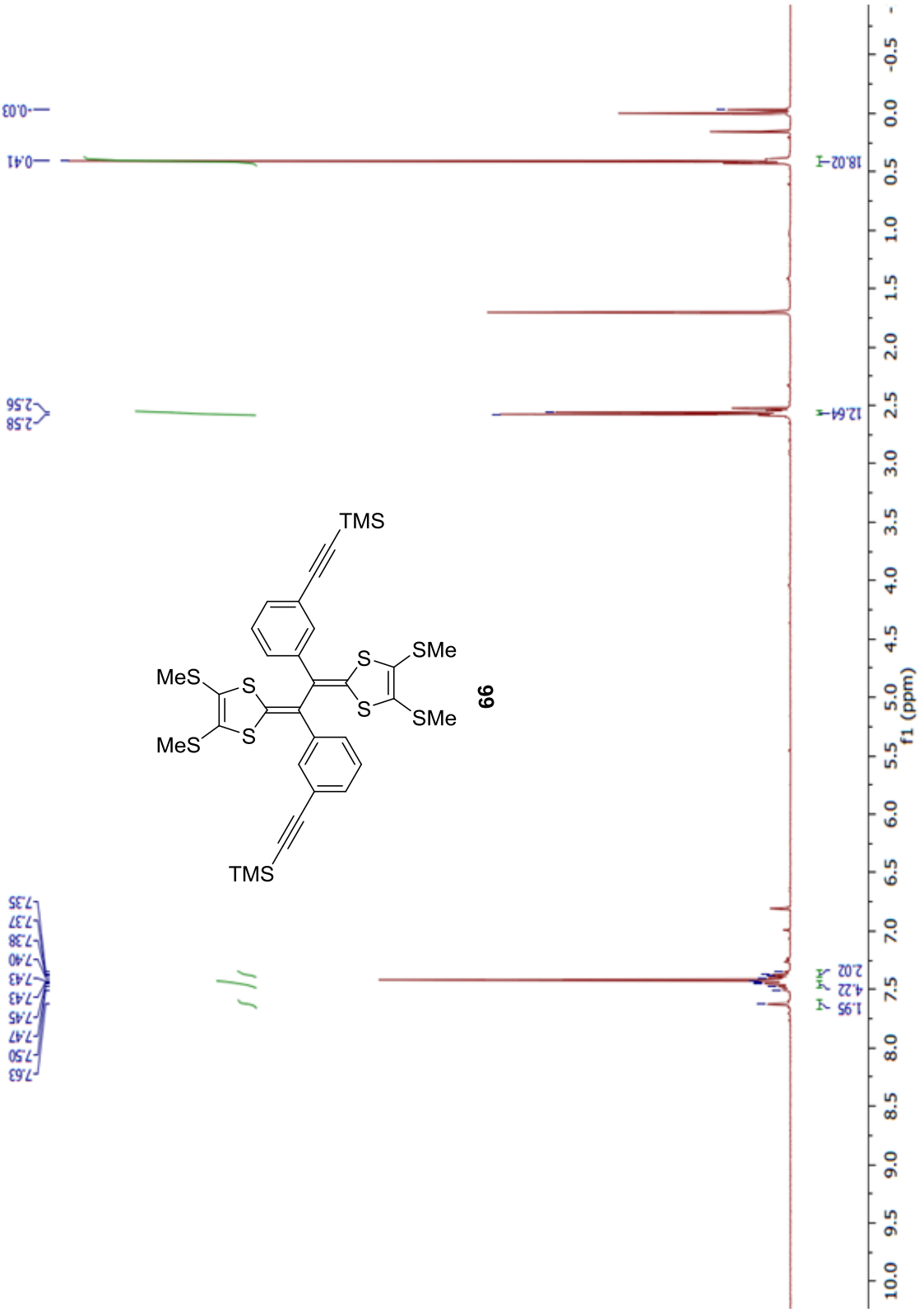
TMS
SMe
MeS
S
MeS
SMe
TMS
99
f1 (ppm)

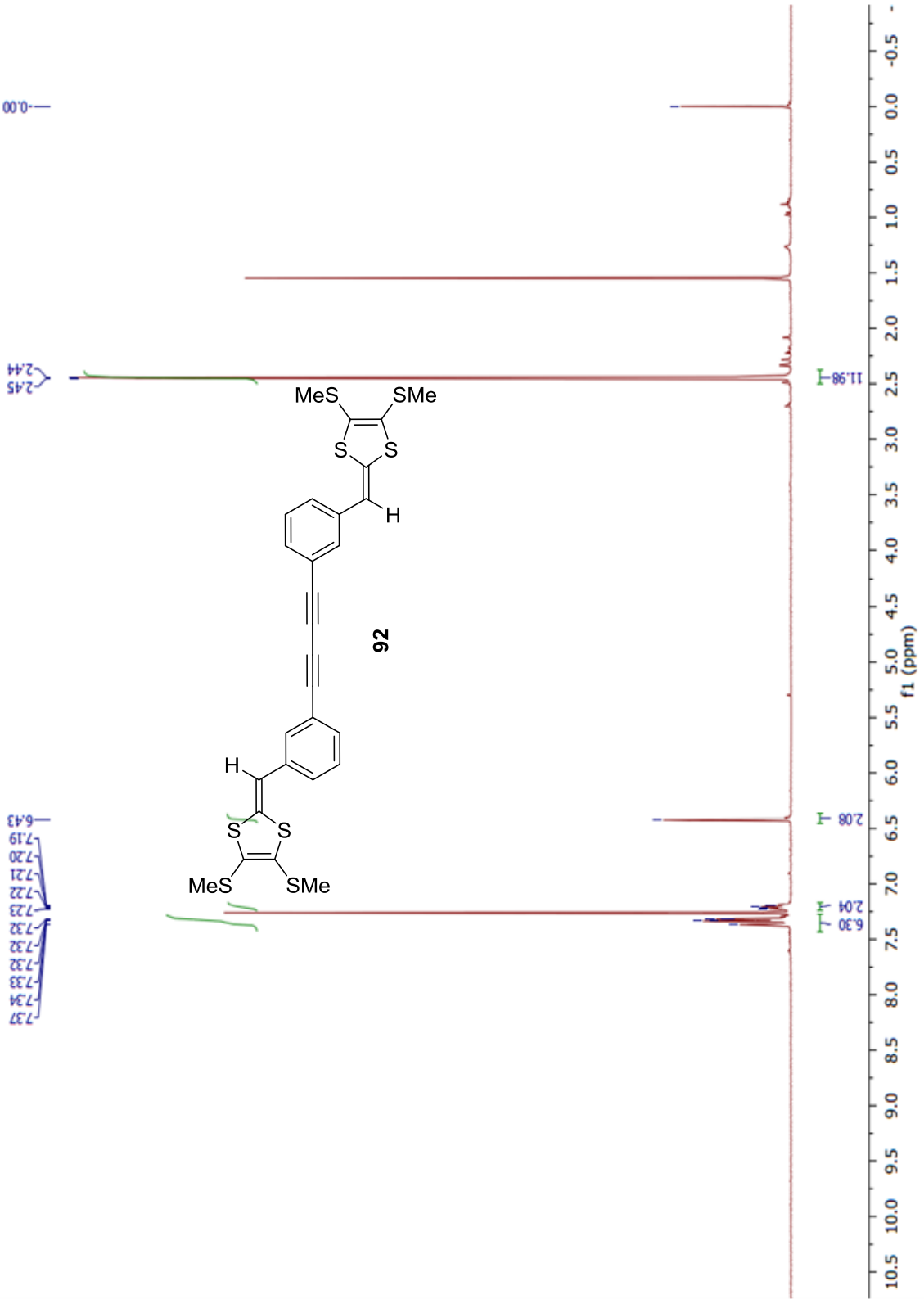
MeS
SMe
S
S
H
92
H
S
S
MeS
SMe
f1 (ppm)

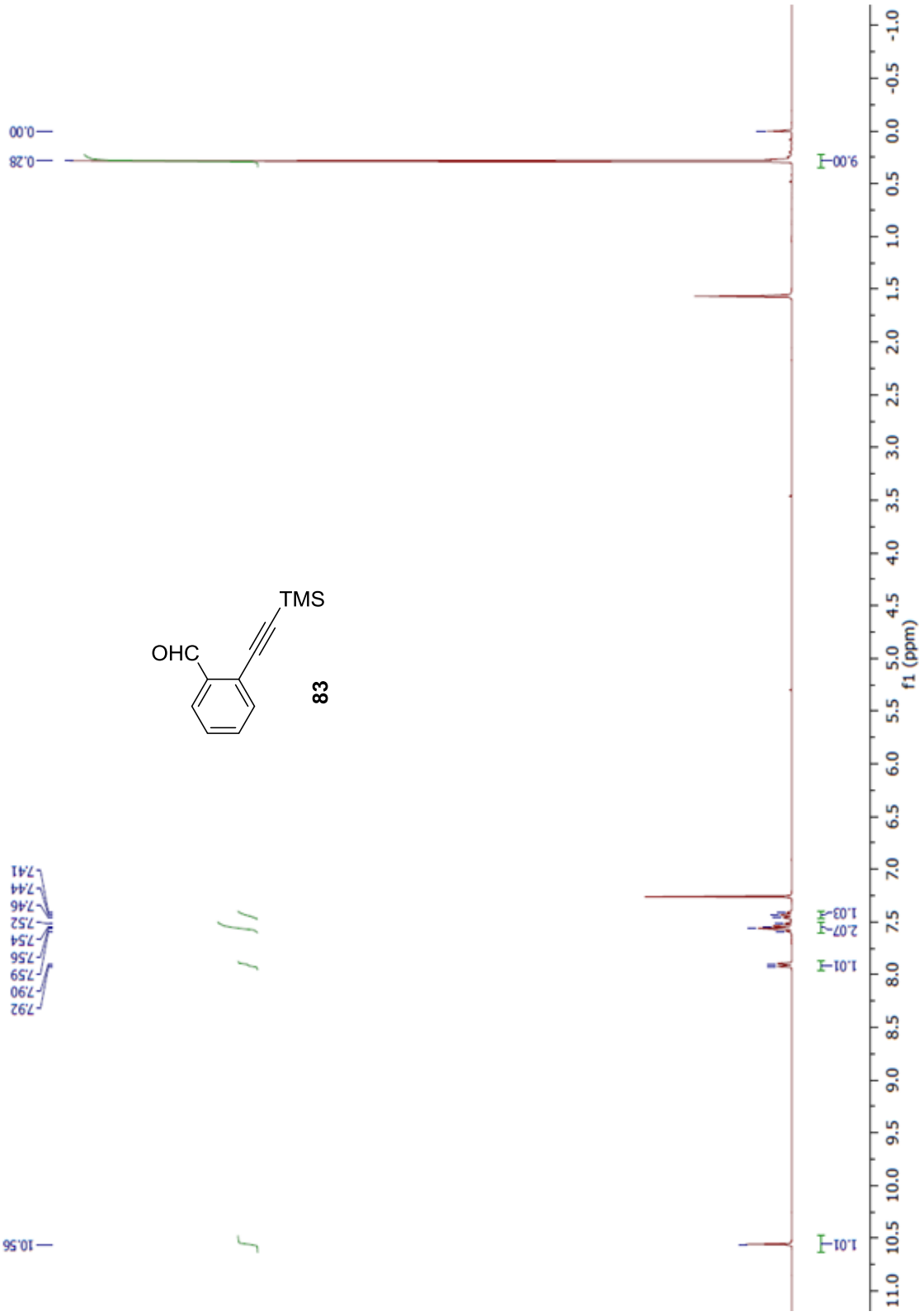
TMS
OHC
83
f1 (ppm)

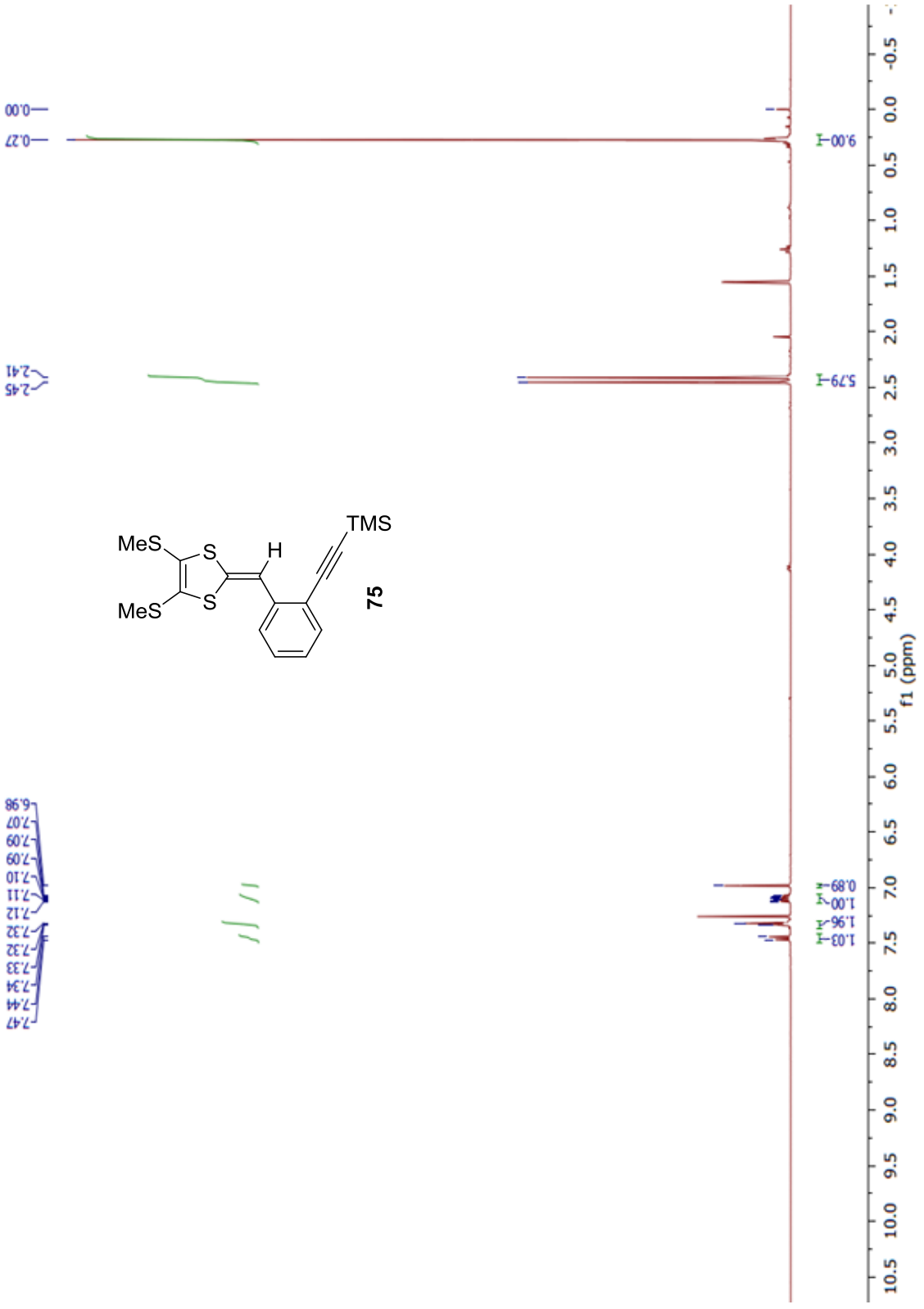
MeS
S
H
TMS
MeS
S
75
f1 (ppm)

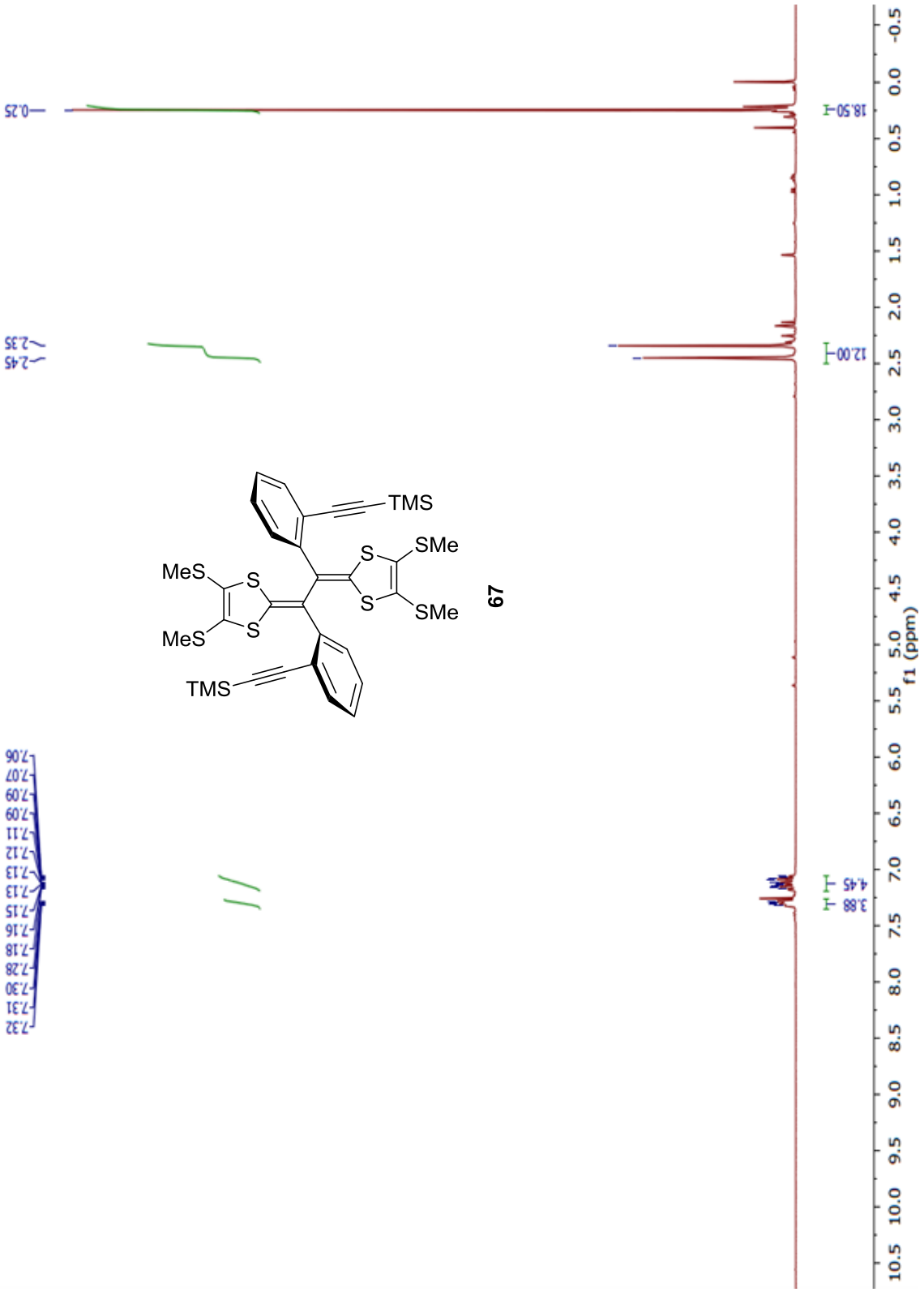
TMS
SMe
MeS
S
S
S
SMe
MeS
TMS
67
f1 (ppm)

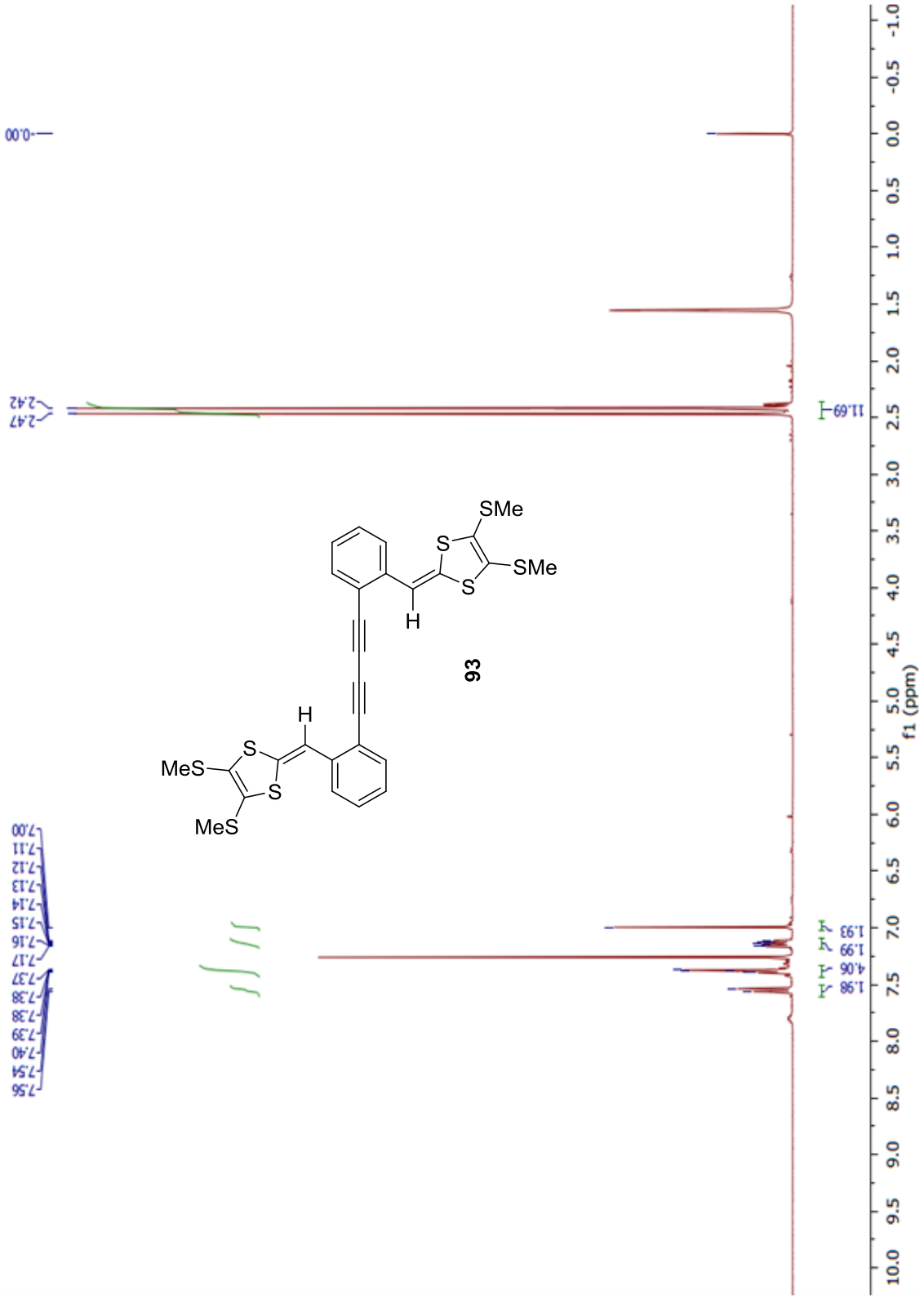
SMe
S
SMe
S
H
93
H
S
MeS
S
MeS
f1 (ppm)

A.2: ^{13}C NMR Spectra

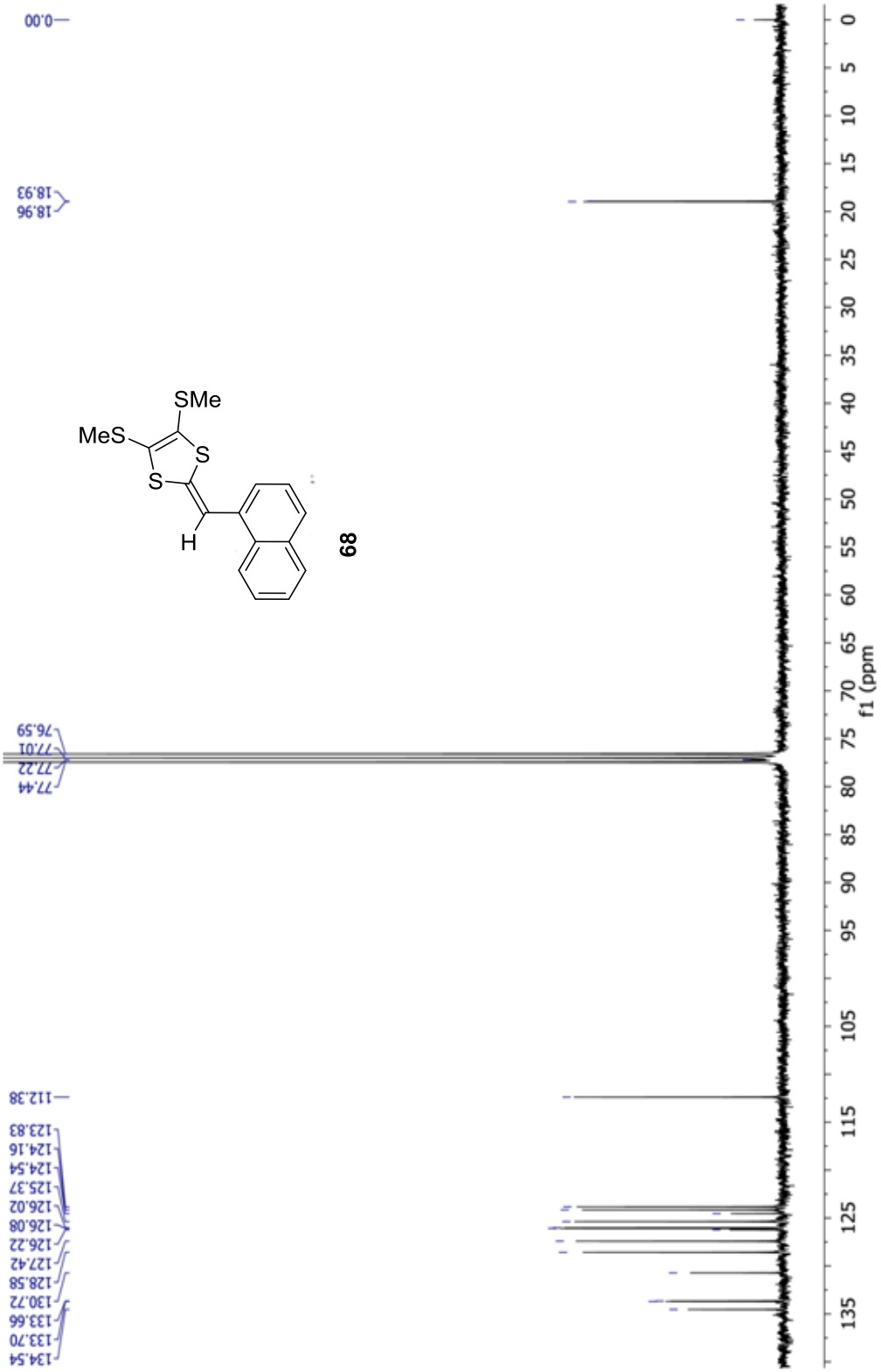
SMe
MeS
S
S
H
68
0.00
18.96
18.93
77.44
77.22
77.01
76.59
112.38
123.83
124.16
124.54
125.37
126.02
126.08
126.22
127.42
128.58
130.72
133.66
133.70
134.54
0
5
10
15
20
25
30
35
40
45
50
55
60
65
70
75
80
85
90
95
105
115
125
135
f1 (ppm

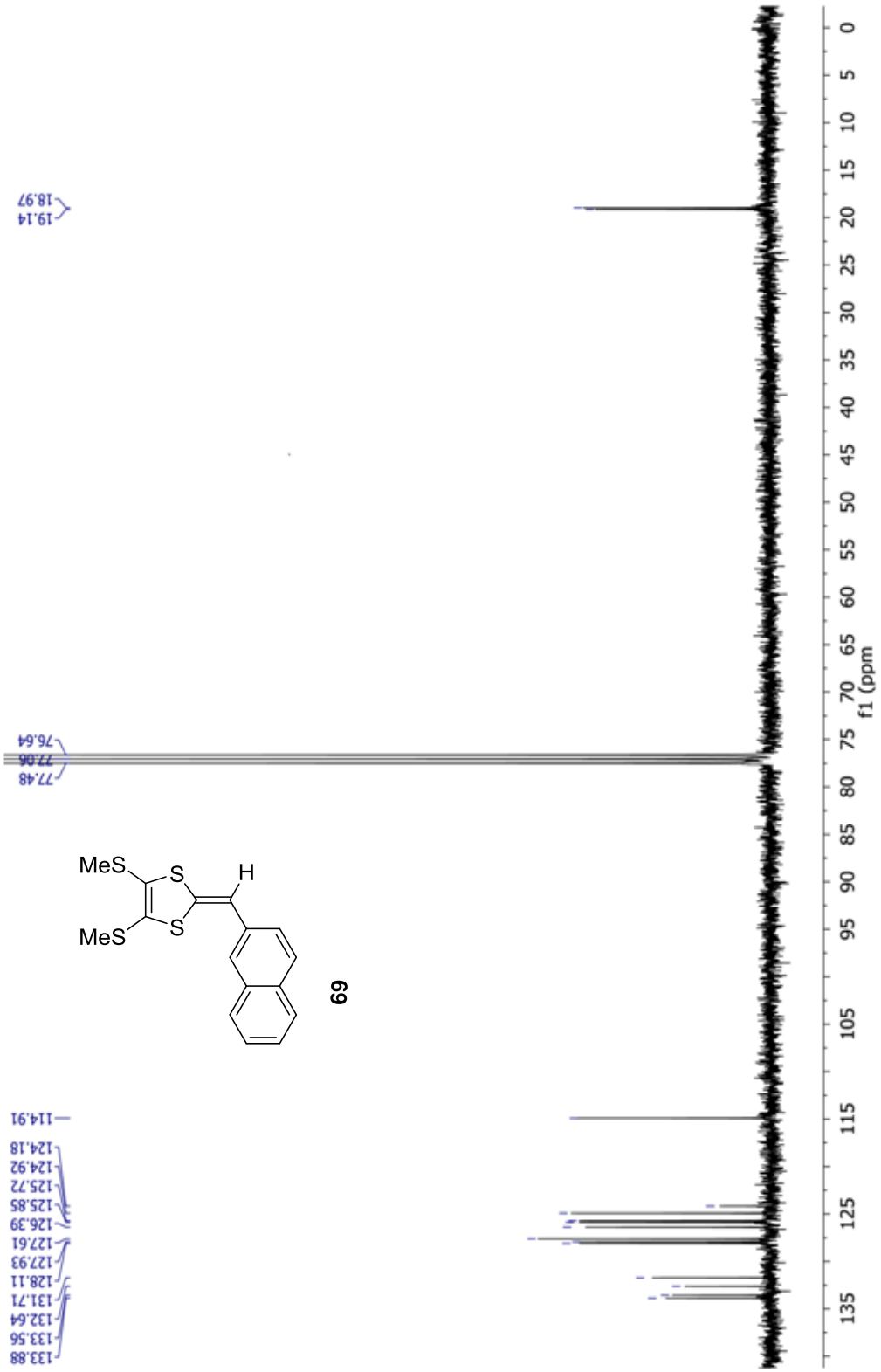
MeS
S
H
MeS
S
69
f1 (ppm)

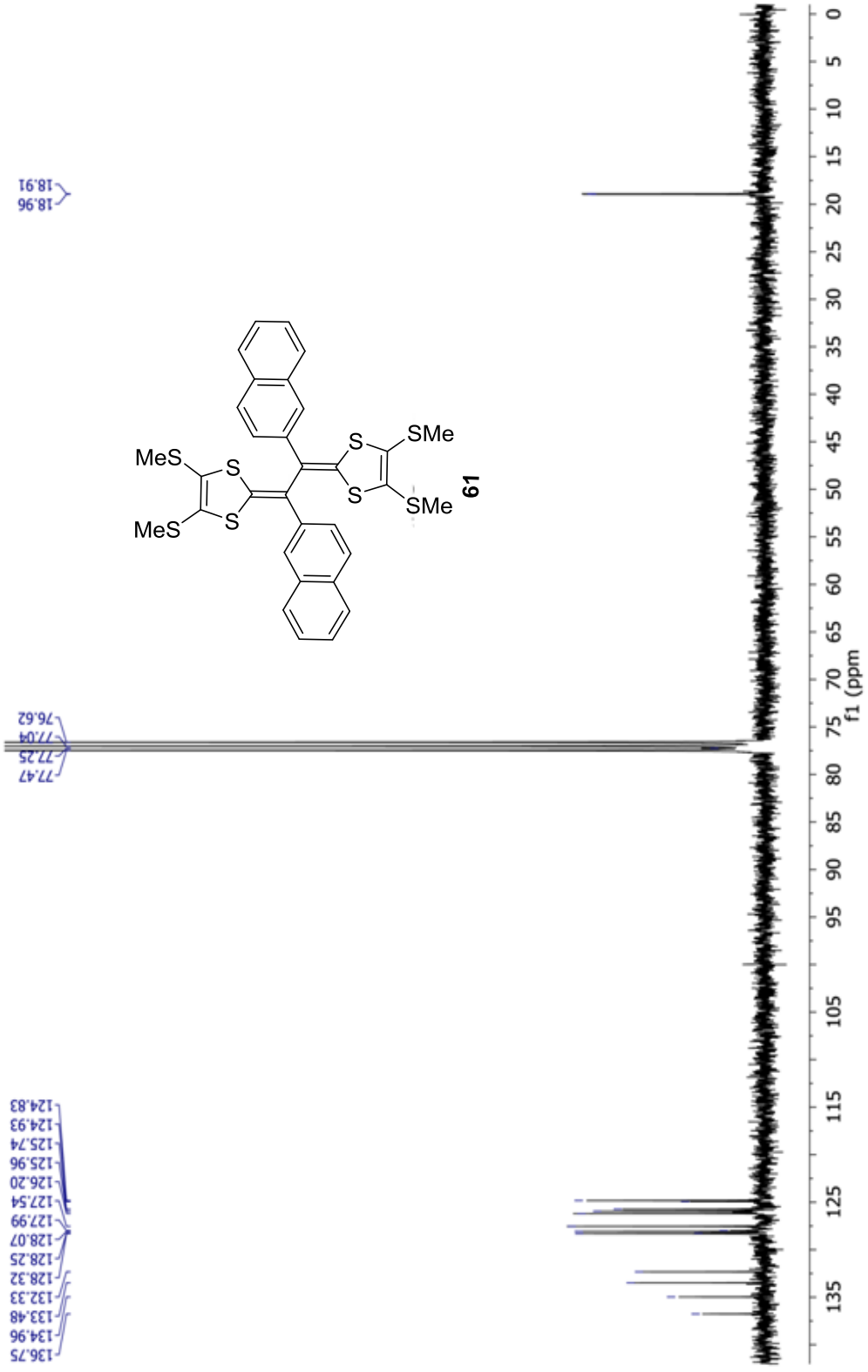
MeS
S
MeS
S
S
SMe
S
SMe
61
18.96
18.91
77.47
77.25
77.04
76.62
136.75
134.96
133.48
132.33
128.32
128.25
128.07
127.99
127.54
126.20
125.96
125.74
124.93
124.83
f1 (ppm

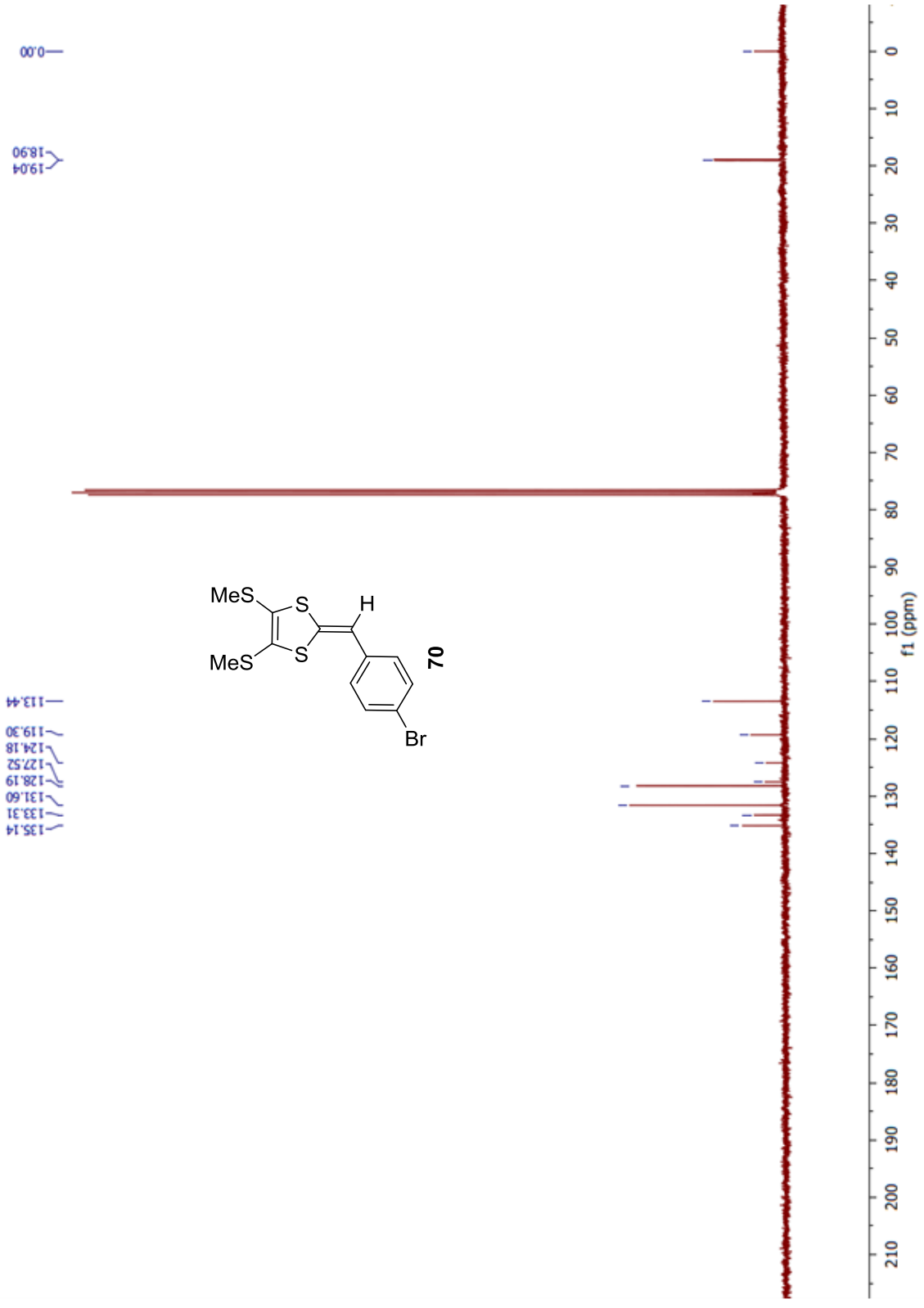
0.00
18.90
19.04
113.44
119.30
124.18
127.52
128.19
131.60
133.31
135.14
MeS
MeS
S
S
H
Br
70
f1 (ppm)

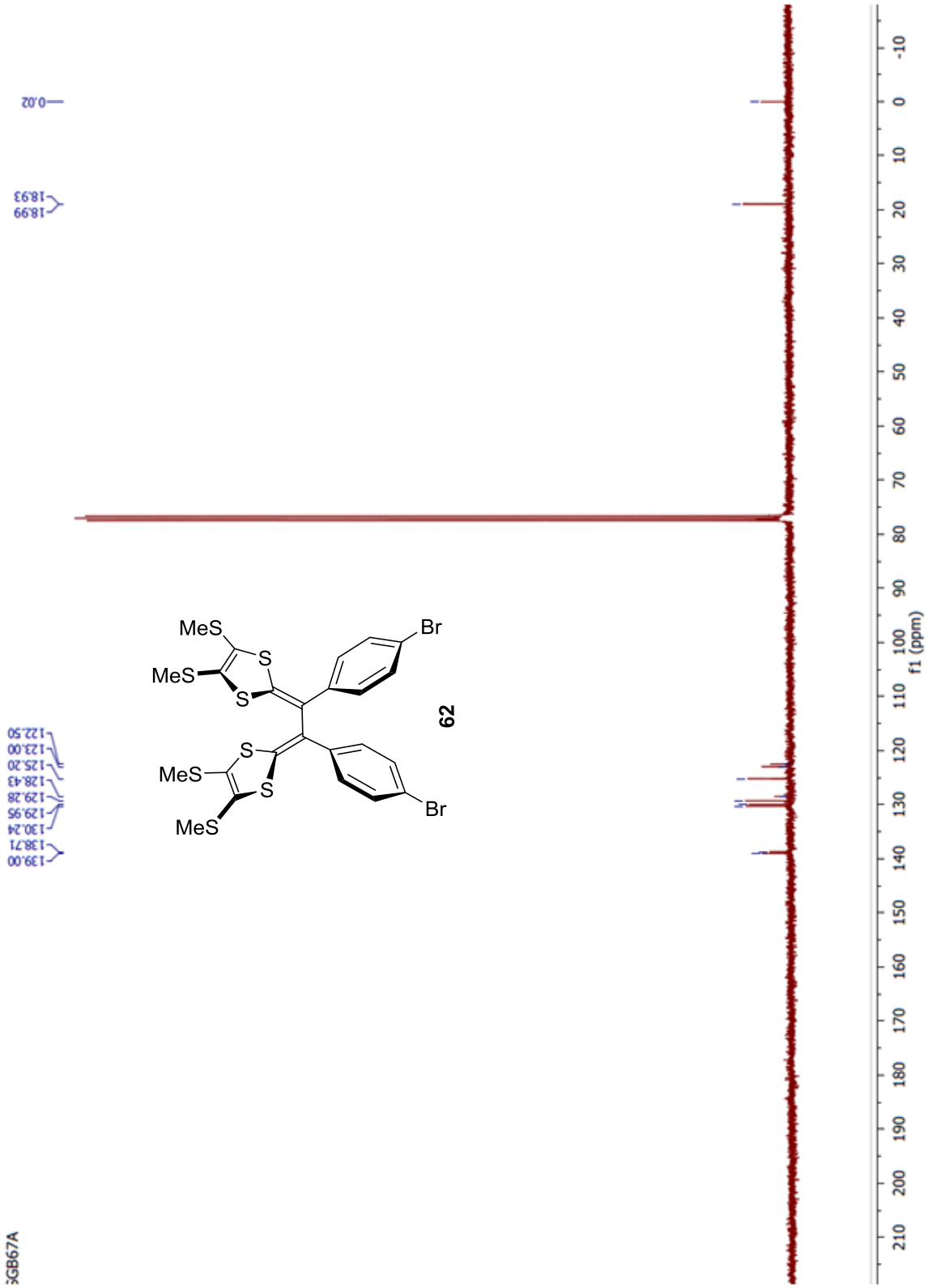
MeS
MeS
MeS
MeS
S
S
S
S
Br
Br
62
f1 (ppm)

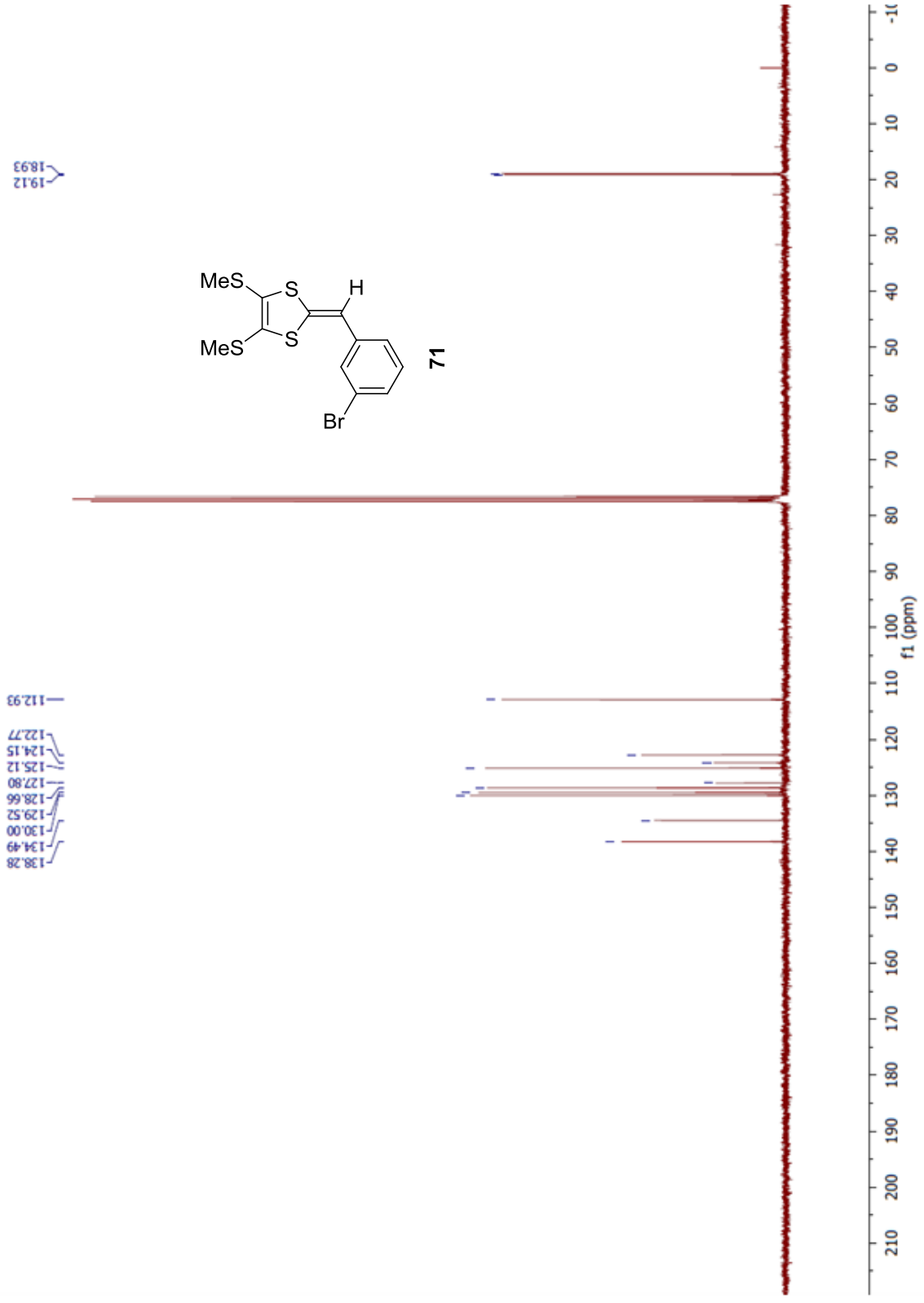
MeS
MeS
S
S
H
Br
71
19.12
18.93
112.93
122.77
124.15
125.12
127.80
128.66
129.52
130.00
134.49
138.28
f1 (ppm)

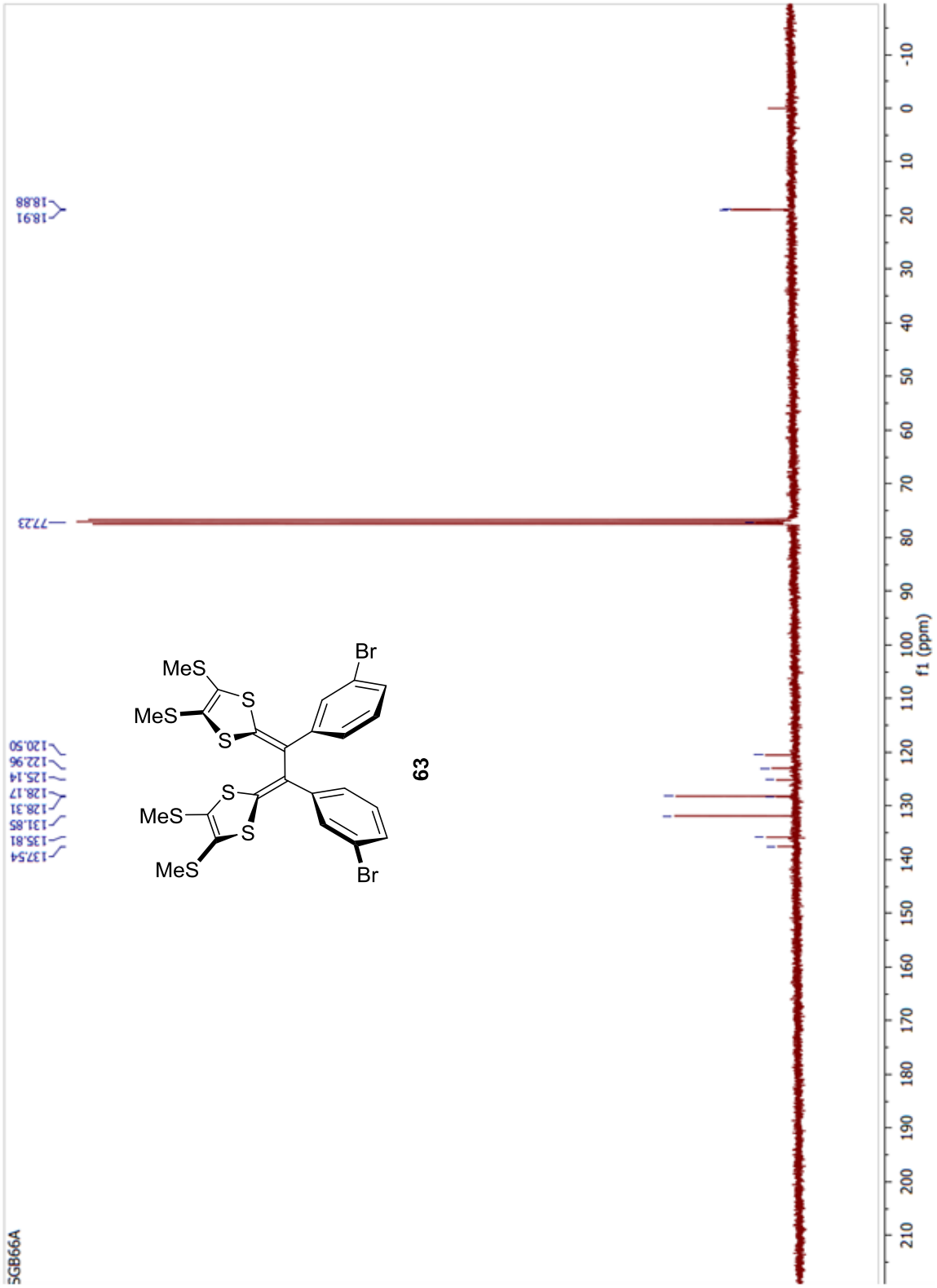
18.91
18.88
77.23
120.50
122.96
125.14
128.17
128.31
131.85
135.81
137.54
MeS
MeS
S
S
Br
S
MeS
S
MeS
Br
63
5GB66A
f1 (ppm)

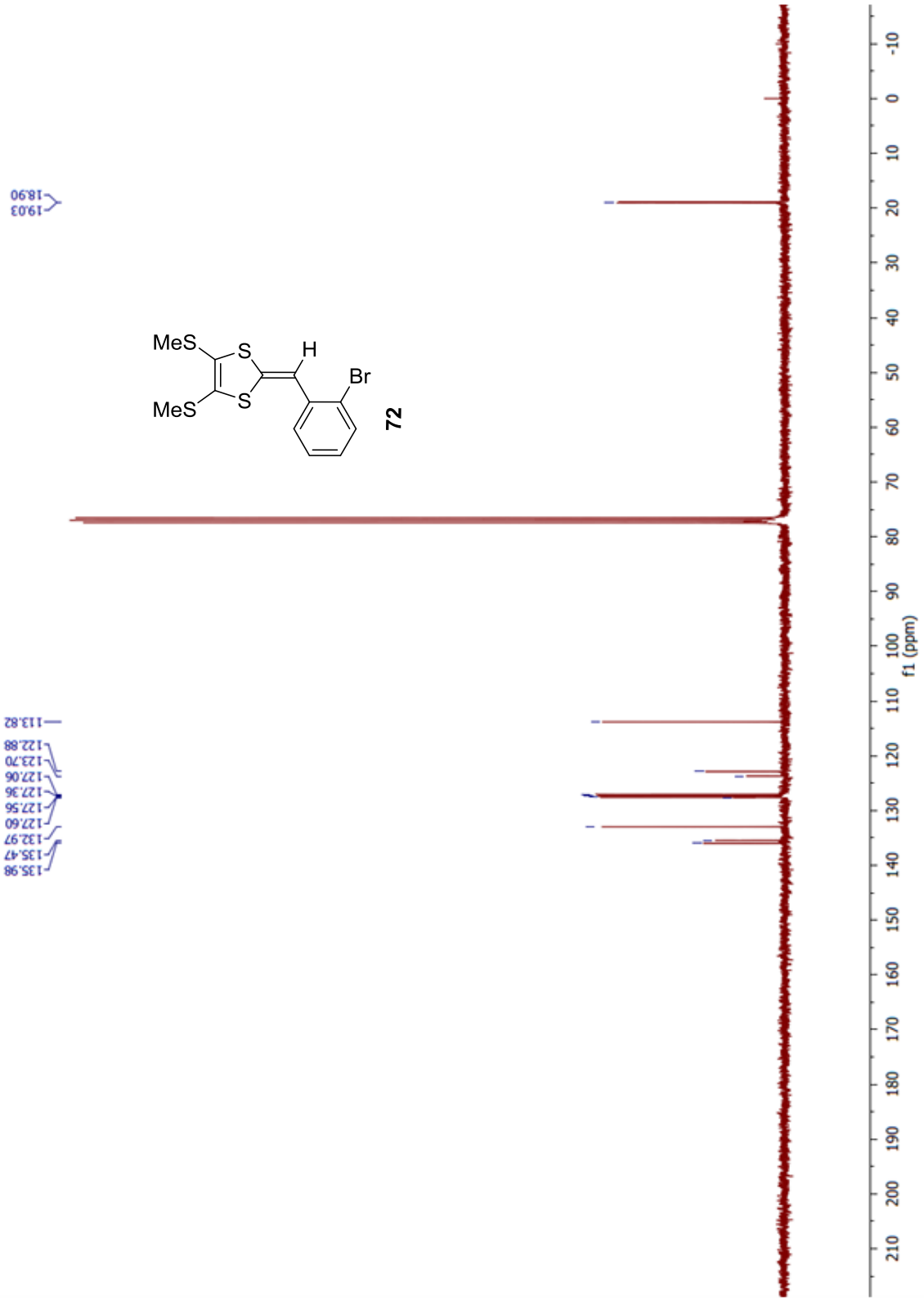
MeS
S
H
Br
MeS
S
72
18.90
19.03
113.82
122.88
123.70
127.06
127.36
127.56
127.60
132.97
135.47
135.98
f1 (ppm)

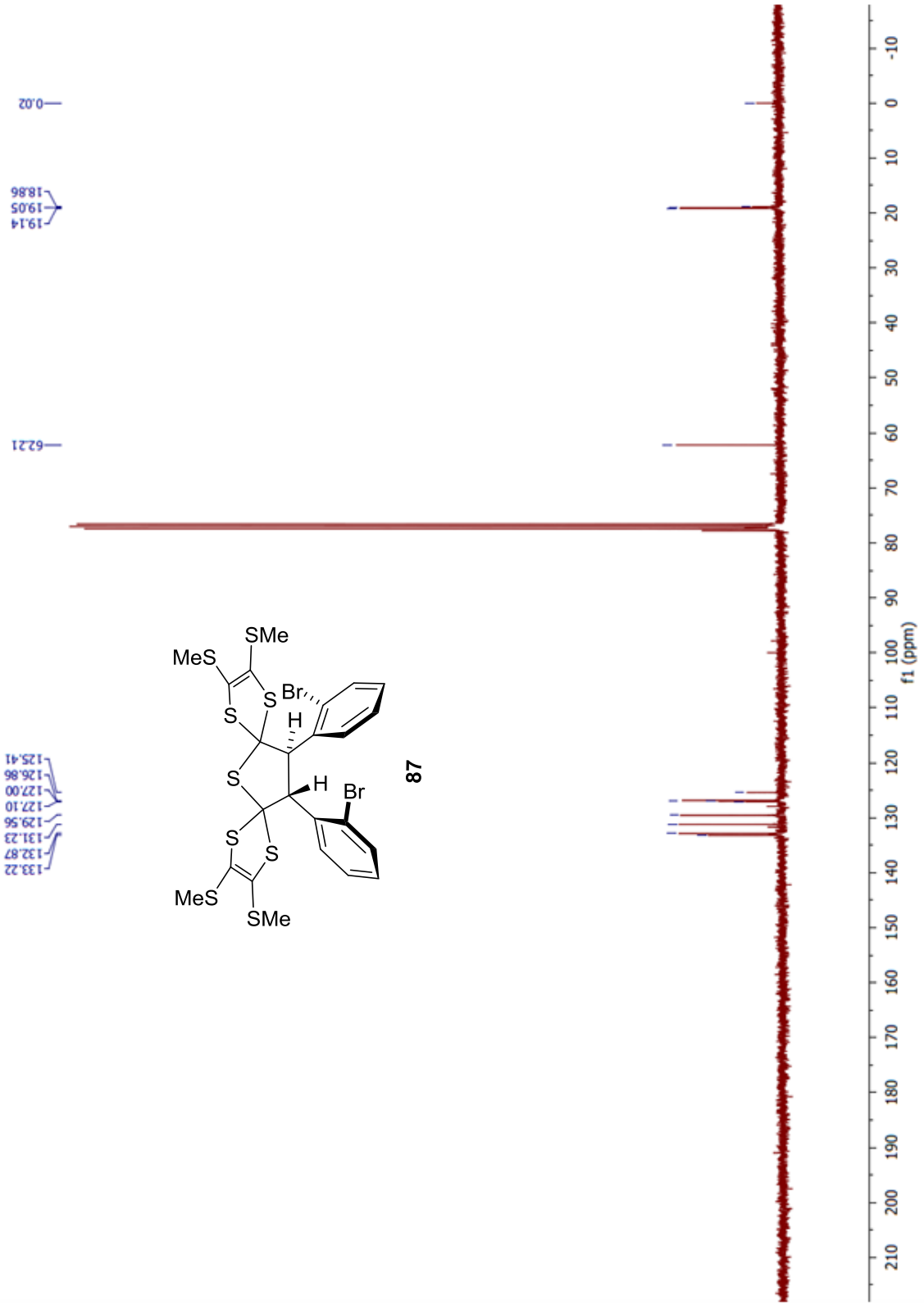
0.02
18.86
19.05
19.14
62.21
125.41
126.86
127.00
127.10
129.56
131.23
132.87
133.22
SMe
MeS
S
S
Br
H
S
H
Br
S
S
MeS
SMe
87
-10
0
10
20
30
40
50
60
70
80
90
100
110
120
130
140
150
160
170
180
190
200
210
f1 (ppm)

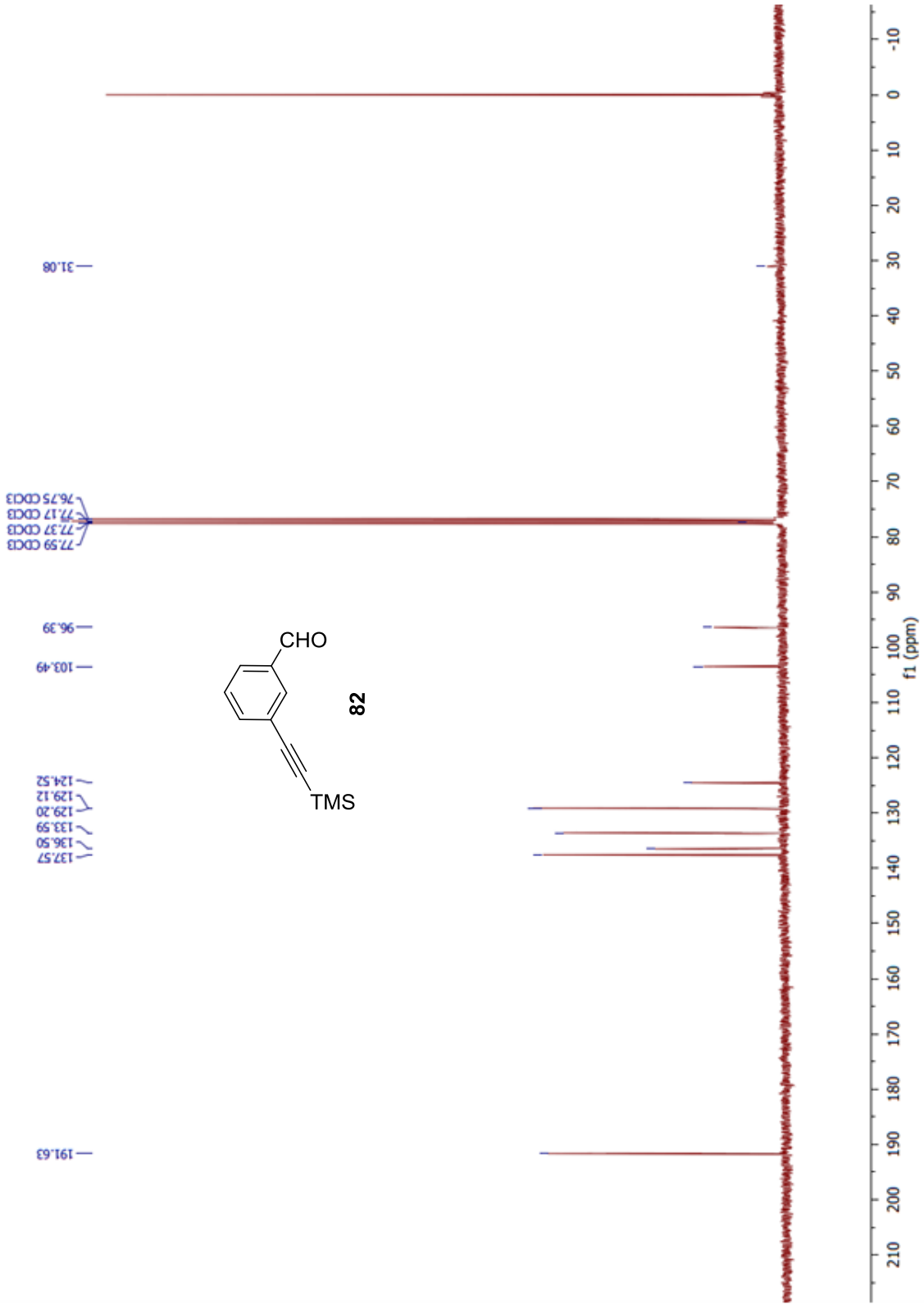
CHO
TMS
82
f1 (ppm)

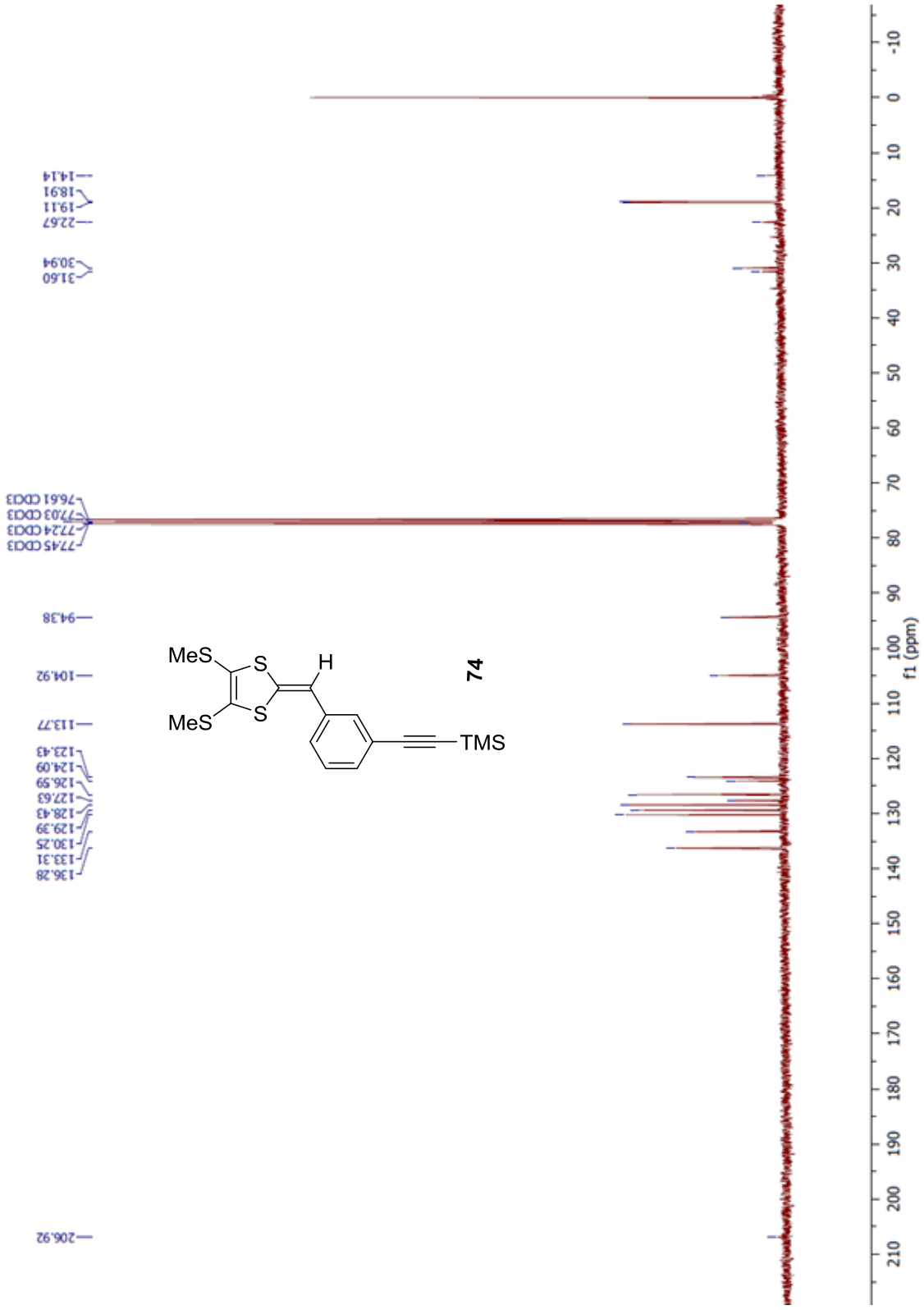
MeS
S
H
MeS
S
TMS
74
14.14
18.91
19.11
22.67
30.94
31.60
76.61 CDCl3
77.03 CDCl3
77.24 CDCl3
77.45 CDCl3
94.38
104.92
113.77
123.43
124.09
126.59
127.63
128.43
129.39
130.25
133.31
136.28
206.92
f1 (ppm)

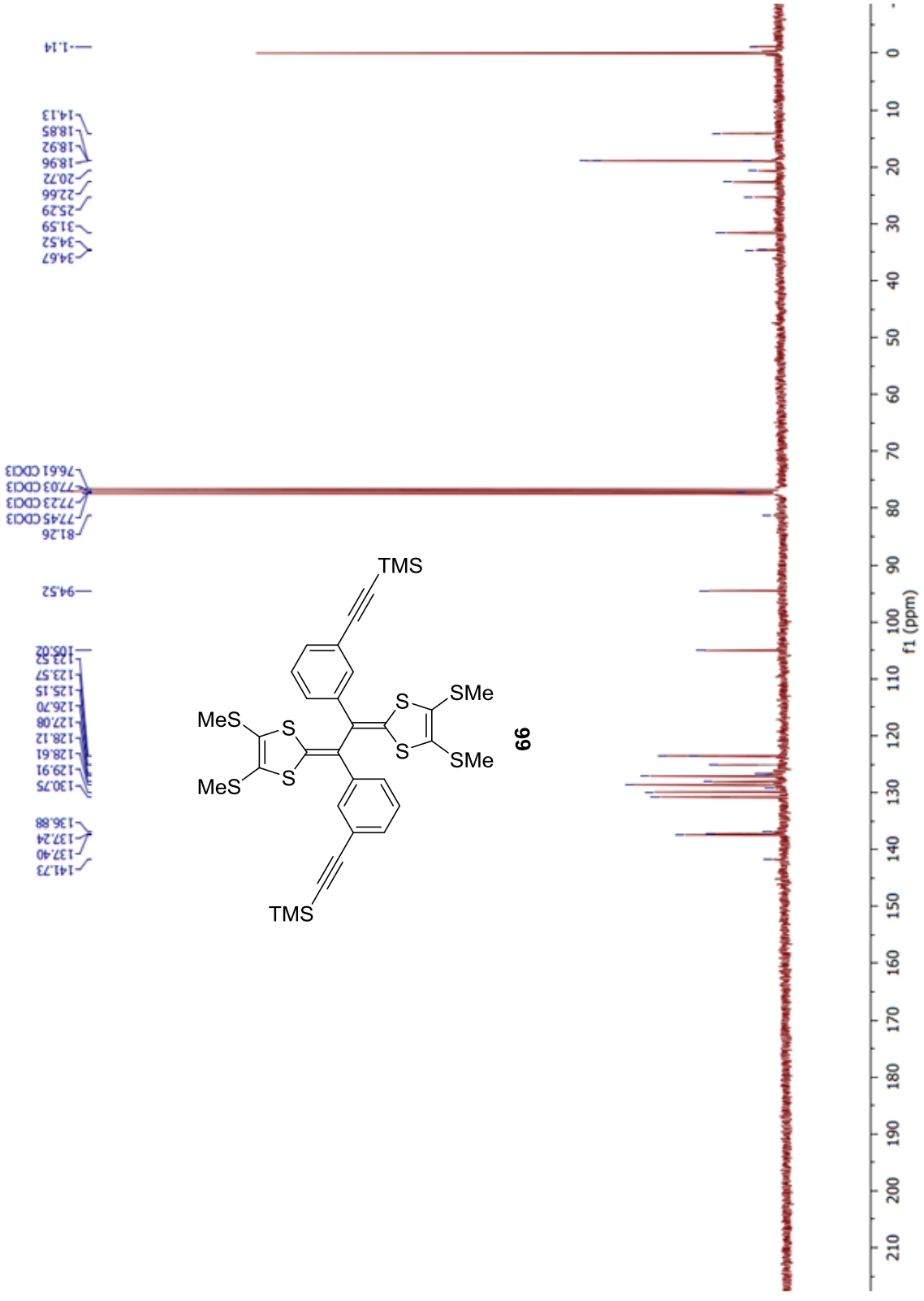
TMS
SMe
SMe
MeS
MeS
S
S
S
S
TMS
99
f1 (ppm)

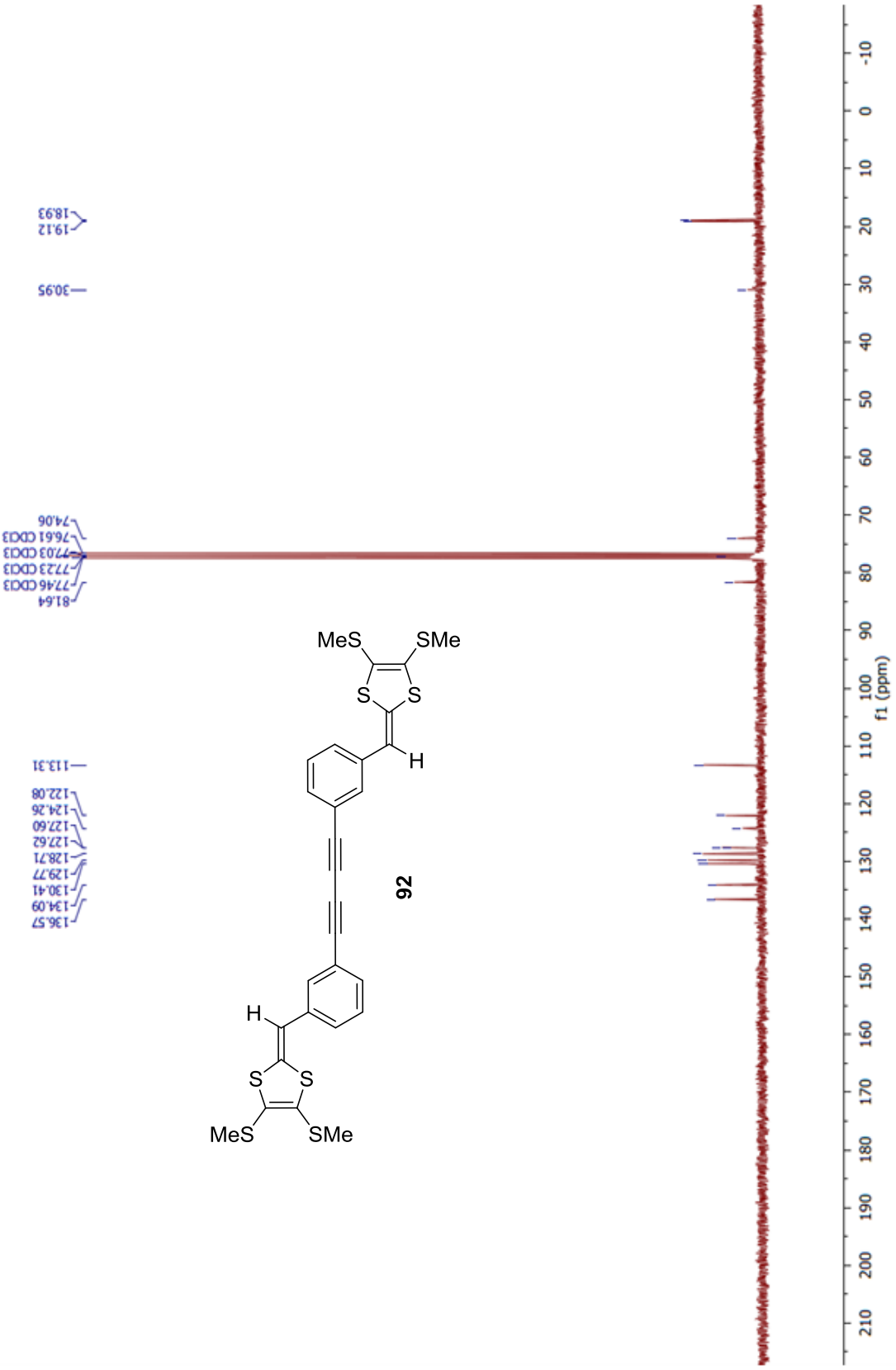
18.93
19.12
30.95
74.06
76.61 CDCl3
77.03 CDCl3
77.23 CDCl3
77.46 CDCl3
81.64
113.31
122.08
124.26
127.60
127.62
128.71
129.77
130.41
134.09
136.57
MeS
SMe
S
S
H
92
H
S
S
MeS
SMe
f1 (ppm)

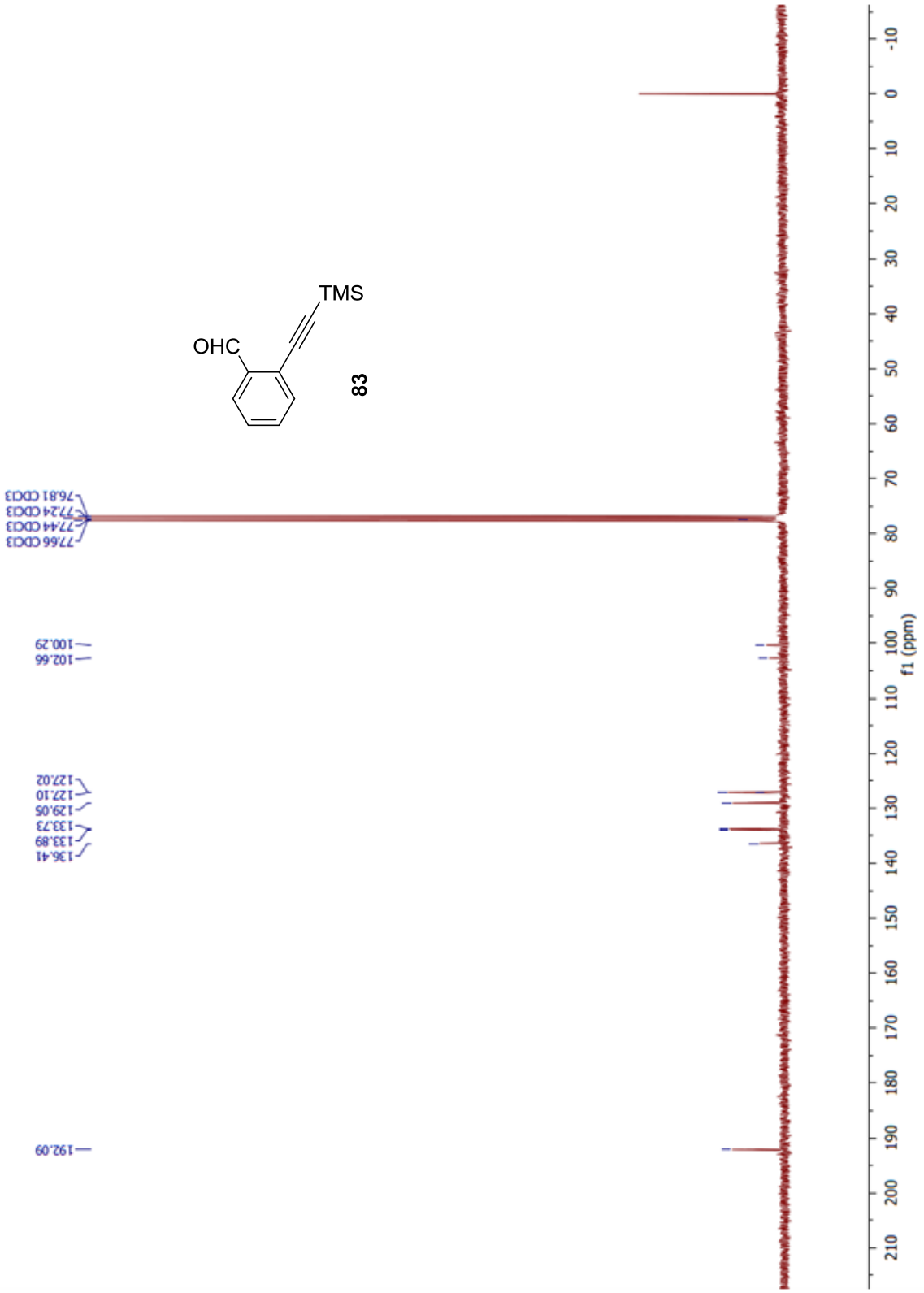
TMS
OHC
83
77.66 CDCl3
77.44 CDCl3
77.24 CDCl3
76.81 CDCl3
100.29
102.66
127.02
127.10
129.05
133.73
133.89
136.41
192.09
f1 (ppm)

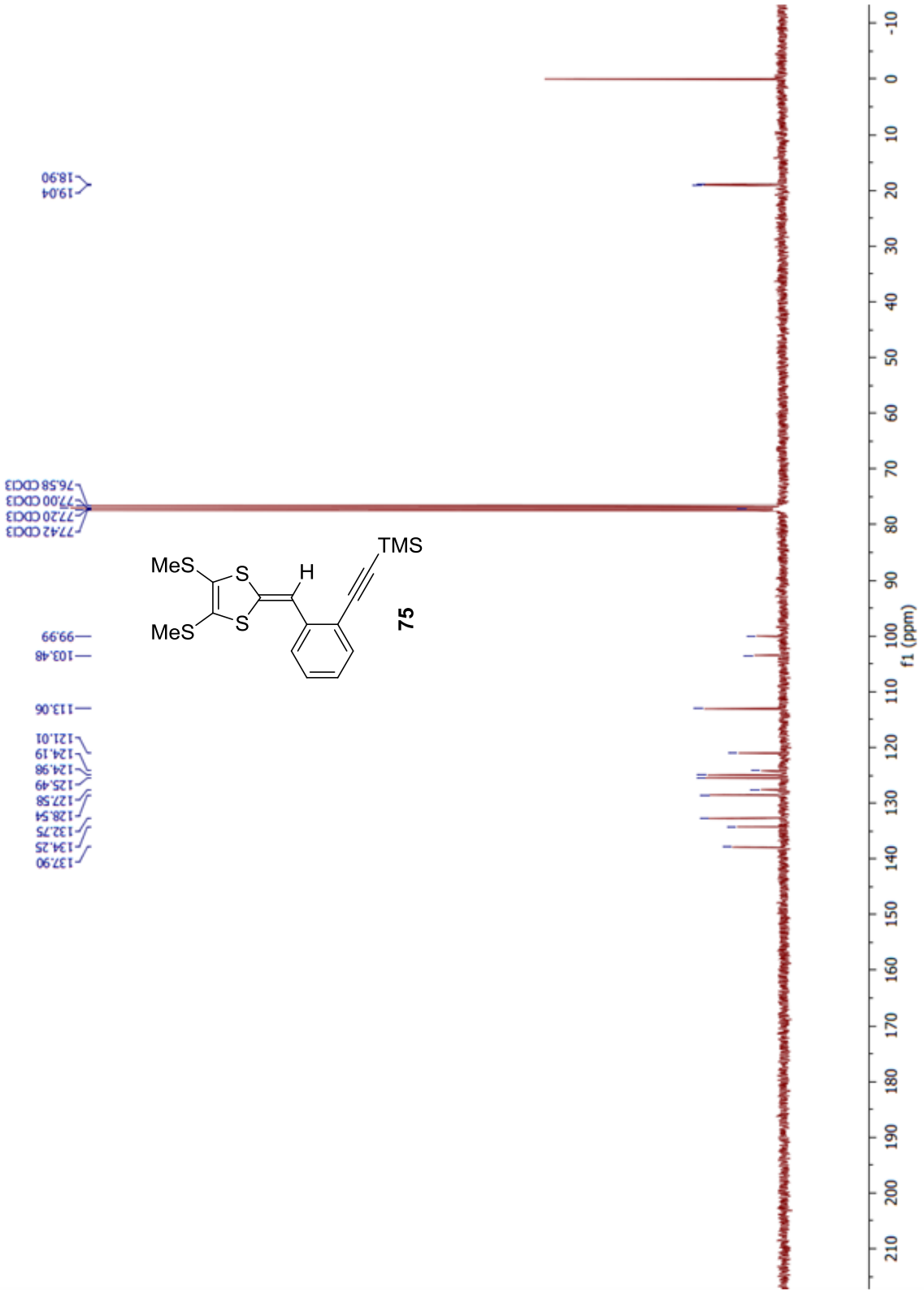
MeS
S
H
TMS
MeS
S
75
f1 (ppm)

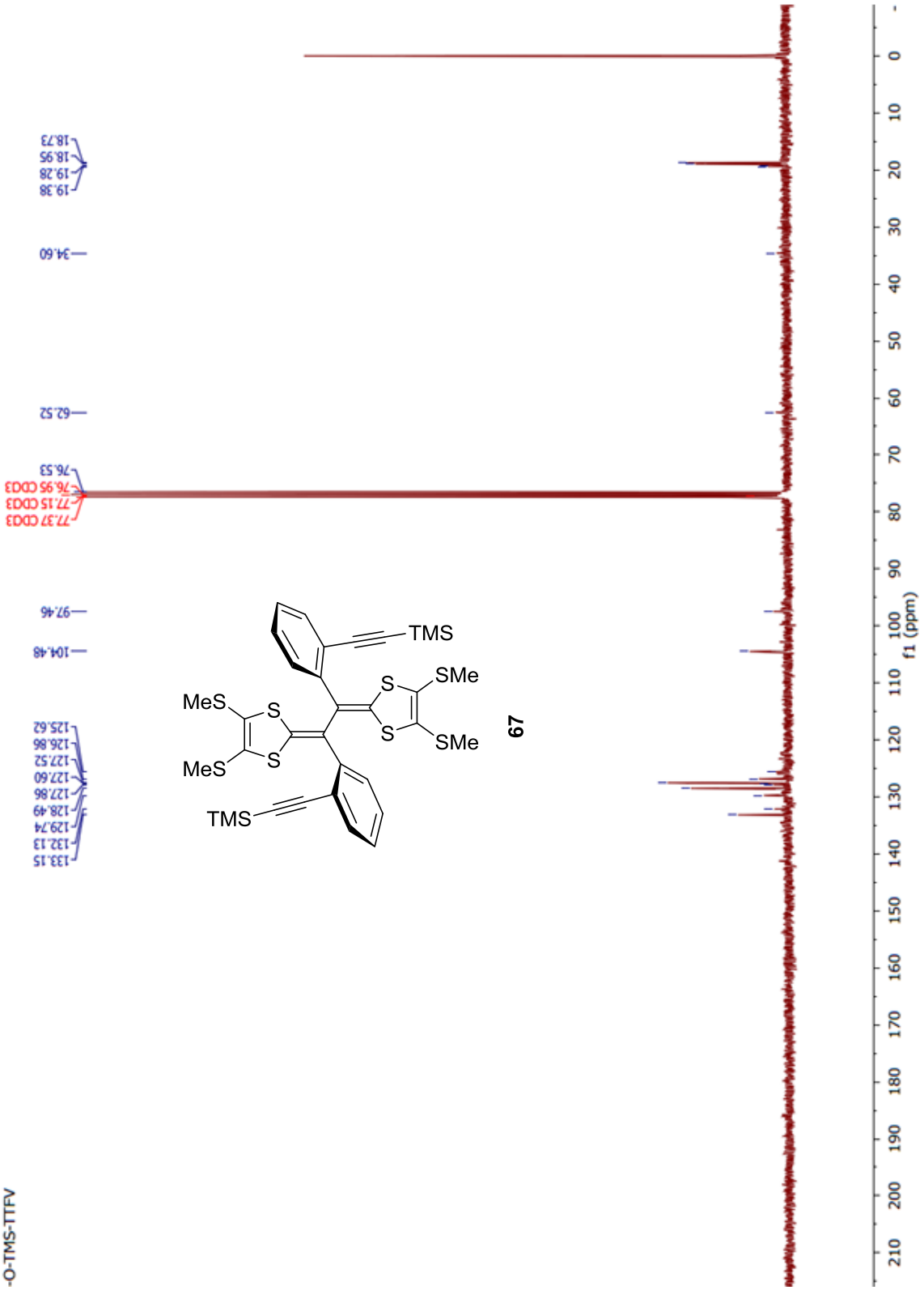
-O-TMS-TTFV
18.73
18.95
19.28
19.38
34.60
62.52
76.53
76.95 CDCl3
77.15 CDCl3
77.37 CDCl3
97.46
104.48
125.62
126.86
127.52
127.60
127.86
128.49
129.74
132.13
133.15
TMS
SMe
SMe
MeS
MeS
S
S
S
S
67
f1 (ppm)

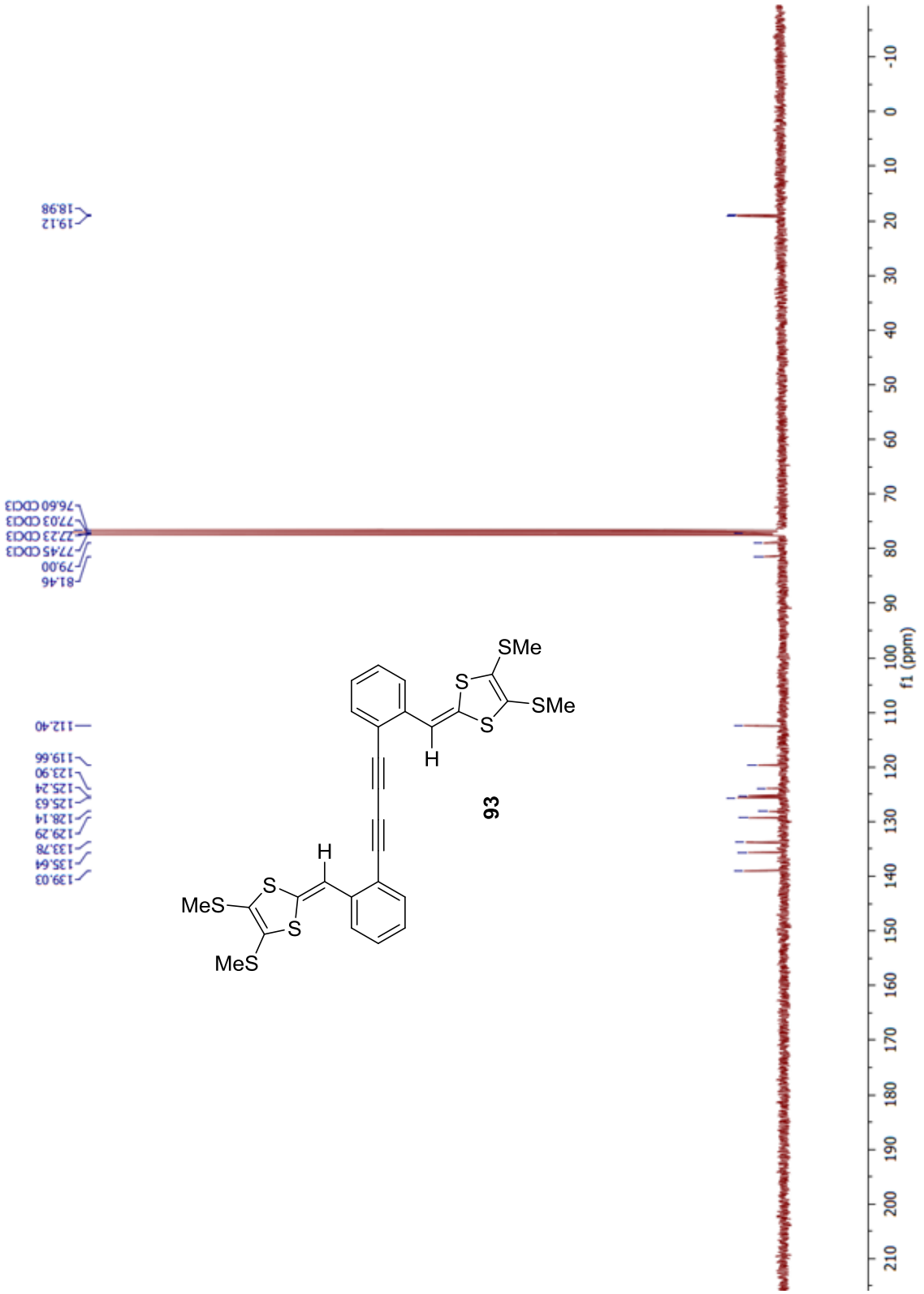
SMe
S
SMe
S
H
93
H
S
MeS
S
MeS
f1 (ppm)